Transport and Mixing in the Tropical Tropopause Layer

Dissertation
zur Erlangung des Doktorgrades
der Naturwissenschaften

vorgelegt beim
Fachbereich Geowissenschaften / Geographie
der Johann Wolfgang Goethe-Universität
in Frankfurt am Main

von

Carine Dorianne Homan, MSc
aus Amsterdam

Frankfurt am Main 2010
D30

Vom Fachbereich Geowissenschaften / Geographie der Johann Wolfgang Goethe-Universität als Dissertation angenommen.

Dekan:	Prof. Dr. Robert Pütz
Gutachter:	Prof. Dr. Ulrich Schmidt, Universität Frankfurt
	Prof. Dr. C. Michael Volk, Universität Wuppertal
Datum der Disputation:	22-12-2010

In the end,
we will conserve only what we love,
we will love only what we understand,
we will understand only what we
are taught.

Baba Dioum

Contents

Overview **1**

1 Introduction **3**
1.1 The Tropical Tropopause Layer (TTL) . . . 3
1.2 Transport in the TTL . . . 6
1.2.1 Diabatic ascent . . . 6
1.2.2 Convection . . . 8
1.2.3 Stratospheric isentropic inmixing into the TTL . . . 8
1.2.4 Isentropic mixing across the subtropical barrier . . . 9
1.3 Use of tracer measurements . . . 9
1.3.1 Vertical tracer profiles . . . 10
1.3.2 Tracer-tracer correlations . . . 11

2 Measurements **13**
2.1 The M55-Geophysica . . . 13
2.2 The High Altitude Gas Analyzer (HAGAR) . . . 16
2.3 The Cryogenically Operated Laser Diode (COLD) and the Fast Ozone Analyzer (FOZAN) . . . 18
2.4 Measurement campaigns . . . 18
2.4.1 SCOUT-O3 . . . 18
2.4.2 AMMA/SCOUT-O3 . . . 25
2.4.3 TROCCINOX, APE-THESEO and ASHOE MAESA . . . 30

3 Tracer measurements in the tropical tropopause layer during the AMMA/SCOUT-O3 aircraft campaign **31**
3.1 Introduction . . . 31
3.2 Analysis of main transport processes . . . 32
3.2.1 Convection . . . 33
3.2.2 Stratospheric isentropic inmixing into the TTL . . . 41
3.2.3 Isentropic mixing across the subtropical barrier . . . 43
3.3 Conclusions . . . 47

4 Influence of boundary layer pollution, convection and the subtropical jet on the TTL over Darwin during the SCOUT-O3 aircraft campaign 49
4.1 Introduction . . . 49
4.2 Measurements . . . 50
4.3 Prevailing meteorology . . . 50
4.4 Results . . . 51
4.4.1 Vertical profiles of O_3, CO, CO_2 and N_2O . . . 51
4.4.2 Tracer-tracer correlations . . . 54
4.4.3 Backward trajectories . . . 58
4.5 Interpretation . . . 64
4.5.1 Horizontal isentropic inmixing . . . 64
4.5.2 Hector . . . 66
4.5.3 Influence of the subtropical jet . . . 70
4.5.4 Influence of boundary layer pollution over Indonesia . . . 73
4.6 Conclusions . . . 81

5 Residence times and vertical transport rates in the background TTL 83
5.1 Introduction . . . 83
5.2 Measurements and method . . . 85
5.3 Results . . . 87
5.4 Discussion and Conclusions . . . 96

6 Conclusions and Outlook 99

A Calibration standards 101

List of abbreviations 103

Bibliography 107

Summary 117

Zusammenfassung 121

Acknowledgements 127

Curriculum Vitae 129

Overview

The future development of the global climate due to increasing greenhouse gas concentrations is still hard to predict. While computer simulations with interactive climate-chemistry models are able to make high resolution predictions for future climate, they still have high uncertainties due to insufficient understanding of radiative, transport and chemical processes and the interaction between these processes. Especially the stratosphere and the transport processes between the troposphere and the stratosphere are still a challenge to represent properly in models (Douglas et al., 2003; WMO, 2007; Gettelman et al., 2009). However, it is clear that especially these processes are very important for the radiative and chemical balance of the atmosphere (Shindell et al., 1998). An example is the transport of short-lived natural and anthropogenic halogenated compounds which, if they reach the lower stratosphere, will be oxidized there producing halogen radicals which could deplete ozone (see e.g. WMO, 2007; Bridgeman et al., 2000). Depleted ozone levels may alter the circulation in the stratosphere, which will in turn affect the surface climate.

Especially the tropics are a region of interest, because they are a source region for much of the air entering the stratosphere (e.g. Holton et al., 1995). Here, the tropical tropopause layer (TTL) forms the transition between the convectively dominated troposphere and the radiatively dominated stratosphere. As discussed first by Brewer (1949), the boundary condition for stratospheric water vapor is likely set in this region. The interaction of convection, the stratospheric wavedriven circulation and horizontal exchange with the midlatitude lower stratosphere governs the transport of ozone, aerosols and other short lived chemical species into the stratosphere. However, the relative roles of these processes in the TTL are still unclear.

In situ measurements provide a useful tool to test and improve computer simulations and help to improve our current knowledge of troposphere to stratosphere transport. Therefore, in 1999 the Institute for Atmospheric and Environmental Sciences at the University of Frankfurt developed the High Altitude Gas Analyzer (HAGAR), an instrument for simultaneous high resolution in situ measurements of long lived trace gases in the stratosphere (Riediger, 2000; Strunk, 1999). Trace gases can be used as tracers of transport whenever their lifetimes are longer than the timescales of the processes transporting them, such that their distributions are mainly determined by dynamics.

This dissertation project builds mainly on two tropical aircraft campaigns performed with the HAGAR instrument. Different transport processes between the tropical troposphere, the tropical stratosphere and the extratropical stratosphere are studied. By improving our understanding of fundamental transport processes in the TTL, a key region for atmospheric

chemistry-climate coupling, this work will contribute to ongoing efforts within the scientific community to obtain more insight into the role of the different transport processes taking place in the TTL. It will thereby help to validate and improve global chemistry-climate models with the goal to provide more reliable predictions of future atmospheric composition and climate.
First, in Chapter 1, a short introduction is given on the definition and the characteristics of the tropical tropopause layer (Section 1.1), the different transport processes that play a role in the tropical tropopause layer (Section 1.2) and the use of tracers to study these transport processes (Section 1.3). In the second chapter, the aircraft platform (Section 2.1) and the instruments that are used in the analyses (Section 2.2 and Section 2.3) will be explained. Furthermore, a description of the two main tropical campaigns is presented (Section 2.4.1 and 2.4.2), as well as a short description of three previous campaigns, from which data are used for comparison (Section 2.4.3).
Chapters 3 to 5 will show the results obtained during the measurement campaigns and scientific analyses thereof. Chapter 3 will present results from the AMMA/SCOUT-O3 campaign over Africa and discuss the different transport processes observed in the tracer data. Chapter 4 will discuss results of the SCOUT-O3 campaign over northern Australia and will focus especially on vertical transport and mixing due to convection, influences of local pollution and the influence of the subtropical jets. The last chapter will focus on the study of slow vertical ascent and the so called "CO_2 tracer clock".

Chapter 1

Introduction

1.1 The Tropical Tropopause Layer (TTL)

Although the troposphere and stratosphere are inseparable in a dynamical sense (Hoskins et al., 1985) they are very different with respect to their vertical transport timescales and their chemical processes. In the troposphere, the layer reaching from the surface up to about 18 km in the tropics, the temperature decreases with height. Vertical transport is therefore dominated by convective processes, in which mixing of air masses takes place on very short time scales. Above the troposphere, in the stratosphere, the temperature increases with height due to the absorption of solar radiation by ozone. This increase of temperature with height makes the stratosphere a very stable layer in the atmosphere. Vertical transport processes are slow and dominated by radiative and large scale processes. In the tropics, the boundary between the troposphere and the stratosphere is not a sharp border, but a region of transition, where both properties of the convectively dominated troposphere and the radiatively controlled stratosphere can be observed. This region is called the Tropical Tropopause Layer or Tropical Transition Layer (TTL). In this region the main transport of air between the troposphere and the stratosphere takes place. Air experiences its final dehydration in the TTL prior to entry into the stratosphere, and transit time scales (together with wash-out processes) greatly affect the flux into the stratosphere of water vapour and short-lived ozone-depleting substances. Hence, the TTL acts in several ways as a "gate to the stratosphere" which greatly enhances its importance for the global climate system (Fueglistaler et al., 2009).
In the past ten years, the concept of a tropical tropopause layer rather than a tropopause surface has been discussed by different authors. Highwood and Hoskins (1998) defined the TTL in the context of the large scale tropical circulation. They define the level of main convective outflow as the base of the TTL. The level of main convective outflow is the level an air parcel can reach by undiluted, nonovershooting ascent. It is located around a potential temperature[1] level of at most 365 K (Folkins et al., 2000). Higher potential

[1] The potential temperature is the temperature an air parcel would attain if it is brought adiabatically to the Earth's surface. The potential temperature is not sensitive to temperature differences due to variations in pressure and can only change due to diabatic processes. Without diabatic processes air parcels will move

temperatures above that level can only be reached by diabatic ascent associated with radiative processes or mixing. As the upper boundary of the TTL Highwood and Hoskins (1998) use the cold point tropopause at around 380 K potential temperature. The cold point tropopause is defined as the lowest temperature in the temperature profile. Above the cold point tropopause, temperature increases with height, which hinders convective motions to penetrate deeply into the stratosphere.
Gettelman and Forster (2002) use a similar definition of the TTL. They define the (absolute) lapse rate minimum, the altitude at which the smallest change of temperature with altitude is observed, and which is associated with convection, at $\sim$ 345-350 K or 10-12 km, as the bottom of the TTL. For the top of the TTL they also choose the cold point tropopause.
With this definition the lower boundary of the TTL is determined by tropospheric processes (convection) and the upper boundary is determined by stratospheric radiative heating and a remote response to convection. However, in the lower part of the TTL the outflow from most of the deep convection subsides again due to radiative cooling, which prevails below the so-called "level of zero net radiative heating" (LZRH). Therefore, other authors (e.g. Folkins et al, 1999; Sinnhuber and Folkins, 2006) argue that this level of zero radiative heating should be used as the base of the TTL, since only air masses detraining from deep convection above this level (at an altitude of about 15.5 km, or about 360 K potential temperature) will reach the stratosphere.
Recently, Fueglistaler et al. (2009) proposed a new definition of the upper boundary of the TTL, primarily motivated by the large-scale dynamical structures. They define the base of the TTL at the level of zero radiative heating as well, but as the upper boundary they propose 425 K or approximately 18.5 km, as they argue that tropospheric influences may reach well above the cold point tropopause.
In this thesis the broader definition of the TTL is used, reaching from the level of main convective outflow until the cold point tropopause or above, as all processes taking place from the level of main convective outflow up to the highest levels overshooting convection may reach are of interest.
Apart from these different definitions for the TTL, there are also variations in the depth and altitude of the TTL over time and space. The top of the TTL, the cold point tropopause, has a single and coherent cycle throughout the tropics which has been linked to seasonal variations in solar radiation and its impact on tropical convection and to remote forcing during boreal winter associated with the intensification of the Brewer Dobson circulation (see Section 1.2.1). The climatological annual- and zonal mean height of the tropical CPT is 16.9 km, with very little north-south variability. Figure 1.1 shows the change of the cold point tropopause height and potential temperature over the year and at different latitudes. During NH winter the cold point tropopause is higher and at a slightly higher potential temperature than in NH summer. The height of the cold point tropopause varies with longitude, with the lowest cold point tropopause at around 160°E, and the highest over northern South America and east of Central America during the NH winter, and over

along lines of equal potential temperature (isentropes). Potential temperature is therefore a useful quantity for studying atmospheric transport processes, and is often used as a vertical coordinate instead of height or pressure.

Africa during other months. The coldest CPT is found over the western tropical Pacific (not shown). (Seidel et al. 2001)

The lower boundary of the TTL shows a larger variation over the tropics. Latitudinal

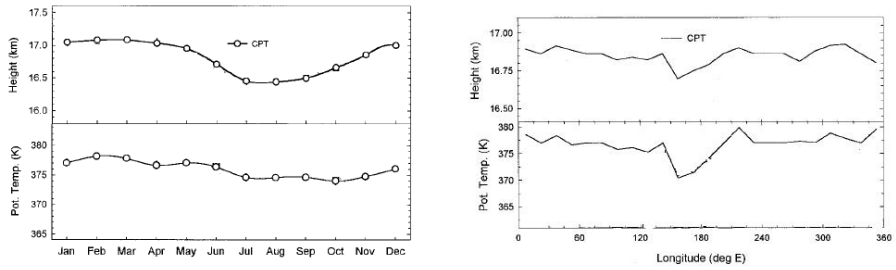

Figure 1.1: Climatological seasonal cycle (left) and annual-mean (right) of height (upper) and potential temperature (bottom) of the cold point tropopause in the equatorial zone (between 10°N and 10°S). Adapted from Seidel et al. (2001).

variations over the seasons are due to the migration of the rising branch of the Hadley circulation. The Hadley circulation consists of rising motion in the tropics, poleward flow in the upper troposphere and sinking in the subtropics. The rising branch migrates seasonally, influenced by the shifting latitude of maximum solar heating and ocean dynamics. It is generally found in the summer hemisphere. Large scale convective systems occur at the rising branch and the level of main convective outflow is higher and at higher potential temperature in these regions.

Longitudinal variations are mainly caused by the Walker circulation. The Walker circulation causes rising motion, and higher levels of main convective outflow, over the Western Pacific and maritime continent, with a maximum over Indonesia (115 - 120°E). Over the eastern Pacific there is a broad region of subsidence, with maximum descent in the coastal region of Ecuador (180°E). Secondary circulation cells of the Walker circulation cause rising motions over the land regions of South America and Africa, with compensating subsidence over the Atlantic and the Indian Ocean. Compared to the Pacific branch of the Walker Circulation, these cells cover smaller longitude ranges and tend to have weaker vertical motions in the annual mean climatology.

The Walker circulation has a pronounced seasonal cycle and interannual variability, which is closely tied to the El Niño and Southern Oscillation climate system. Changes in ENSO therefore also influence the TTL. During El Niño phases, the characteristic temperature pattern at tropopause levels attenuates, and temperatures are fairly uniform. Consequently, troposphere to stratosphere transport in the TTL is more zonally uniform during El-Niño than during La Niña (Fueglistaler and Haynes, 2005).

Also of influence to the TTL, and closely linked to the Walker circulation, are the east-west circulations in the subtropics caused by the largescale monsoon circulations and the convergence of the trade winds, the Quasi Biennial Oscillation (QBO, ∼2 years), the solar cycle (11 years), volcanic eruptions, and changes due to anthropogenic forcing of the climate system.

1.2 Transport in the TTL

Transport processes in the TTL are driven by the global-scale processes described in the previous section, as well as more local processes such as radiative heating, convection and horizontal exchange with the midlatitude lower stratosphere.
Figure 1.2 shows the different transport processes in the TTL as described in the overview paper of Fueglistaler et al. (2009). The processes are equal in both hemispheres although the strength of the processes varies between different seasons and (longitudinal) regions. As described in the previous section, Fueglistaler et al. (2009) define the TTL as the region between the level of clear sky zero radiative heating and the 425 K potential temperature level (the grey area in Figure 1.2). However, in this section all the different transport processes taking place between the level of main convective outflow and the 425 K level will be described, as these will be relevant for the following chapters. Only a short description will be given here, more details can be found in the relevant chapters.

1.2.1 Diabatic ascent

On the global scale, transport into the stratosphere is constrained by the Brewer-Dobson circulation. The Brewer-Dobson circulation is thought to be controlled by the non-local response to breaking gravity and Rossby waves in the extratropical stratosphere (Haynes et al., 1991). This wave-driven force induces a pumping action whereby air is sucked up from the tropical lowermost stratosphere, transported meridionally toward the poles, where it is pushed downward again. Due to the upward motion of air in the equatorial region the air will become colder than radiative equilibrium and this difference is compensated by radiative heating ('d' in Figure 1.2), whereas in the polar regions the air is radiatively cooled.
The radiative heating in the upper part of the TTL is a result of heating from the absorption of infrared radiation by ozone and carbon dioxide balanced by infrared cooling mostly from water vapor (Thuburn and Craig, 2002). The level at which the background clear sky radiative heating rate (Qclear) changes from a net cooling to a net heating is called the level of zero net radiative heating (LZRH) (Sherwood, 2000; Folkins et al., 2000). An air parcel has to be lifted to this level for the background atmospheric net radiative heating to lift it diabatically into the stratosphere. Although the velocity of this large-scale vertical advection by the Brewer Dobson circulation and radiative heating in the upper TTL is low, between 2 and 3 months for the upward transport from a potential temperature of 350 K up to 390 and 420 K, respectively (e.g. Andrews et al., 1999), this process is thought to dominate vertical transport above 15-17 km (Gettelman, 2009). The Brewer-Dobson circulation is confined to the winter season and strongest over the NH. Diabatic ascent rates are therefore faster during NH winter (Randel et al., 2007).

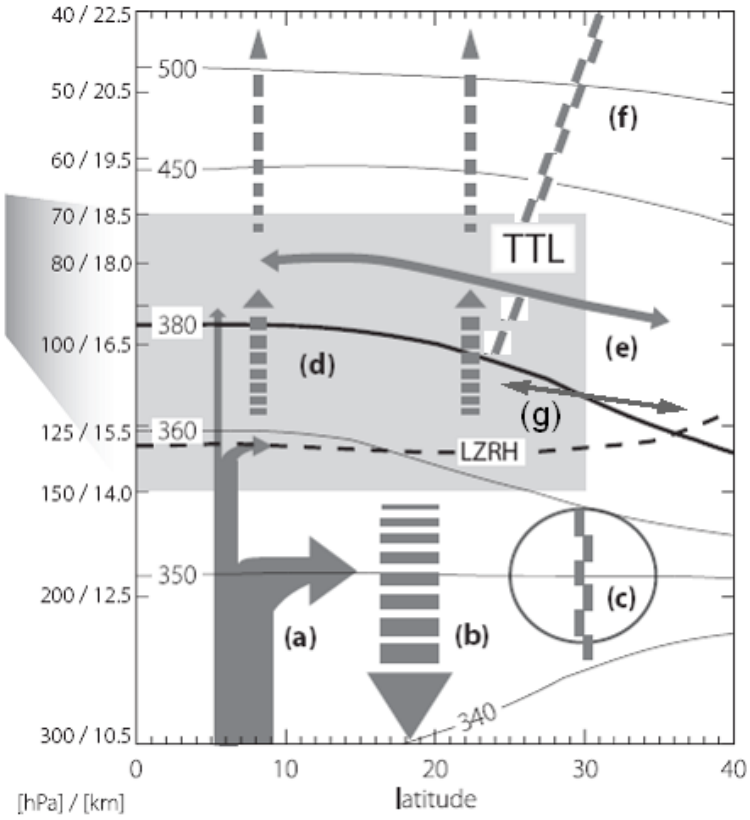

Figure 1.2: Overview of transport processes in the TTL. a) convection, b) radiative cooling (subsidence), c) subtropical jet, transport barrier, d) radiative heating (clear sky ascent), e) rapid meridional outflow, f) subtropical barrier, g) horizontal transport along the isentropes. Adapted from: Fueglistaler et al. (2009).

1.2.2 Convection

Convection (indicated by the 'a' in Figure 1.2) plays an important role in determining the thermodynamic and chemical properties of the TTL. It can provide a fast pathway for halogenated very short lived species and other boundary layer trace gases to reach the TTL and subsequently the stratosphere, where they could contribute to the depletion of ozone. The amount of very short lived species that can reach the stratosphere thus depends crucially on the convective mass flux into the TTL as well as the maximum altitude level that is reached by deep convection.
There are two mechanisms by which convection contributes to vertical transport through the TTL. The first is direct convective uplift to the level of neutral buoyancy, which is located at a potential temperature of at most 365 K (the large arrows of 'a')(Folkins et al., 2000). At this level the potential temperature first becomes equal to the highest equivalent potential temperatures[2] realized in the marine boundary layer. It is therefore near the maximum altitude an air parcel from the boundary layer can reach by undiluted, non overshooting ascent (Reid and Gage, 1981). This convection up to the level of neutral buoyancy is followed by slow diabatic ascent up to and across the tropopause as described in the previous section.
The second mechanism by which convection can influence the TTL, to much higher levels than its neutral buoyancy level, is irreversible mixing of air following dynamic overshooting (the smallest arrows of 'a') (Danielsen, 1982; Danielsen, 93; Sherwood, 2000). When an air parcel overshoots its level of neutral buoyancy it will be colder than the surrounding air and start descending back to its equilibrium level. However, when it entrains and mixes with warmer surrounding air it will come to rest at a warmer, higher equilibrium level, i.e. its potential temperature increases (Danielsen, 1982). The deepest overshooting of convection occurs predominantly above continental areas (Liu and Zipser, 2005; Zipser et al., 2006) and in large mesoscale convective systems (Rossow and Pearl, 2007), thereby providing a fast pathway for boundary layer air into the upper TTL or even the lower stratosphere. Although the existence of this mechanism is generally accepted, its importance at global scale is less clear.

1.2.3 Stratospheric isentropic inmixing into the TTL

Horizontally, the tropical tropopause layer is confined by the subtropical jets ('c' in Figure 1.2). The strength and position of these jets vary by season, with a strong jet close to the equator in the winter hemisphere and a weak, poleward shifted jet in the summer hemisphere. Haynes and Shuckburgh (2000) show that a strong subtropical jet forms an effective transport barrier for the meridional, isentropic transport between the lower part of the TTL and the extratropical lower stratosphere.
Isentropic, quasi-horizontal transport from the extra-tropical stratosphere ('g' in Figure 1.2) may play a significant role in determining the chemical (trace species) and

[2]The equivalent potential temperature is the potential temperature an air parcel would reach if all the water vapor in the parcel would condense and thereby remove all latent heat.

radiative character of the TTL (Gettelman and Forster, 2002). Analysis of previous aircraft measurements suggests that there may be significant quasi-isentropic transport from the lower mid-latitude stratosphere toward the tropics (Tuck et al., 2003; Marcy et al., 2007).

1.2.4 Isentropic mixing across the subtropical barrier

Except for its lowest part where isentropic mixing with the extratropics is still relatively strong, the tropical stratosphere is more or less isolated from the extratropical part of the stratosphere (Volk et al., 1996; Minschwaner et al., 1996). The subtropical barrier ('f' in Figure 1.2) constitutes a region of strong horizontal shear and maximum PV gradient along isentropes, thereby prohibiting fast isentropic mixing between the tropical stratosphere and mid-latitude stratosphere, especially in the winter hemisphere.

1.3 Use of tracer measurements

Satellite observations and 2-D or 3-D transport models provide a general picture of the TTL, but typically cannot well resolve spatial, in particular vertical, variations within the layer. Hence, highly resolved in situ measurements of trace gases and their use as tracers of atmospheric transport have proven extremely useful for studying the radiative, chemical, and dynamical properties of the TTL (e.g. Park et al., 2007). Tracers are compounds whose chemical lifetimes are longer than the timescales of the processes transporting them, such that their distributions are mainly determined by dynamics.
Since the troposphere and stratosphere have different chemical signatures, tracers can be used to study transport processes between these two regions. Stratospheric air for example, has high ozone and odd nitrogen mixing ratios, whereas tropospheric air has low ozone mixing ratios and large mixing ratios of anthropogenic trace gases such as carbon monoxide. Observations of the spatial distribution of tracers with different lifetimes and source or sink regions are used to investigate different transport processes.
Convection, for example, can best be studied using tracers that show a different mixing ratio in the boundary layer compared to the upper troposphere/lower stratosphere, for example ozone for maritime convection, and CO and CO_2 for continental convection. Low O_3 mixing ratios from the marine boundary layer will be found again at the level of main convective outflow in case of frequent convection. Overshooting convection may mix higher O_3 mixing ratios from the upper TTL with lower mixing ratios from the lower TTL and cause mixing lines in the so called "background profile", as will be described in the next section.
CO can be enhanced in the boundary layer due to biomass burning or polluted air masses. If these air masses with enhanced mixing ratios are found again in the TTL this is an indication of convection. CO_2 is a more complicated tracer, because of its variability in the boundary layer. Uptake of CO_2 during the day by vegetation reduces CO_2 mixing ratios in the boundary layer air, while pollution, biomass burning and release of CO_2 during the night will increase the mixing ratios in the boundary layer. The seasonal cycle of CO_2

however, can very well be used to trace the time since air left the troposphere, and will be used to define the slow ascent rates in Chapter 5.
Stratospheric intrusions can be identified by stratospheric tracers, like N_2O, CH_4 and CFC's, whose mixing ratios decrease in the stratosphere. If vertical stratospheric inmixing from the tropical stratosphere or horizontal inmixing along the isentropes from the extratropical stratosphere takes place, lower mixing ratios of N_2O, CH_4 and CFC's will be observed in the measured air masses.
Interhemispheric mixing can be identified by tracers that have a distinct interhemispheric gradient due to differences in emission rates in both hemispheres. Tracers used to study interhemispheric mixing are for example CO, SF_6 and H-1211 ($CBrClF_2$).

1.3.1 Vertical tracer profiles

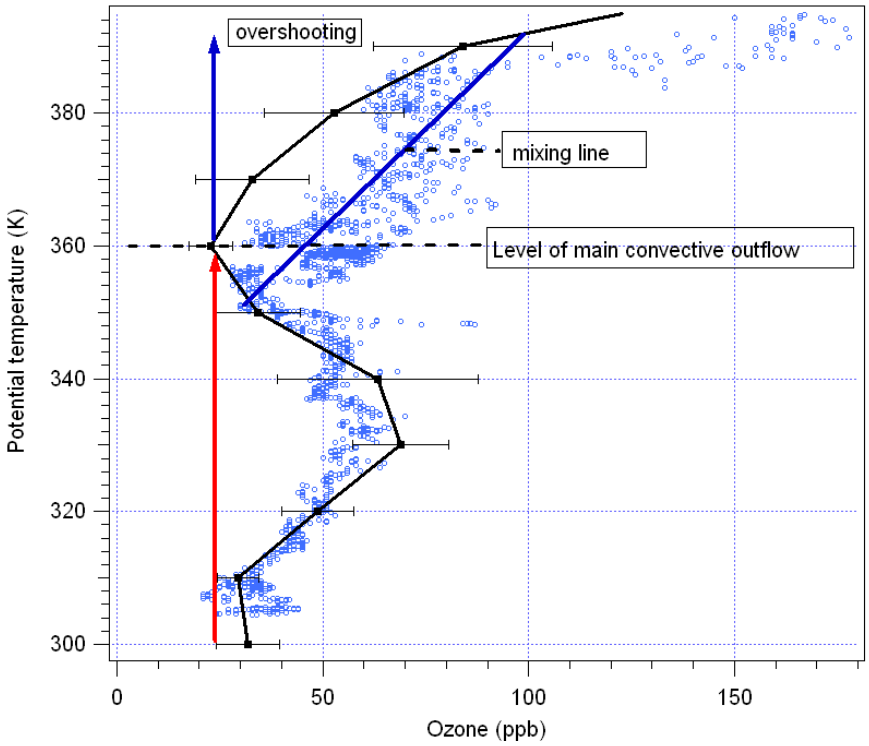

Figure 1.3: Example of vertical mixing in a vertical tracer profile. See text for explanation. Data: SCOUT-O3 flights 051130a (blue dots), 051123 and 051125 (black line)

An example of a vertical profile of a trace gas versus potential temperature, in this case O_3, is shown in Figure 1.3. In the boundary layer, ozone mixing ratios of 30 ppb are found, whereas in the free troposphere mixing ratios increase. Due to convection, the boundary layer air with a low mixing ratio is transported upwards to about 360 K, the level of main

convective outflow, where therefore again low mixing ratios are observed (red arrow). Above that level the ozone mixing ratios increase due to photochemical production of ozone.
Mixing events can be observed as a deviation of this "background profile". When mixing occurs, e.g. due to overshooting convection, air with a certain potential temperature level will first be transported to a level with another potential temperature (blue arrow). The air parcels will then start to travel back to their equilibrium level (at the original potential temperature), but during this transport the air will be mixed with the surrounding air and thereby increase or decrease its potential temperature and its mixing ratio of trace gases. The air parcels will therefore find a new equilibrium along a so called mixing line. In the example, the blue dots indicate a flight where mixing presumably has occurred, in contrast with the "background" profile in black. The air parcels overshoot their level of neutral buoyancy (which is equal to the level of main convective outflow, around 355-360 K), and are being transported into air masses with a potential temperature of 390 K in this case. The air then starts to descend again and obtains a new potential temperature and ozone mixing ratio due to mixing between 360 and 390 K along the mixing line (blue line). A note of caution however should be taken into account, as such a signature can also be caused by other processes (e.g. horizontal inmixing from the extratropical stratosphere, or influence of lightning and biomass burning). Whether vertical mixing or other processes have occurred has to be clarified by comparing signatures of different tracers with each other.

1.3.2 Tracer-tracer correlations

Different transport processes cannot only be seen in the vertical profile of the tracers but also in the correlation between the mixing ratios of two different tracers. In the stratosphere, the correlation between two long-lived tracers (tracer to tracer correlation) often turns out to be very compact (Plumb and Ko, 1992). The form and curvature of the correlation curve is dependent on the lifetimes of the tracers and on transport processes. Different atmospheric regions may exhibit different correlation curves between tracers. Variations from these correlations may be caused by mixing between the regions or by chemistry. Hence, tracer-to-tracer correlations are a particularly useful tool to study transport and mixing between the troposphere and the stratosphere (e.g. Hoor et al., 2002), or between the tropical and extratropical stratosphere (e.g. Volk et al., 1996).

Figure 1.4 shows an example of mixing (presumably following overshooting) seen in a tracer-tracer plot. Without mixing, the tracer-tracer relationship between a tropospheric (e.g. CO, CO_2) and a stratospheric tracer (e.g. O_3) will form an L-shape, with in the troposphere an almost constant mixing ratio of the stratospheric tracer and much variation in the mixing ratio of the tropospheric tracer (blue colours), and the opposite in upper TTL and the stratosphere (green/yellow/red colours). Thus, the tracer-tracer plot exhibits two distinct branches for the stratosphere and the troposphere, which meet in the lower TTL. If mixing takes place, a mixing line develops between the stratospheric and the tropospheric branch, mixing the air between these two regions. The higher the overshooting air reaches, and the more recent the mixing is, the clearer the mixing line can be observed. In the example air with a CO mixing ratio of around 130 ppb, ozone mixing ratio of 50 ppb, and a potential temperature of $\sim$350 K overshoots to a level with a potential temperature

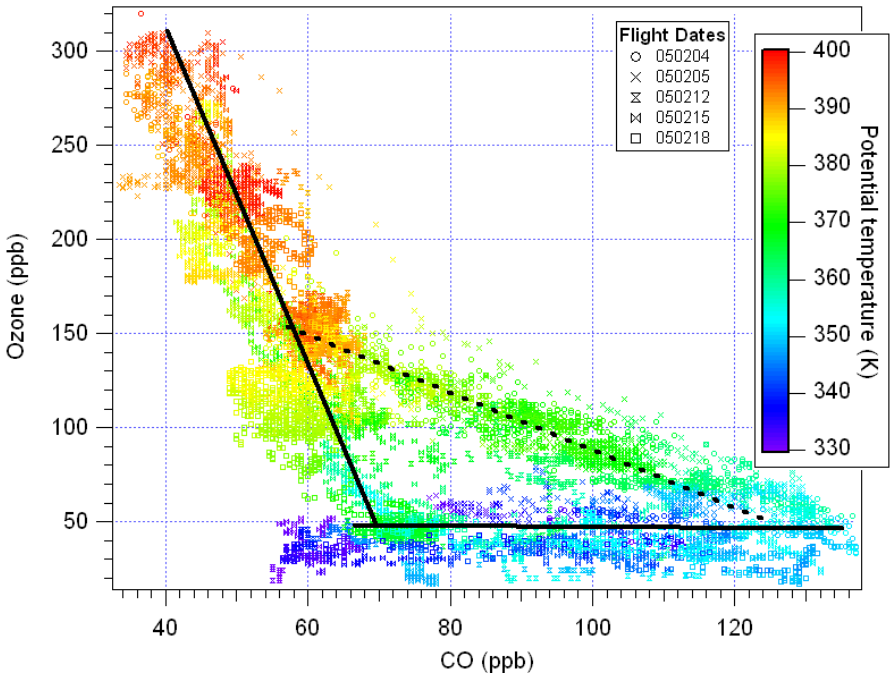

Figure 1.4: Example of mixing as seen in a tracer-tracer plot. See text for explanation. Data from TROCCINOX.

between 380-395 K, a CO mixing ratio of 60 ppb and an ozone mixing ratio of 150 ppb. When the air descends again it mixes with the surrounding air and finds a new equilibrium along the mixing line (dotted line). Again, as in the previous section, it has to be clarified with other tracers whether overshooting convection or other processes are causing this signature.

Chapter 2

Measurements

This dissertation project builds mainly on two tropical measurement campaigns that were conducted in 2005 and 2006 as part of this thesis with the High Altitude Gas AnalyzeR (HAGAR) on board the M55-Geophysica aircraft, but will also use data from three previous tropical field campaigns to gain better insight into the processes that take place in the TTL. Tracer data provided by two other instruments on board the aircraft are analysed along with the HAGAR data.
In this chapter a description of the M55 Geophysica (Section 2.1), the HAGAR instrument (Section 2.2) as well as a short description of the two other instruments, namely FOZAN and COLD will be given (Section 2.3). The aircraft campaigns performed with HAGAR on board the Geophysica are described in Section 2.4, with the two main tropical aircraft campaigns, namely the SCOUT-O3 and AMMA/SCOUT-O3 campaigns, described in Section 2.4.1 and 2.4.2, respectively. Section 2.4.3 will shortly describe the three previous aircraft campaigns which are used as comparison in the following analyses.

2.1 The M55-Geophysica

The M55 Geophysica is a Russian aircraft developed and operated by Myasishchev Design Bureau (MDB), Russia (Figure 2.1). It is the only truly stratospheric aircraft platform in Europe and has been successfully deployed during several campaigns since 1996. It has a good maneuverability at all altitudes and can reach an altitude of 21 km at a cruise speed of about 200 ms^{-1}. The maximum flight time is 6 hours, limiting the operative radius to approximately 3500 km. Its maximum payload is 1.5 tonnes. For scientific measurements, instruments can be installed in the different bays. On board are instruments from various European institutes which measure trace gases and aerosols in situ or by use of remote sensing techniques. The payload during the SCOUT-O3 and AMMA/SCOUT-O3 campaign is given in Table 2.1.
The aircraft transmits all flight parameters, as for example altitude, ambient air pressure and temperature, angles of bank and attack, latitude, longitude and Greenwich time every second via the UCSE (Unit for Connection to the M55 Geophysica airborne Scientific Equipment) device to the individual instruments, allowing one to perform high-quality analysis of the

results immediately after the flight and to compare the data easily with the data of all other scientific instruments onboard.

Figure 2.1: The M55 Geophysica (photo: M. Mahoney)

Table 2.1: Payload of the M55 Geophysica during the SCOUT-O3 and AMMA/SCOUT-O3 campaigns

Instrument	Institute	Measured parameter	Technique	Averaging time	Accuracy	Precision
MiPAS	MPI-Karlsruhe	H_2O, CH_4, N_2O, O_3, CFC-11, HNO_3 and others, clouds	Mid-IR emission limb sounder			
CRISTA-NF	FZJ	H_2O, O_3, CFC-11, HNO_3 and others, clouds	IR emission limb sounder	1 min per profile, 500m vert. Res.		
MARSCHALS[a]	RAL	H2O, CO, O3	MW limb sounder			
FOZAN	CNR	O_3	Dye chemiluminescence + ECC	1 s	0.01 ppmv	8%
FOX	DLR	O_3	UV absorption	2 s	5%	2%
FISH	FZJ	H_2O (total)	Lyman-alpha photo-fragment fluorescence	1 s	0.2 ppmv	4%
FLASH	CAO	H_2O (gas phase)	Lyman-alpha	8 s	0.2 ppmv	6%
ACH	CAO	H_2O (frost-point), H_20 (gas phase)	mirror hygrometer with digital feedback	minutes when H_2O is a few ppm		
SIOUX	DLR	NO, NOy, Particle NOy, HNO_3	Chemiluminescence,Au-converter+Subisokinetic inlet	1 s,1 s	10%, 12%	3%, 5%
HALOX	FZJ	ClO, BrO, $ClONO_2$	Chemical-conversion resonance fluorescence + thermal dissociation	20 s, 100 s	20%, 35%	5%, 20%
HAGAR	Univ. of Frankfurt	N_2O, CFC-12, CFC-11, H-1211, SF_6, CH_4 , H_2, CO_2	GC/ECD, IR absorption	90 s,5 s		0.7%, 0.6%, 0.8%, 1.6%, 2.2%, 0.8%, 1.1%, 0.3 ppm
ALTO	INOA	N_2O, CH_4	TDL	5 s,1 s	5%, 4%	2%, 1%
TDL[b]	INOA, Univ. of Groningen	CO, H_2O isotopes	TDL, Cavity-Ring-Down TDL	5s	5%	2%
COPAS (tail boom only)	Univ. of Mainz	Condensation nuclei (CN-total, CN-non-volatile)	2-channel CN counter, one inlet heated	1 s	10%	5%
FSSP3000 or FSSP100	Univ. of Mainz	Size speciated aerosols (0.4-40 x 10-6 m)	Laser-particle spectrometer	20 s	20%	10%
Cloud Particle Image	Univ. of Mainz	Particles 100 x 10-6 m				
MAS Aerosol optical properties	CNR	multi wavelength scattering	10 s	5%	5%	
MAL up/MAL down	Obs. Neuchatel	Remote Aerosol Profile (2km from aircraft altitude)	microjoule -lidar	30-120 s	10%	10%
WAS	MPI-Heidelberg	Trace gas isotopes,Water Isotopes,VSLS	whole air sampler			
TDC Rosemount probe	CAO	Temperature, horizontal wind	PT100, 5 hole probe	0.1 s,0.1 s	0.5 K, 1 m/s	0.1 K, 0.1 m/s
MTP[b]	JPL	Vert. Profile of temperature and potential temperature	Microwave passive sensor			

[a] only on board during SCOUT-O3
[b] only on board during AMMA/SCOUT-O3

2.2 The High Altitude Gas Analyzer (HAGAR)

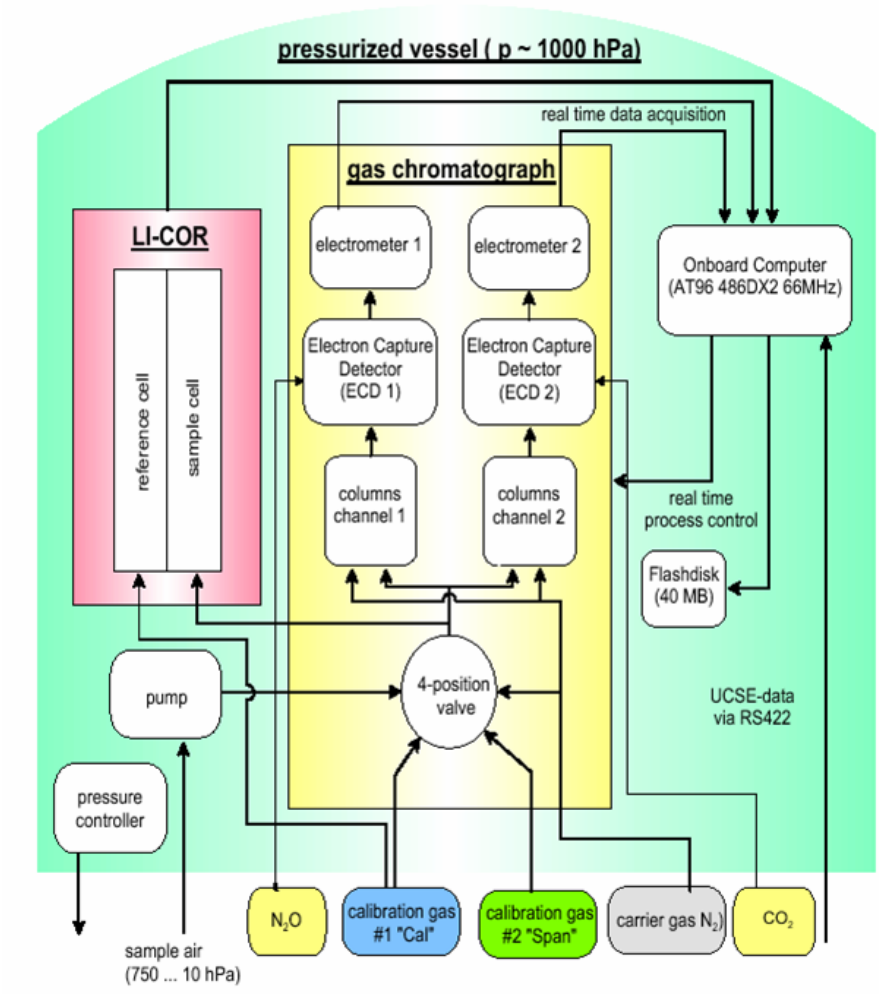

Figure 2.2: Principal scheme of the HAGAR instrument. From Werner (2007).

The Institute for Atmospheric and Environmental Sciences at the University of Frankfurt developed the High Altitude Gas Analyzer (HAGAR), an instrument for simultaneous high resolution in situ measurements of long-lived trace gases in the stratosphere in 1998. HAGAR is a two-channel in situ gas chromatograph (GC) that is combined with a CO_2 sensor (LI-COR 6251).
Only a short overview of the instrument and the processing of the data is given here. Detailed descriptions about the measurement of trace gases with gas chromatography, the technical characteristics of HAGAR and the laboratory calibrations are given in Riediger (2000), Strunk (1999), and Werner (2007). Details about the in-flight calibrations, and the

processing schemes of the chromatograms can be found in Ivanova (2007).
Figure 2.2 shows the principal scheme of the instrument. The instrument is completely pressurized and temperature controlled and operates fully automatically. In the configuration used in 2005 and 2006 it weighs about 85 kg (including the mounting frame and gas bottles) and has a cylindrical shape with 45 cm diameter and 55 cm height. Sample air is pumped into the instrument and transported with the carrier gas N_2. The airstream is divided between the CO_2-LICOR and the two gas chromatographic channels. In the first GC channel CH_4, SF_6 and H_2 are measured, the second channel measures N_2O, CFC-12, CFC-11 and H-1211, both with a time resolution of 90 seconds. Chromatograms are obtained with electron capture detectors (ECD), which measure the change in current due to the capture of electrons by electronegative molecules. The passing of a substance is recognized as a peak in the chromatogram and the area below the peak or the peak height is proportional to the mixing ratio of a molecule in the air sample.
To measure substances that do not capture electrons directly (for example CH_4 and N_2O), a doping gas is applied that leads to electron capture in a couple of ion chain reactions. The first channel is doped with N_2O and the second channel with CO_2.
The CO_2 sensor achieves a time resolution of 5 seconds using non-dispersive infrared absorption (NDIR). CO_2 concentrations are calculated from the difference between the absorption of the sample air and the reference air (CAL gas). In order to avoid interference with water vapour, which causes pressure broadening of absorption lines, the sample air passes through a desiccant column filled with magnesium perchlorate before entering the CO_2-analyzer.
In-flights calibration is achieved using two different calibration gases, one with mixing ratios of tropospheric air (CAL), and one with mixing ratios of about 50-60% (for CO_2: ∼95%) of tropospheric values (SPAN), that are alternatively injected after every fifth injection of sample air (i.e. every 7.5 minutes). They account for drifts in the detector sensitivity, for example due to small temperature and pressure variations of the detectors, which mostly happen during ascent and descent when the instrument's environment changes rapidly. A possible fluctuation of the mixing ratios in the CAL and SPAN 2L gas bottles itself is checked by laboratory calibrations between the flights. A table of CAL and SPAN values for all species is given in Appendix A.
The final air mixing ratios are calculated from the response of the air sample and the response of the two calibration gases. The relation between the detector response and the mixing ratio of a substance is described by a polynomial of at least second order. This relation is determined in the laboratory by measuring a series of standard gases covering the whole range of mixing ratios from the tropospheric background to zero. These standard gases are accurately calibrated against a NOAA/CMDL[1] standard.
Finally, the peaks in the chromatogram are smoothed with a Savitzky- Golay filter (cf. Werner, 2007) and integrated with either a tangent baseline fitted below the peak (N_2O, CFC-12, CFC-11, SF_6, H_2) or a Gaussian peak fit (H1211 and CH_4)(cf. Ivanova (2007)). For the CO_2 data a third order polynomial function is used to calculate the mixing ratio from the voltage output of the sample cell.

[1]National Oceanic and Atmospheric Administration/Climate Monitoring and Diagnostics Laboratory, USA

The precision of the single measurements is calculated using the local variance of the CAL and SPAN measurements (cf. Werner, 2007). Accuracies of the HAGAR measurements are limited by the precision and are thus only slightly larger than these precision values. The mean precisions for all flights of the SCOUT-O3 and AMMA/SCOUT-O3 campaign are given in the sections describing the campaigns (Section 2.4.1 and 2.4.2).
Over 100 flights were absolved with HAGAR since 1998, therefore providing a unique data set of tracer data in different regions and seasons over both hemispheres.

2.3 The Cryogenically Operated Laser Diode (COLD) and the Fast Ozone Analyzer (FOZAN)

Additionally to the tracer and CO_2 data measured by HAGAR the CO data of the COLD instrument and the O_3 data measured by the FOZAN instrument will be used in the analysis.
The Cryogenically Operated Laser Diode (COLD) was developed by the Italian Institute INOA (Istituto Nazionale di Ottica Applica). It was realized as a general purpose instrument for airborne measurement of stratospheric trace gases and different gases can be measured by changing the laser source or even the laser operation region only. In recent years it was optimized for in situ CO measurements in the UT/LS and since 2005 it was successfully deployed during three tropical campaigns: TROCCINOX-2 (Tropical Convection Cirrus and Nitrogen Oxides Experiment) in Brazil, SCOUT-O3 (Stratospheric Climate Links with Emphasis on the Upper Troposphere and Lower Stratosphere) in Australia and AMMA/SCOUT-O3 in Burkina Faso. The instrument is currently installed in the central bay (bay 2) of the unpressurized fuselage of the M55 Geophysica, and it operates autonomously for the full flight. The instrument has a time resolution of 4 s, and measures with a precision of 1% and accuracy of 6-9%. Detailed information can be found in Viciani et al. (2008).
Ozone was measured with the Fast Ozone ANalyzer (FOZAN). It was developed and manufactured at the Central Aerological Observatory (CAO) in collaboration with the Italian CNR Institute for Atmospheric and Ocean Studies (ISAO). The fast-response (< 1 s) ozonometer is designed for operation in a wide range of analyzed air pressures (1100-30 mbar, 0-22 km) and temperatures (from -95 to +40 degrees Celsius). Its measured concentration range is 10-500 $\mu g/m^3$. The device has a built-in reference ozone generator (relative error of $< 6\%$) allowing one to autocalibrate the device in flight. The accuracy of the instrument is 10%. Detailed information can be found in Ulanovsky et al. (2001).

2.4 Measurement campaigns

2.4.1 SCOUT-O3

The SCOUT-O3 (Stratosphere-Climate Links with Emphasis on the Upper Troposphere and Lower Stratosphere) campaign took place based in Darwin, Australia in November/December 2005. Darwin (12°S, 130°E) is located at the northern tip of Australia and at the southern border of the so called “Tropical Warm Pool”. This region is thought to be

most important in troposphere-to-stratosphere transport (TST) (Fueglistaler et al., 2004). The campaign was part of the larger SCOUT-O3 project. SCOUT-O3 is a European Commission Integrated Project with 70 partner institutions and over 400 scientists involved from 19 countries. The five and a half year project commenced on 1 May 2004 and ended 31 August 2009. The overall aim of the SCOUT-O3 project is to provide predictions about the evolution of the coupled chemistry/climate system, with emphasis on ozone change in the lower stratosphere and the associated UV and climate impact, in order to provide vital information for society and public use (see www.ozone-sec.ch.cam.ac.uk/scout_o3).
The Darwin campaign was intended to feed the following three aspects of this overarching aim (see also Vaughan et al., 2008):

1) to understand the tropical mechanisms of troposphere- to-stratosphere transport (TST),
2) to understand past changes in stratospheric trace gas concentrations and humidity, and
3) to enable a prediction of future stratospheric trace gas concentrations and humidity.

This led to the following objectives for the SCOUT-O3 Darwin experiment:

i) How does air undergo TST?
ii) Where is air transported from the troposphere to the stratosphere?
iii) How is air processed during its passage through the TTL and what is its composition?
iv) How is air dehydrated during TST?
v) How well do numerical weather prediction models represent mesoscale and large-scale transport processes in the tropical Pacific/Maritime Continent region?

The campaign took place during the pre-monsoon, when a mesoscale deep convective system colloquially known as “Hector” develops almost daily over the Tiwi Islands some 100 km north of Darwin (Keenan and Carbone, 1992). It is triggered by island heating and can reach up close to the tropopause. The high predictability of the Hector system was a major motivation for conducting the SCOUT-O3 campaign in Darwin.
The campaign included both survey flights designed to sample the background TTL and flights sampling the plume, turret, and outflow of the deep convective cell 'Hector'. A total of eight (mostly northbound) local flights were conducted within the TTL and the lower stratosphere (up to 20 km). Twelve transfer flights were made between Oberpfaffenhofen (Germany) and Darwin. An overview of the flights is given in Table 2.2. A map of the flight paths of the local flights is given in Figure 2.3. More information about the SCOUT-O3 field campaign and the meteorological conditions during the campaign can be found in Vaughan et al. (2008) and Brunner et al. (2009).

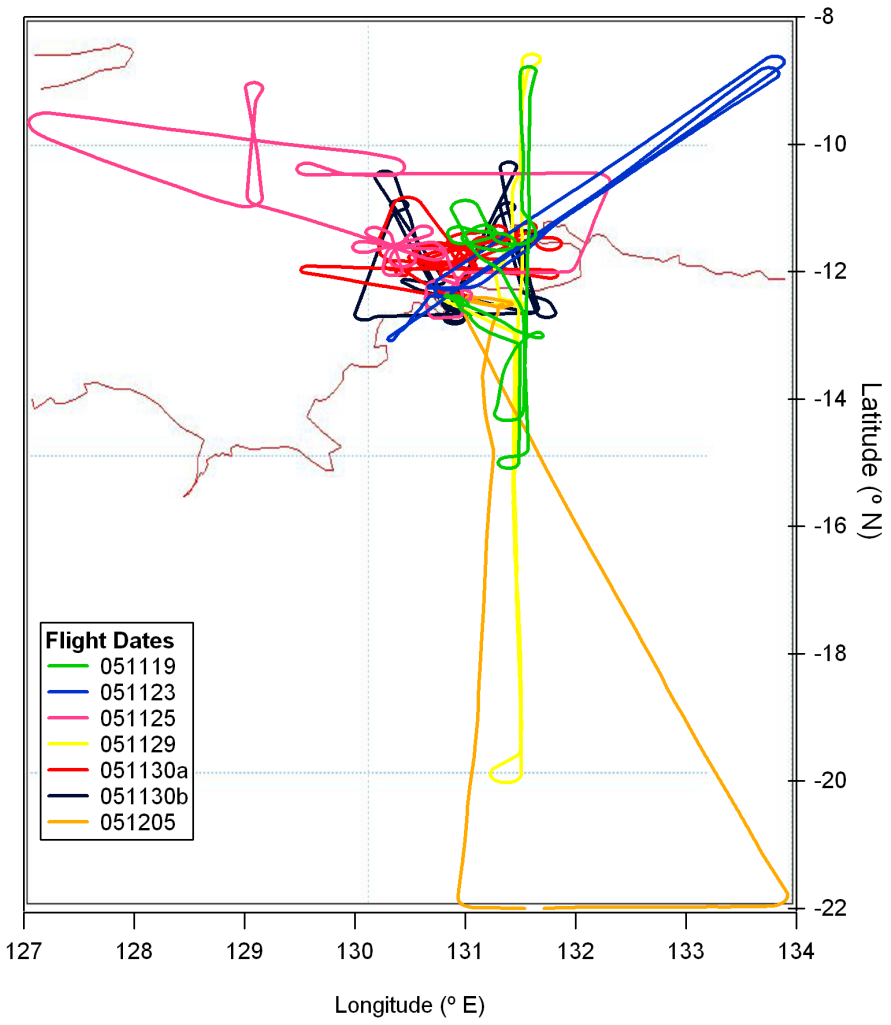

Figure 2.3: SCOUT-O3 local flight paths

Table 2.2: Overview of flights during the SCOUT-O3 campaign

Date of flight	Scientific goals
31-10-2005	Test flight: Oberpfaffenhofen
04a-11-2005	Transfer flight: Oberpfaffenhofen - Larnaca
04b-11-2005	Transfer flight: Larnaca - Dubai
08-11-2005	Transfer flight: Dubai - Hyderabad
09-11-2005	Transfer flight: Hyderabad - U-Tapao
11-11-2005	Transfer flight: U-Tapao - Brunei
12-11-2005	Transfer flight: Brunei - Darwin
16-11-2005	Hector, upwind survey, anvil
19-11-2005	Cirrus, Hector
23-11-2005	TTL survey
25-11-2005	Cirrus, late Hector
29-11-2005	Mesoscale convective systems, north-south profile
30a-11-2005	Hector
30b-11-2005	post Hector, cirrus
05-12-2005	Envisat satellite validation
10a-12-2005	Transfer flight: Darwin - Brunei
10b-12-2005	Transfer flight: Brunei - U-Tapao
13-12-2005	Transfer flight: U-Tapao - Hyderabad
14-12-2005	Transfer flight: Hyderabad - Dubai
16-12-2005	Transfer flight: Dubai - Larnaca
17-12-2005	Transfer flight: Larnaca - Oberpfaffenhofen

HAGAR performance during SCOUT-O3

An extensive data set of the TTL was collected during the SCOUT-O3 campaign. However, some problems occurred which are listed below:

- Just before the SCOUT-O3 campaign one of the two Siemens ECDs broke, which made it necessary to build in the spare ECD. To avoid acoustic oscillations in Channel 1 the ECDs were 'crossed', i.e. the column which normally is connected to ECD 1 was connected to ECD 2 and vice versa. This situation was maintained until 5 December. A summary of the performance of the two ECDs is given here:

  ECD 1:

  - Used for channel 2 up to flight 051130b.
  - Showed bad reproducibility starting 051128 (particularly bad during 051130a).
  - Switched back to channel 1 before 051205 (also replacing electrical cables and inlet fitting).
  - Was partially saturated during the flight of 051205, and erratic and very noisy during the other parts of the flight. No useful data were obtained.
  - After the 051205 flight the ECD was completely dead (saturated baseline) and could not be revived. This was possibly caused by an electrical problem.

  ECD 2:

  - Used for channel 1 up to 1130b.
  - Had to be flown always without N_2O doping to prevent a very high baseline (up to saturation).
  - An electrical problem caused a saturated baseline from 051119 to 051125, therefore no data were recorded. This was solved by replacing the disintegrated electrical contacts with new cables before 051128.
  - Still no data were recorded for 051128 and 051129 as the electrical contact apparently interrupted when the temperature of the ECD reached 347°C (the ECD saturated during flight). This was solved thereafter by keeping T at 345°C.
  - The 051130a signal goes below 0 after 1 h. The reason for this is unknown.
  - After H_2-bakeout, the ECD worked well for flight 051130b.
  - Switched back to Channel 2 before 051205, worked well for 051205 and rest of the campaign (with now T=340°C to be on the safe side).

- Part of these ECD problems was probably caused by a thunderstorm on November 14. The huge thunderstorm on this day crossed Darwin and rain leaked through the roof of the hangar. Because the vessel of HAGAR was open at that time, water dropped into HAGAR and different parts of the instrument had to be build apart and be dried before the instrument was able to work again. Other problems because of this thunderstorm were:

  - The heater of the vessel had to be off for the rest of the campaign to prevent a short.
  - The mass flow controller of the LI-COR broke down (likely because of an electrical short) just before the flight on 19 November and was removed on November 21. From 28 November a mass flow meter was installed to at least measure the Licor sample flow.

- Other problems:

  - There was an N_2O contamination during the test flight. This has been corrected by using the Cal-to-pump measurements as described in Werner (2007).
  - During the transfer flight on November 9 the carrier gas ran out and only one hour of data are available.
  - During the first local flight on 16 November no data were recorded by HAGAR due to a program hangup before the start (due to improper program start configuration).
  - The CO_2 signal showed some low-frequency oscillations and drift during almost all flights, which could not be reproduced in the laboratory and therefore could not be corrected. As a result of this, the mixing ratios during ascent are approximately 1 ppm higher than during descent.

The precisions of the HAGAR instrument during the SCOUT-O3 campaign is given in Table 2.3.

Table 2.3: Precision of flights during the SCOUT-O3 campaign in percent (CO_2: ppm).

Flight date	N2O	CFC-12	CFC-11	H-1211	SF_6	CH_4	H_2	CO_2
20051031	1.35	1.21	1.91	1.39	2.81	not measured (no doping applied)		0.23 ppm
20051104a	1.20	1.52	0.98	5.48	3.15			0.23 ppm
20051104b	1.12	0.50	0.76	1.66	1.88			0.20 ppm
20051108	0.73	0.64	0.44	1.34	2.27			0.23 ppm
20051109	1.88	0.83	1.26	1.31	3.43			0.19 ppm
20051111	0.59	0.40	0.62	1.58	2.62			0.22 ppm
20051112	1.11	0.68	0.51	1.18	3.44			0.19 ppm
20051116	no data recorded (software error)							
20051119	0.83	0.78	1.12	1.05	ECD1 failure	not measured (no doping applied)		0.50 ppm
20051123	1.24	1.13	1.31	1.63				0.26 ppm
20051125	0.44	0.36	0.54	1.88				0.50 ppm
20051128	5.95	3.13	4.28	8.56				0.23 ppm
20051129	2.05	2.00	1.86	9.97				0.24 ppm
20051130a	6.54	3.61	6.63	12.63				0.29 ppm
20051130b	1.53	1.41	1.65	5.60	1.27			0.26 ppm
20051205	0.49	0.30	0.44	3.08	ECD1 failure			0.25 ppm
20051210a	0.38	0.33	0.39	1.97				0.25 ppm
20051210b	0.27	0.25	0.32	1.17				0.24 ppm
20051213	0.23	0.20	0.26	1.47				0.22 ppm
20051214	no data							
20051216								
20051217								

2.4.2 AMMA/SCOUT-O3

In July/August 2006 another tropical field campaign, the AMMA/SCOUT-O3 campaign (http://amma.igf.fuw.edu.pl/) took place over West Africa, based in Ouagadougou (12°N, 1°W), Burkina Faso, within the frame of the international AMMA project (African Monsoon Multidisciplinary Analysis).
The AMMA project was set up by an international scientific group and is funded by a large number of agencies, especially from France, UK, US and Africa. Scientists from more than 20 countries, representing more than 40 national and pan-national agencies are involved in this multi-year project.
The main three goals of AMMA are:

- to improve our understanding of the West African Monsoon and its influence on the physical, chemical and biological environment, regionally and globally.
- to provide the underpinning science that relates variability of the West African Monsoon to issues of health, water resources, food security and demography for West African nations and defining and implementing relevant monitoring and prediction strategies.
- to ensure that the multidisciplinary research carried out in AMMA is effectively integrated with prediction and decision making activity.

To achieve these objectives model and data assimilation, field campaigns, satellite remote sensing and long-term collection of atmospheric and oceanic data are performed. The field campaigns are divided into three periods: the long term observing period (LOP)(2002-2010) to study interannual-to-decadal variability of the West African Monsoon, the enhanced observing period (EOP)(2005-2007) to study annual cycles and to serve as a link between the LOP and the SOPs, and the special observing periods (SOPs) to study specific processes and weather systems at various key stages during the rainy season in the summer of 2006.
Within this frame, the AMMA and SCOUT-O3 European projects together funded a specific campaign addressing the study of dynamical, microphysical and chemical processes in the TTL. The AMMA/SCOUT-O3 campaign took place during the special observing period in 2006 between 31 July and 17 August. During this field campaign, 5 aircraft, stratospheric balloons and a large number of sondes performed intensive measurements in the wet phase of the monsoon season, from the troposphere to the lower stratosphere. The flights took place from Niamey (Niger) and Ouagadougou (Burkina Faso).
Since Africa is one of the main sources of biomass burning emissions and the main source of atmospheric dust aerosol, one of the key objectives of AMMA/SCOUT-O3 was also to investigate (1) the convective outflow dynamics; (2) the fate of the chemical species and water vapour injected into the upper troposphere by MCS; (3) the impact on the global scale. In addition, the AMMA/SCOUT-O3 campaign was a unique opportunity to validate the upper-troposphere/lower-stratosphere aerosol distribution provided by the CALIPSO satellite lidar. Specifically, the campaign was designed to provide observations to answer the following key questions:

- Do continental mesoscale convective systems penetrate into the stratosphere?
- In how far is this overshooting impacted by the diurnal variation of convection?
- How much moisture could be lifted above the tropopause?
- Are cirrus clouds forming at the cold point?
- What is the composition of lifted air?
- Could chemically active Very Short Lived Species (VSLS) be transported into the lower stratosphere by this mechanism?
- How much of NOx produced by lightning could also be present in the TTL?
- What is the impact, at global scales, of chemical species and water vapour uplifted by convection over West Africa?

The Geophysica, based in Ouagadougou, performed a total of nine flights with measurements from the free troposphere up to the tropical lower stratosphere at 20 kilometers. Four transfer flights were made between Verona (Italy), Marrakech (Morocco) and Ouagadougou (Burkina Faso). Five local flights between 4°N and 17°N and 3°W and 3°E were made to study mesoscale convective systems (MCS), long range transport, and for satellite validation. A brief overview of the flights is given in Table 2.4. The flight paths of the local flights are displayed in Figure 2.4. A more extended overview of the flights and the Geophysica campaign can be found in Cairo et al. (2009).
More detailed information about AMMA in general can be found in Redelsperger et al. (2006). An overview of the summer monsoon over West-Africa in 2006 can be found in Janicot et al. (2008).

Table 2.4: Overview of flights during AMMA/SCOUT-O3.

Date of flight	Time (UTC)	Scientific goals
29-07-2006	5.50-9:32	Test Flight
31-07-2006	9:15-13:15	Transfer flight-UTLS profile
01-08-2006	10:59-14:59	Transfer flight-UTLS profile
04-08-2006	8:26-12:13	Long range transport
07-08-2006	12:15-16:07	MCS close up
08-08-2006	11:46- 15:31	CALIPSO satellite validation
11-08-2006	14:44- 18:22	MCS aged outflow
13-08-2006	12:50- 16:23	Long range transport
16-08-2006	13:27-15:16	Transfer flight-UTLS profile
17-08-2006	4:10- 7:51	Transfer flight-UTLS profile

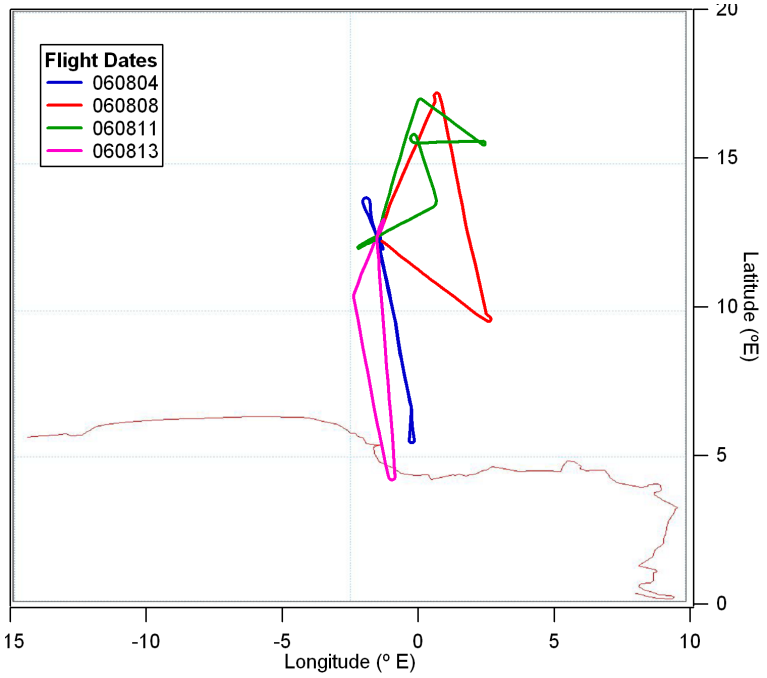

Figure 2.4: AMMA/SCOUT-O3 local flight paths.

HAGAR performance during AMMA/SCOUT-O3.

In between the SCOUT-O3 and the AMMA/SCOUT-O3 campaigns the Siemens ECD of channel 1 was exchanged for a Shimadzu ECD (May 2006) with the same configuration as during the EUPLEX campaign (Werner, 2007). It was doped with 0.5% N_2O in N_2 at a pressure of 5.5 bar to yield a (calculated) N_2O doping mixing ratio of ∼70 ppb in the ECD, similar to EUPLEX as well (Werner, 2007).
In general HAGAR performed very well during the AMMA/SCOUT-O3 campaign. Only few problems were encountered which are listed here:

- During the transfer flights and the first two local flights there were frequent switching problems between the SPAN, CAL and air samples for channel 2. Due to this problem there are many data gaps and a somewhat lower precision on 4 August for channel 2. After replacing a broken Valvo rotor adapter this problem was solved.
- During the second transfer flight and the first local flight the baseline of channel 1 was found to be too high, causing low SF_6 precisions.
- A potential bias in the CO_2 signal may have occurred in the first four flights due to the mass flow meter after the LICOR sample cell (which replaced the broken MFC of the SCOUT-O3 campaign). This flow meter caused a flow restriction (although small) at the cell exit and caused the sample cell pressure to become dependent on the sample flow. A potential bias occurred whenever the sample flow during measurement deviated much from the flow during the calibration. It took multiple flights before the right pump set pressure (975 mb) was found at which the blank-to-pump flow matched this of Cal and Span. The possible bias was found to be max. 0.5 ppm during the test flight, decreasing to max. 0.1 ppm during the flight of 31 July and to be negligible during the flights on 1 and 4 August.
- Due to a program hangup during start no data were measured on 7 August.
- During the flight of 11 August a sudden baseline increase and sensitivity loss of channel 1 was observed after about 50 minutes. This resulted in a lower precision for SF_6, H_2 and CH_4.
- The N_2O signal on Channel 2 was contaminated by N_2O in the vessel during the flights of 1 and 17 August. This has been corrected by using the Cal-to-pump measurements as described in Werner (2007).

The precisions of the HAGAR instrument during the flights of the AMMA/SCOUT-O3 campaign is given in Table 2.5.

Table 2.5: Precision of flights during the AMMA/SCOUT-O3 campaign in percent (CO_2: ppm).

Flight date	N_2O	CFC-12	CFC-11	H-1211	SF_6	CH_4	H_2	CO_2
20060729	0.46	0.53	1.08	1.40	1.86	0.74	0.94	0.32 ppm
20060731	0.34	0.49	1.81	1.96	1.42	0.34	1.45	0.30 ppm
20060801	0.44	1.19	0.54	1.05	2.33	0.69	0.68	0.30 ppm
20060804	1.31	1.07	0.88	1.27	2.11	0.91	1.22	0.31 ppm
20060807	no data recorded (software error)							
20060808	0.30	0.28	0.39	0.85	1.87	0.26	1.04	0.31 ppm
20060811	0.52	0.39	0.45	2.89	2.93	2.20	4.63	0.30 ppm
20060813	0.51	0.46	1.02	1.11	2.02	0.75	0.93	0.30 ppm
20060816	0.38	0.52	0.97	1.42	1.64	0.59	0.63	0.30 ppm
20060817	0.39	0.34	0.84	1.81	2.20	1.01	1.68	0.30 ppm

2.4.3 TROCCINOX, APE-THESEO and ASHOE MAESA

The TROCCINOX campaign (Tropical Convection and Nitrogen Oxides Experiment) took place in February/March 2005 from Aracatuba, Brazil (21°S, 50°W). The main goals of the TROCCINOX project were to investigate the impact of tropical deep convection on the distribution and the sources of trace gases, cloud and aerosol particles, focusing on processes in the upper troposphere and lower stratosphere. A total of 16 flights, including 8 transfer flights between Oberpfaffenhofen, Germany, and Aracatuba were performed with the M55 Geophysica and the DLR Falcon.
The APE-THESEO campaign was held from 15 February to 15 March 1999 from the Seychelles in the western Indian Ocean. APE-THESEO stands for 'Airborne Platform for Earth observation - (contribution to) the Third European Stratospheric Experiment on Ozone'. The campaign aimed to study processes controlling the low water content of the stratosphere, including the mechanisms of cloud formation in the tropical tropopause region, and transport processes, studied using measurements of long-lived trace gases and ozone. Again the M55 Geophysica was operated together with the DLR Falcon, and performed a total of seven local flights from Mahe, Seychelles (4°S and 55°E). An overview of the campaign is given by Stefanutti et al. (2004).
The Airborne Southern Hemisphere Ozone Experiment (ASHOE) was designed to examine the causes of ozone loss in the Southern Hemisphere lower stratosphere and to investigate how the loss is related to polar, mid-latitude, and tropical processes. ASHOE was conducted together with the MAESA campaign (Measurements for Assessing the Effects of Stratospheric Aircraft), whose focus was to provide information about stratospheric photochemistry and transport for assessing the potential environmental effects of stratospheric aircraft. These combined objectives were met by a series of flights of the National Aeronautics and Space Administration (NASA) ER-2 high-altitude research aircraft from Christchurch, New Zealand, and on transfer flights from Moffett Field, California, to Christchurch via Hawaii and Fiji. ASHOE/MAESA took place in four phases through the Antarctic winter of 1994: late March to early April, late May to early June, late July to early August, and October. The tropical flights were made during transfer in March and October 1994. An overview of the campaign is given by Tuck et al. (1997).

Chapter 3

Tracer measurements in the tropical tropopause layer during the AMMA/SCOUT-O3 aircraft campaign

This chapter is based on: Homan, C.D., Volk, C.M., Kuhn, A.C., Werner, A., Baehr, J., Viciani, S., Ulanovski, A., and Ravegnani, F.: Tracer measurements in the tropical tropopause layer during the AMMA/SCOUT-O3 aircraft campaign, Atmos. Chem. Phys., 10, 3615-3627, 2010.

3.1 Introduction

Over the last decade various field campaigns have taken place to obtain in situ observations of the TTL and get more insight into the different processes taking place in this layer of the atmosphere. Several European campaigns were conducted with the Russian M55-Geophysica high-altitude aircraft. Cairo et al. (2008) show with observations made above a tropical cyclone during the APE-THESEO campaign that cyclones may induce horizontal stirring of the lower stratosphere, possibly promoting irreversible entrainment of midlatitude stratospheric air into the tropical zone. Konopka et al. (2007) show with a comparison of the in situ measurements made during TROCCINOX of ozone, water vapour, NO, NOy, CH_4 and CO with CLaMS model simulations that vertical mixing, mainly driven by the vertical shear in the tropical flanks of the subtropical jets and, to some extent, in the outflow regions of large-scale convection, offers an explanation for the upward transport of trace species from the main convective outflow at around 350 K up to the tropical tropopause around 380 K. Schiller et al. (2009) found highly localised layers of enhanced water vapour up to 420 K which could be traced to direct injection by overshooting turrets during the SCOUT-O3 campaign.

In situ measurements of tracers in the TTL have also been conducted using the NASA ER-2 and WB-57F aircraft. Marcy et al. (2007) have presented measurements of HCL, O_3, HNO_3, H_2O, CO, CO_2 and CH_3Cl in the tropical upper troposphere and lower stratosphere (UT/LS) during the Pre-AVE campaigns over Costa Rica in January 2004. They infer that a significant amount of stratospheric air and O_3 were present in the TTL, making it distinct from both the stratosphere and the remainder of the troposphere. Park et al. (2007a) have presented CO_2 measurements during the Pre-AVE, CR-AVE and TWP-ICE campaign in Costa Rica and Australia. They suggest that the TTL is composed of two layers, the lower TTL which is subject to significant inputs of convective outflow, and the upper TTL, where air ascends slowly and ages uniformly. They calculate a mean age of air entering the lower stratosphere of 26 days during NH winter. Tuck et al. (2003) have analyzed tracers and thermodynamical data from various ER-2 and WB57F aircraft campaigns and documented significant transport from the lower midlatitudes stratosphere toward the tropics, coming to the conclusion that the characteristics of the TTL are determined by a trade-off between subtropical jet stream dynamics and inner tropical ascent via deep convection.
Until now, in situ measurements of tracers throughout the TTL have not been reported during NH summer and none have been made above the African continent. However, this region may play an important role in troposphere-to-stratosphere transport. Ricaud et al. (2007) present satellite data of N_2O, CH_4 and CO and radar data in the tropical tropopause region during NH spring and suggest that rapid uplift over land convective regions, in particular over Africa, may be the dominant process of troposphere-to-stratosphere exchange. However, this view is in contrast to a number of other studies showing that the African region is not an important contributor to troposphere-to-stratosphere transport compared in particular to Southeast Asia and the Western Pacific (Fueglistaler et al., 2004; Berthet et al., 2007; Barret et al., 2008, Park et al., 2007b).

In this chapter in situ tracer data obtained on board the M55 Geophysica aircraft during the AMMA/SCOUT-O3 project are analysed to study the principal transport processes that control the chemical composition of the TTL and the lower tropical stratosphere above West-Africa. Vertical profiles and correlations between the various species, serving as stratospheric tracers, as boundary layer tracers, or age-of-air tracers will be used to contrast observations of the background TTL with convectively influenced air, to diagnose irreversible mixing of convectively overshooting air with the background TTL, to assess isentropic mixing across the subtropical tropopause and to study the morphology of the stratospheric subtropical transport barrier.

3.2 Analysis of main transport processes

The results of the analysis of the different transport processes occurring in the summer TTL over West-Africa will be discussed in the following sections. Section 3.2.1 describes both main convective outflow as well as overshooting convection, Section 3.2.2 describes isentropic stratospheric inmixing across the subtropical tropopause and Section 3.2.3 describes isentropic mixing across the subtropical barrier in the lower stratosphere.

3.2.1 Convection

The AMMA/SCOUT-O3 campaign took place at the peak of the monsoon period when many mesoscale convective systems are generated in the West-African region and travel to the west. Rossow and Pearl (2007), analyzing the International Satellite Cloud Climatology Project cloud data set, found that penetrating convection occurs especially in these larger, organised, mesoscale convective systems.
In this section, the AMMA/SCOUT-O3 tracer data will be analysed for signals of this deep convection. Section 3.2.1 will study the level of main convective outflow and the influence of local and aged convection on the CO_2 profiles. Section 3.2.1 will examine the data for signals of overshooting convection.

Main convective outflow

CO_2 can be used as a tracer for continental convection because its mixing ratio is reduced in the boundary layer due to uptake by vegetation during daytime. Deep convection during the African monsoon season peaks in the evening (Sultan et al., 2007) when boundary layer CO_2 is expected to be around its minimum. Convective transport of boundary layer air into the TTL during the monsoon season therefore results in a layer of low CO_2 mixing ratios around the level of main convective outflow. Above this level, diabatic ascent is expected to dominate convection, vertical mixing and mixing of older air from mid-latitudes into the tropics. Hence, a coherent "tape recorder" signal due to the monotonic aging of the slowly ascending air and the progressing CO_2 seasonal cycle in the tropospheric boundary layer can be observed (Boering et al., 1996; Park et al., 2007a). In this section the strength and height of the main convective influence is discussed with help of the CO_2 profiles and is compared with results of an analysis by Law et al. (2010). Law et al. (2010) calculate the fraction of measured air sampled between 350 and 365 K that has potentially been influenced by recent convection with help of ECMWF backtrajectories and infrared satellite images identifying convective clouds. They label an airmass as possibly recently convectively influenced when its backward trajectory crossed a region whose cloud top radiance was below 200 K within a longitudinal band from 30° W to 40° E, corresponding to an age of at most three to four days.
Figure 3.1 shows the vertical CO_2 profiles for the four local flights on August 4, 8, 11 and 13, respectively. Mixing ratios as low as 372 ppm are observed in the daytime boundary layer over Ouagadougou; even lower values could be present in rural areas. The influence of vegetative uptake of CO_2 is getting smaller in the free troposphere, resulting in higher mixing ratios of around 380 ppm. Convection during afternoon and evening transports the CO_2-depleted boundary layer air up to about 13-14 km, or a potential temperature level of 350 K (Figure 3.2), where again a distinct layer with low mixing ratios is observed. Above this level the typical coherent "tape recorder" signal is observed.
The flight of 11 August shows the highest and strongest outflow signature, with mixing ratios as low as 374 ppm found up to 370 K. This flight aimed specifically at sampling air influenced by a large and intense MCS that had crossed westward across Burkina Faso dur-

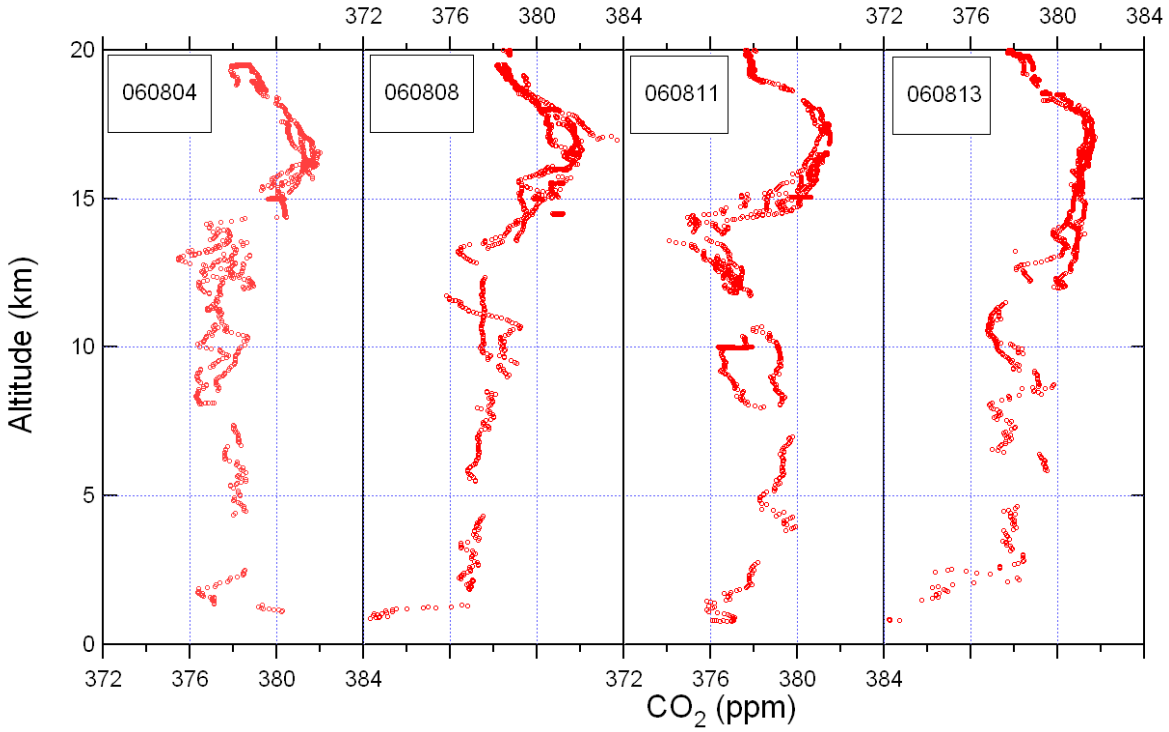

Figure 3.1: Vertical profiles of CO_2 for the local flights on August 4th, 8th, 11th and 13th, respectively.

ing the previous days (Cairo et al., 2010). Law et al. (2010) also find that of all flights performed during the campaign, the TTL sampled during the flight on 11 August was most influenced by recent convection. They calculate that for this flight ∼55% of the measured air between 350 and 365 K was possibly influenced by recent convective activity. Our CO_2 observations suggest that convective outflow of this intense MCS in fact reached unusually high potential temperatures of 370 K.

For the flight of 8 August, Law et al. (2010) also indicate possible convective influence for ∼40% of the air sampled between 350 and 365 K. This agrees well with the CO_2 profile, which shows a level of main convective outflow at 350 K, albeit with a CO_2 minimum that is less pronounced than on 11 August. However, above this level the "tape recorder" signal is less compact than during the other flights, which might be an indication of overshooting convection, which will be discussed in the next section.

For the flight of 4 August, the CO_2 profile shows again a recognisable level of main convective outflow at 355 K, again less distinct as for the flight of 11 August. Law et al. (2010) infer here a possible influence of recent convection for only ∼10% of the air between 350 and 365 K during that day.

Least influence of convection is evident in the profile of 13 August, where an outflow level

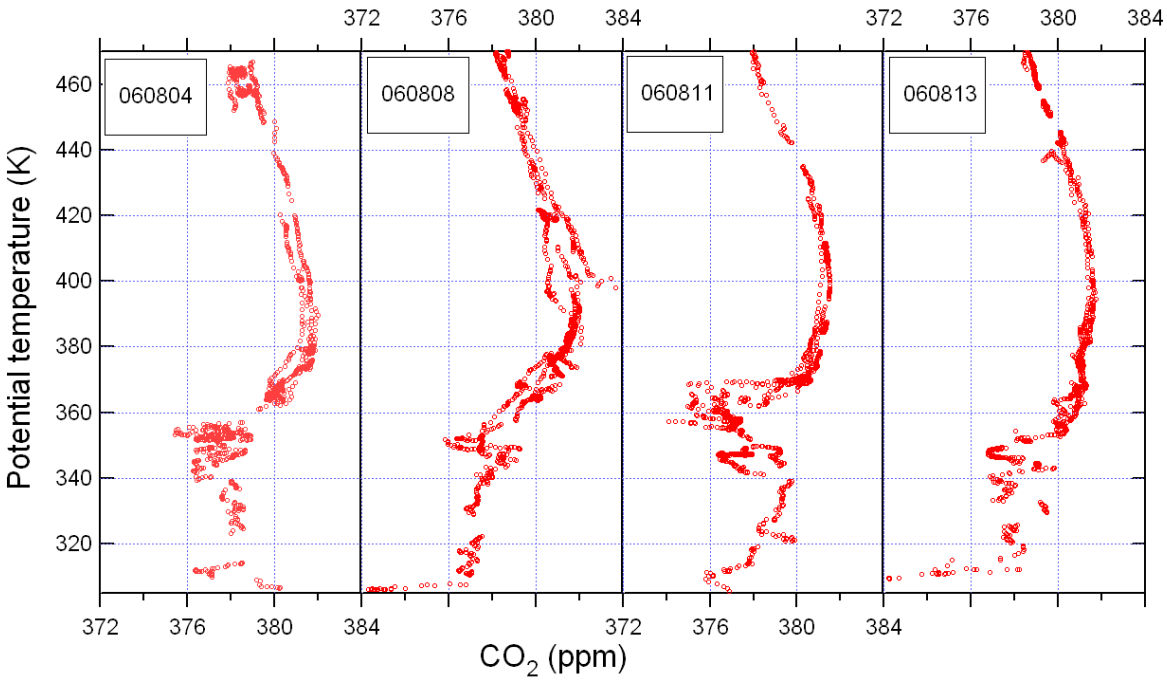

Figure 3.2: Vertical profiles versus potential temperature for CO_2 for the flights on August 4th, 8th, 11th and 13th, respectively.

can hardly be discerned, with mixing ratios at 13 km as high as in the free troposphere. This again agrees well with the analysis of Law et al. (2010), who also find least possible influence of recent convection (∼5%) during this flight, and in fact not even convective uplift of the trajectories within the previous 10 days.

Overall, the observed features in the CO_2 profiles and their relative strengths are thus qualitatively in line with the fractions of sampled air having recently (within about 4 days) passed over convective systems, as calculated by Law et al. (2010). An exception is the flight of 4 August where the observed pronounced CO_2 reductions by 2-3 ppm in the convective outflow region cannot easily be explained by the small recent convective input of 10%, unless regional boundary layer mixing ratios are much lower on the average than those actually observed over Ouagadougou. Another, more likely, explanation is that the CO_2 minima are not only due to recent convection, but to a larger part caused by older convection having occurred more than four days earlier. Since CO_2 is chemically conserved in the TTL, it is not possible to distinguish between the effects of recent and older convection with help of the CO_2 profiles. However O_3 profiles can give an indication whether the convection was of recent or of older origin.

In the tropical boundary layer typical ozone mixing ratios range from 15 to 40 ppb (Folkins and Martin, 2005). Deep convection will transport this O_3 poor air together with ozone pre-

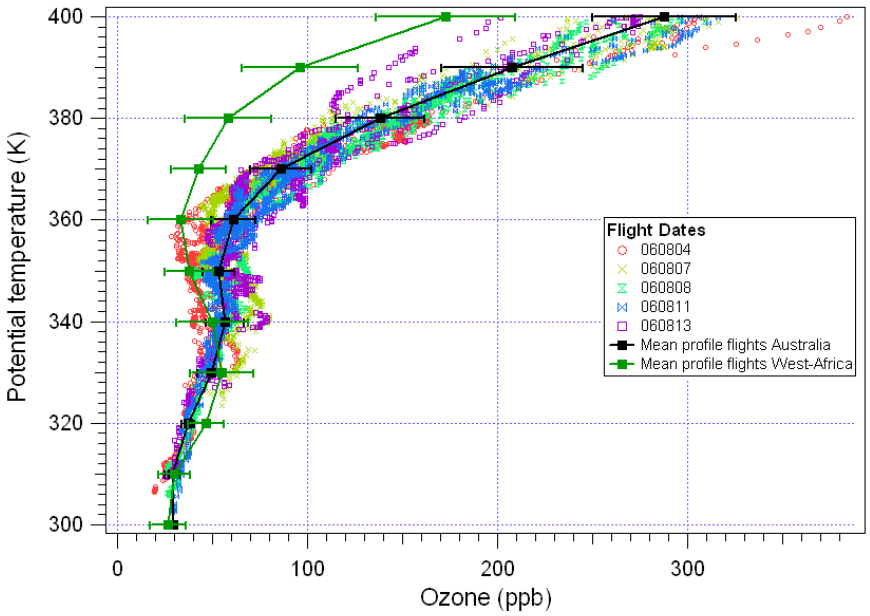

Figure 3.3: Ozone profiles during AMMA/SCOUT-O3 for the five local flights with in black the average profile. The green line represents the average ozone profile for the SCOUT-O3 campaign over Australia. Error bars indicate one standard deviation of the measurements in the given potential temperature bin.

cursors from the tropical boundary layer into the TTL, where, as long as no new convective input takes place, the mixing ratio will steadily increase by photochemical production until it reaches its steady state. Therefore, O_3 mixing ratios are an indication for the convective replacement timescale over a region.
However, not only convection, photochemical production, and the time since the air has last experienced convective flushing determine the O_3 mixing ratios in the TTL. The O_3 budget in the TTL can also be significantly affected by isentropic stratospheric inmixing bringing in extratropical stratospheric air with high O_3 mixing ratios. Vertical mixing, e.g. following overshooting of air, may also mix down higher ozone concentrations from higher altitudes. We show in Section 3.2.2 that horizontal stratospheric inmixing, however, is not significant during the four flights considered here. Mixing following overshooting will be discussed in the next section (Section 3.2.1).

Figure 3.3 shows the ozone profiles during the AMMA/SCOUT-O3 campaign. The average profile of all five local flights is indicated as the black line. For comparison, the dark green line represents the average ozone profiles during the SCOUT-O3 campaign, which took place in November and December 2005 above northern Australia. This latter profile shows the typical S-shape, with low O_3 mixing ratios of 30 ppb over the marine boundary layer, increasing concentrations in the free troposphere, again low O_3 mixing ratios at the level of main convective outflow, and above that increasing mixing ratios due to the photochemical

production of O_3 in the lower stratosphere.
The AMMA/SCOUT-O3 profiles also show this S-shape profile, although less pronounced. Again, concentrations are average to about 30 ppb in the boundary layer; this mean value above Ouagadougou agrees also well with that observed in the boundary layer over Niamey, Niger, by regularly launched ozone sondes (Cairo et al., 2010) and is thus thought to be fairly representative for a wider region. In the free troposphere O_3 increases with height up to around 60 ppb at a potential temperature level of 340 K. O_3 mixing ratios at the level of main convective outflow, however, are much higher on average than those observed during the SCOUT-O3 campaign or in the boundary layer during AMMA/SCOUT-O3. For most of the flights no boundary layer values are observed at the main level of convective outflow (355 K), thereby suggesting that there is no major flushing of the TTL by recent convection of O_3-poor boundary layer air. The absence of this flushing results in increased O_3 mixing ratios due to production by LiNOx (e.g. Thompson et al., 2000; Sauvage et al., 2007; Barret et al., 2010) and other ozone precursors. Law et al. (2010) indicate that a large part of the air in the TTL originated from Asia about a week earlier, where uplift of these ozone precursors could have taken place. An exception appears to be the flight on 4 August when values as low as 30 ppb observed at a level of 355 K indicate more recent convective flushing. Above 370 K the O_3 mixing ratios are up to twice as high as during the SCOUT-O3 campaign. Randel et al. (2007) show that in a narrow vertical layer between ∼16 and 19 km (∼375-450 K) approximately a factor 2 change in ozone between the minimum (during NH winter) and maximum (during NH summer) takes place due to variations in vertical transport associated with mean upwelling in the lower stratosphere (the Brewer Dobson circulation). Thus, the higher mixing ratios observed during AMMA/SCOUT-O3 in the lower stratosphere are probably caused by the seasonal difference in upwelling due to the Brewer Dobson circulation.
In summary, the CO_2 profiles show that the region around West-Africa is highly influenced by convection up to 355 K, during 11 August even up to 370 K. Clearly pronounced levels of main convective outflow are observed during three of the four flights.
However, O_3 profiles strongly suggest that this convective influence is mostly of older origin, and has been transported for at least several days before measured. Only the observations of 4 August exhibit some signatures of recent convection in the O_3 profile. Overall, these results are in good agreement with the findings of Law et al. (2010).

Overshooting of convection

In this Section potential signatures of overshooting convection in the tracer data are examined by observations of CO, CO_2 and O_3.
In Figure 3.4 the CO_2 profiles during AMMA/SCOUT-O3 are plotted in one figure, with their average represented by the black line. On August 8 there are large deviations from this average between 390 and 420 K. Both enhanced and reduced values of CO_2 can be found at this level. On August 4 there are also some reduced values between 400 and 420 K. The enhanced values on August 8 cannot be explained by transport processes; given they occur shortly after a calibration phase of the instrument an unusual instrumental instability cannot completely be ruled out . The low values could be an indication of irreversible mixing

of overshooting air.
If irreversible mixing takes place during or following convective overshoot, air parcels originating from the boundary layer with a potential temperature of 350-360 K (the level of neutral buoyancy) will mix with air masses with a higher potential temperature along a mixing line. In practice, mixing may proceed along a multitude of such mixing lines resulting in a mixing band in a profile plot (provided sufficient sampling). In Figure 3.4, two possible idealized mixing lines are displayed. They indicate that, in order to explain the signatures, mixing would have occurred between air parcels with potential temperatures of approximately 355 K and 400- 420 K, that is overshooting convection would have reached up to 17-18 km.
Overshooting convection can also be diagnosed in tracer-tracer correlations as described in

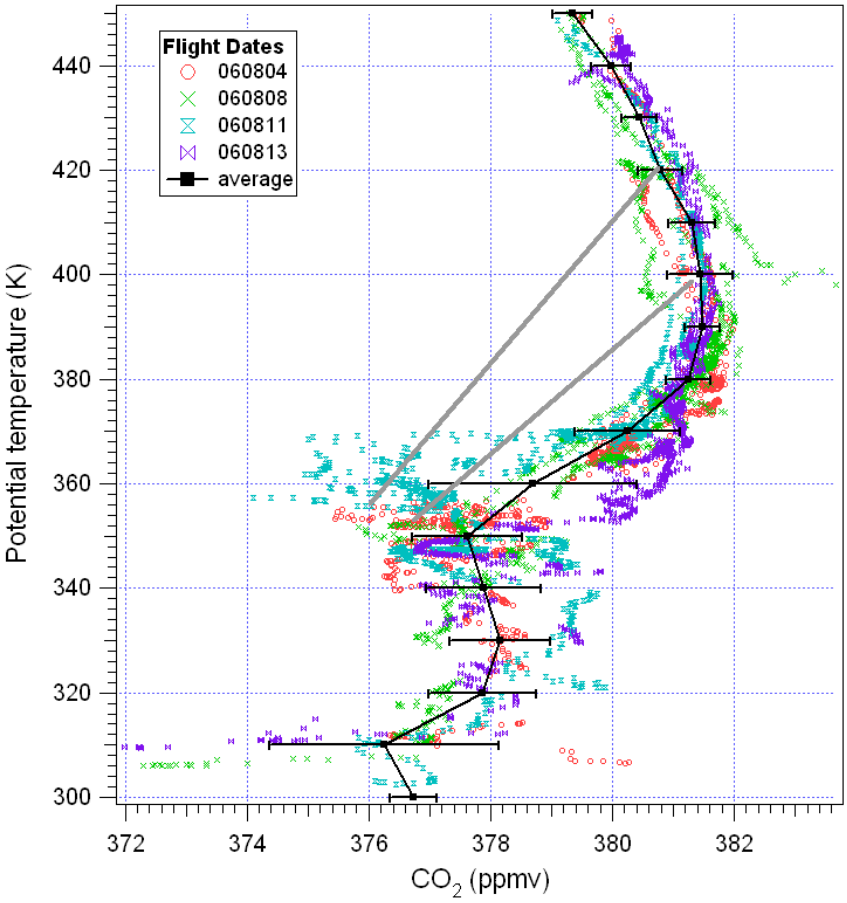

Figure 3.4: CO_2 profiles for the local flights during AMMA/SCOUT-O3 with the average profile in black. The grey lines give two examples of possible mixing lines. Error bars indicate one standard deviation of the measurements in the given 10K potential temperature bin.

Chapter 1.3. Figure 3.5 shows the correlation plot between O_3 and CO_2 for the local flights,

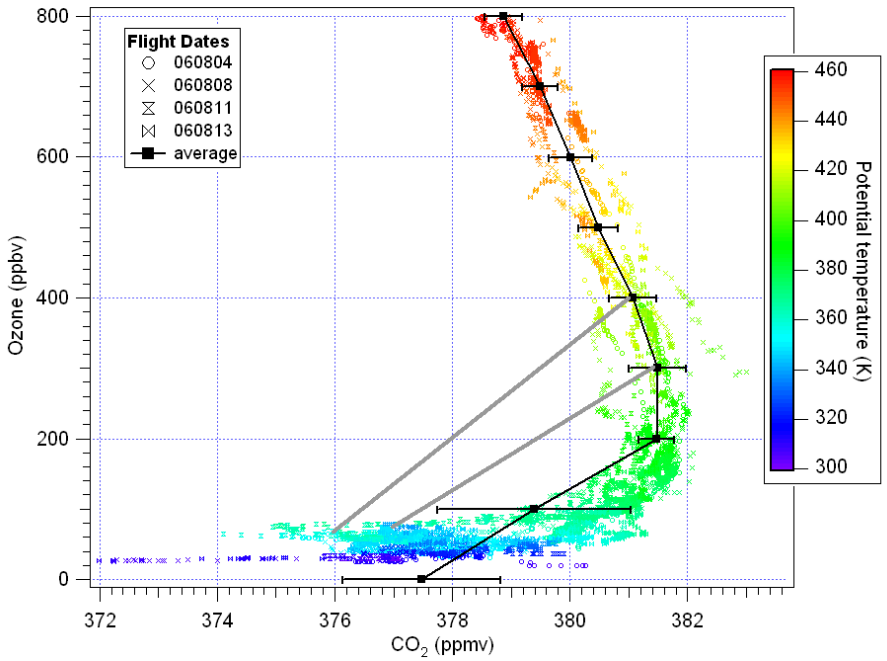

Figure 3.5: Correlation between O_3 and CO_2. The data are coloured to potential temperature. The black line represents the average CO_2 profile for all local flights. The grey lines are the possible mixing lines which are displayed as well in Figure 3.4. Error bars indicate one standard deviation of the measurements in the given 100 ppb O_3-bin

coloured according to potential temperatures and with the average correlation in black. The figure shows a flipped L-shape with variable CO_2 mixing ratios and constant O_3 mixing ratios in the troposphere up to about 360 K, and above that increasing O_3 mixing ratios and slowly decreasing CO_2 mixing ratios. Again, the correlation plot shows a deviation from the average correlation curve between potential temperatures of about 360 and 420 K. They occur along mixing lines corresponding to those displayed in Figure 3.4.
However, similar signatures are not observed during that part of the flight in other species like H_2O, NO_y and particles (not shown). If overshooting of convection had occurred one would expect clear signals of enhanced H_2O and particles as moister air with more particles from the boundary layer would be entrained. Voigt et al. (2008) indicate layers with enhanced particles and NOy, but these are found at other locations during the flight. The latter study does, however, show with backtrajectories that the air measured during this flight was located above a mesoscale convective system for at least 1.5 days prior to the measurements, with cloud top levels up to at least 120 hPa (16 km altitude).

As during the flight of August 7 CO_2 was not measured due to a software failure of the HAGAR instrument only the CO data measured by the COLD instrument are examined.

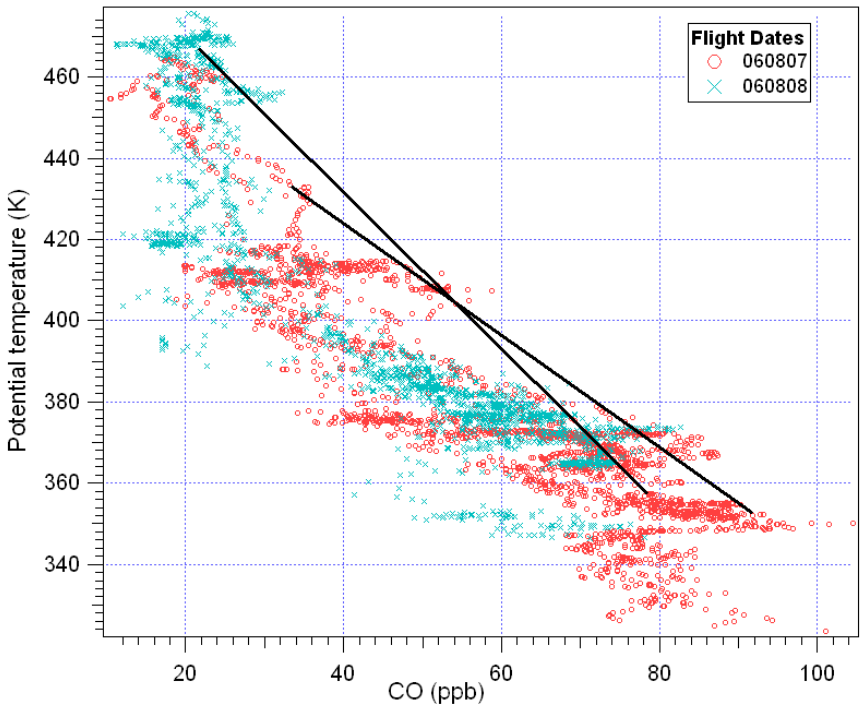

Figure 3.6: CO profiles for August 7 and 8. The black line represents the mixing line that would have to exist to explain the high CO values at 410 K.

Figure 3.6 shows the CO profiles for both August 7 and 8 (the only flights during which COLD measured). Around 410 K very high CO mixing ratios are observed, which could again be an indication of vertical mixing following overshooting. This feature is also present in the correlation plot between CO and O_3, which is shown in Law et al. (2010).
However, as the two possible mixing lines in Figure 3.6 indicate, this would imply mixing of air from the main convective outflow level (355 K) with air parcels at potential temperatures of at least 430 K, i.e. overshoot to extremely high levels.
Again, other tracers do not show similar signatures. Although enhancements are observed in mixing ratios of NO_y and CCN during that day, these only indicate an influence up to 14-15 km, and during a later section of the flight (not shown). Water vapour mixing ratios do not show any signatures indicative of overshooting convection (not shown).
Overall, it can be concluded that signatures potentially indicating impact of overshooting convection are observed in the lower stratosphere in the CO and CO_2 mixing ratios during the AMMA/SCOUT-O3 campaign. However, these signatures are not corroborated by measurements from other instruments on board the airplane. Thus, evidence for the impact of overshooting is inconclusive. In particular, there is no clear indication that overshooting of convection plays a major role in troposphere-to-stratosphere transport during the time of the campaign.

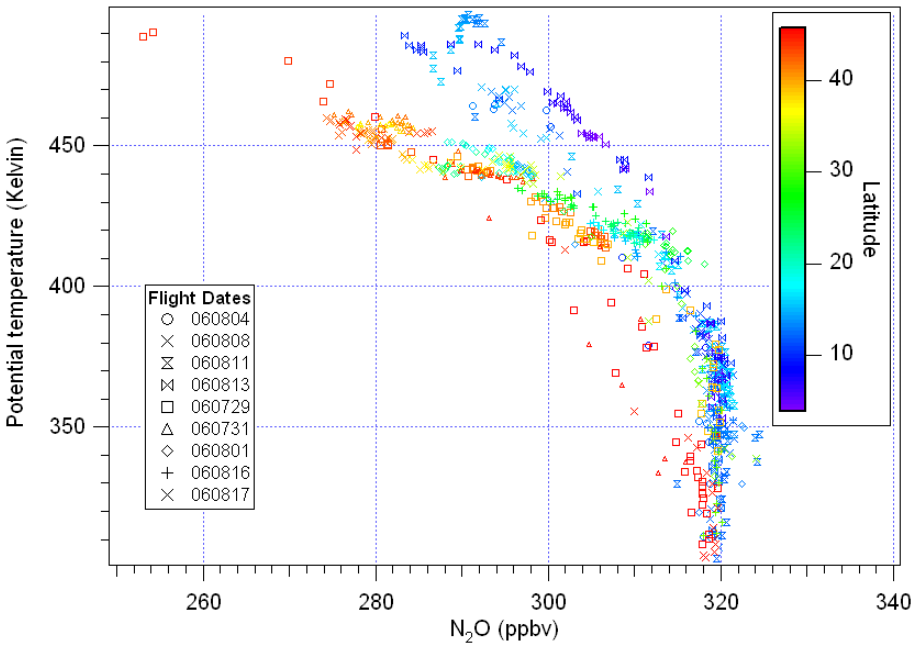

Figure 3.7: Vertical profiles versus potential temperature for N_2O coloured to latitude.

3.2.2 Stratospheric isentropic inmixing into the TTL

In order to quantify the amount of extratropical stratospheric air entering the TTL the N_2O data are examined. N_2O has its source located at the surface and is well mixed throughout the troposphere. Photochemical sinks in the mid-stratosphere result in declining N_2O mixing ratios above the tropopause. Reductions in N_2O mixing ratios below the typical tropospheric value therefore indicate entrainment of stratospheric, photochemically aged (in the order of years) air masses.

The profiles of N_2O shown in Figure 3.7 exhibit constant tropospheric concentrations for the local flights, and a well defined decrease from the tropopause upward, indicating that mixing with stratospherical older air masses is exceedingly rare below the tropopause, whereas the decrease just above the tropopause indicates increasing in-mixing of older air masses. The measurements made in Verona and during the transfer flights ($> 30° N$) show decreasing N_2O values above 330 K, indicating the level of the tropopause in the extratropical region. In order to estimate the fraction of air transported from the extratropical lower stratosphere the N_2O mixing ratios of the extratropical stratosphere are compared with the values in the TTL. The fraction of aged extratropical air (χ) can be expressed as:

$$\chi = \frac{([N_2O] - [N_2O]_{trop})}{([N_2O]_{extratrop} - [N_2O]_{trop})} \tag{3.1}$$

where $[N_2O]$ is the measured N_2O mixing ratio; $[N_2O]_{trop}$ is the average N_2O mixing ratio at the bottom of the TTL, inferred as the average between potential temperatures of 320 K and 350 K between 0-20 °N; $[N_2O]_{extratrop}$ is the average N_2O mixing ratio of the extra-tropical lowermost stratosphere, inferred as the average between potential temperatures of 350 K and 400 K during all flights northward of 40 degrees. The values derived here are $[N_2O]_{extratrop}$ = 309 ± 3.4 ppb and $[N_2O]_{trop}$ = 320 ± 1.4 ppb.

Figure 3.8 shows the derived fraction of extratropical air in the TTL. The blue line repre-

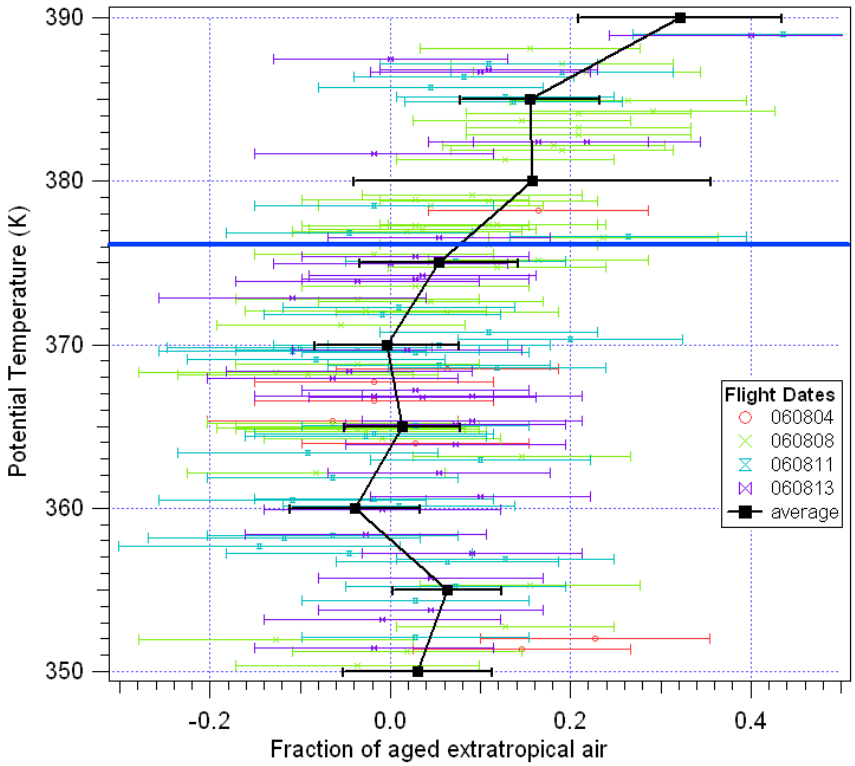

Figure 3.8: Fraction of aged extratropical air. The blue line represents the average height of the tropopause. Error bars indicate the error due to uncertainty in the fixed boundary values.

sents the average height of the cold point tropopause during the campaign. The fraction of aged extratropical air in the TTL is around zero in the lower part up to 370 K and is only slightly increasing toward the top of the TTL (here defined as the cold point tropopause). Note that this result refers to in-mixing of photochemically aged air only and thus does not necessarily rule out in-mixing of extra-tropical stratospheric air altogether. In fact active isentropic exchange across the weak summer subtropical jet with a net export of air masses from the TTL to the extratropical stratosphere is known to flush the lowermost stratosphere with young air over the course of the summer. Any re-entrainment of these young air masses into the TTL would not be detected by the above diagnostic (but would also be of little

relevance for the chemical composition of the TTL).

3.2.3 Isentropic mixing across the subtropical barrier

Except for its lowest part where isentropic mixing with the extratropics is still relatively efficient, the tropical stratosphere is more or less isolated from the extratropical part of the stratosphere (Volk et al., 1996; Minschwaner et al., 1996). The subtropical barrier constitutes a region of strong horizontal shear and maximum PV gradient along isentropes, thereby prohibiting fast isentropic mixing between the tropical stratosphere and mid-latitude stratosphere, especially in the winter hemisphere.
Due to the isolation of the tropical stratosphere, tracer pairs with differing source/sink structures (e.g. O_3-N_2O, O_3-NO_y) show different correlation slopes in the tropical and extratropical stratosphere (Volk et al., 1996; Fahey et al., 1996). At mid-latitudes, where quasi-horizontal mixing is faster than both vertical transport and chemical time scales, a compact correlation evolves whose slope at any point is determined by the ratio of globally integrated sources and sinks of the two species above the given altitude (Plumb and Ko, 1992). Further, since the sources and sinks for O_3 and N_2O are insignificant in the lower stratosphere, this ratio remains approximately constant there, and thus the lower stratospheric correlation is fairly linear. In the tropics, on the other hand, quasi-horizontal mixing is slower, and the correlation is to a large part determined by vertical ascent and local chemistry (Volk et al., 1996); in situ production of O_3 in the lower stratosphere thus results in a correlation slope different from the mid-latitudes. The correlation slope is thus a reliable indicator for the origin of an air mass. A change in the slope of these correlation branches marks the position of the subtropical barrier. Mixing events between the two regions manifest themselves as lines or bands connecting the characteristic tropical and extratropical correlation branches.
Figure 3.9 shows the correlation between O_3 and N_2O for the local and the transfer flights during AMMA/SCOUT-O3. The colours indicate the latitude of the measurements. Different correlation slopes are observed at different latitudes.
The slopes of these correlations are visualised in Figure 3.10 by plotting the ratio of the differences between the measured O_3 and N_2O values from tropospheric reference values, i.e. plotting the correlation slope from the tropospheric origin of the correlation (chosen as 320 ppb N_2O and 50 ppb O_3). The figure shows only data above a potential temperature of 415 K, above which a significant separation between the tropical and midlatitude correlations can be discerned.
The lowest slope values of 0.02 observed southward of 15°N indicate air within the isolated tropical region (the "tropical pipe"), whereas the midlatitudes exhibit slope values exceeding 0.04. Values in between these extremes are found in a band between 10°N and 30°N, suggesting a wider transition zone rather than a sharp subtropical barrier.
In order to examine whether the subtropical barrier might nevertheless be sharp, but undulate within that latitude band due to wave motions, the slope values are also plotted against equivalent latitude in Figure 3.11. Reversible wave motions should be mostly eliminated in this projection as they occur at roughly conserved potential vorticity, and thus equivalent latitude. Nevertheless, the transition between inner tropical and midlatitude slope values

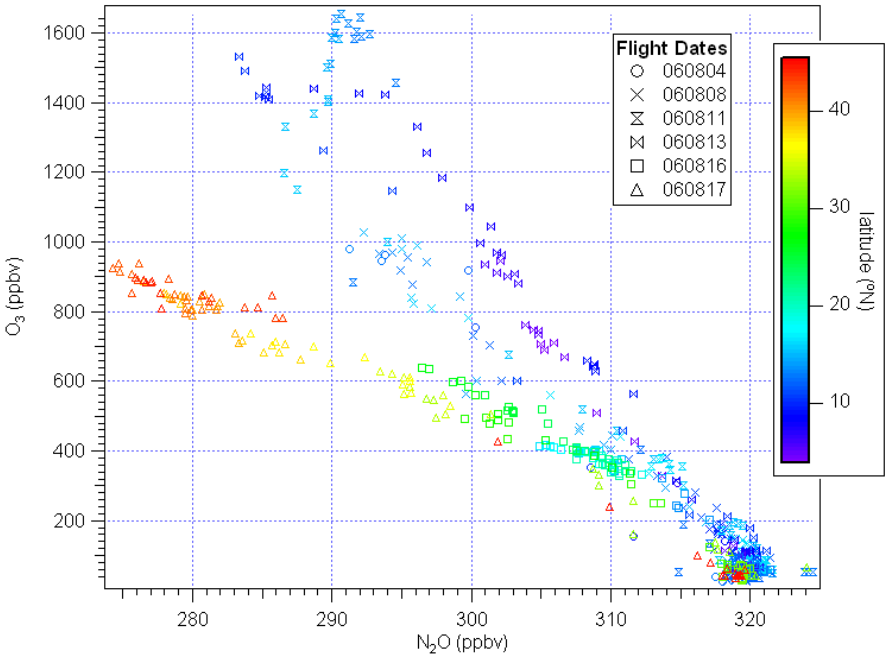

Figure 3.9: N_2O plotted against O_3 coloured to latitude.

still spans a band between 10°N and 25°N equivalent latitude. It thus appears that during AMMA/SCOUT-O3 there is not a sharp barrier but a subtropical transition zone with a width of about 15 degrees latitude.

In Figure 3.12 the data of the AMMA/SCOUT-O3 campaign are compared with the correlation slopes (N_2O vs O_3) found earlier during the ASHOE/MAESA campaign in March and October/November 1994. The slope values from AMMA/SCOUT-O3 data are coloured and plotted against latitude. The ASHOE/MAESA slopes (in grey) can be viewed in analogy to the NOy/O_3 ratios published in Fahey et al. (1996) and in fact show fairly sharp transitions between low tropical values and extratropical values in March (around 10°N) and in October (around 15°N). In contrast, the transition during AMMA/SCOUT-O3 in August is more gradual and ranges between 10°N and 25°N.

It should be noted here that the ER-2 data from ASHOE/MAESA in the region in question are on average sampled at a higher altitude than the M55 data from AMMA/SCOUT-O3, the former being mostly collected during transfer flights at maximum altitude (20-21 km). As the subtropical barrier increases in strength above 20 km, the ASHOE/MAESA data are thus expected to be more suitable to indicate the location and width of the barrier, whereas the Geophysica during AMMA/SCOUT-O3 may have sampled at an altitude range (below 20 km) at which the barrier is weaker and thus more permeable to mixing. On the other hand, the subtropical barrier is also expected to be weakest during summer on the summer hemisphere due to the absence of strong wave activity in the surf zone, which tends to sharpen the barrier. Thus the observed differences between ASHOE/MAESA and

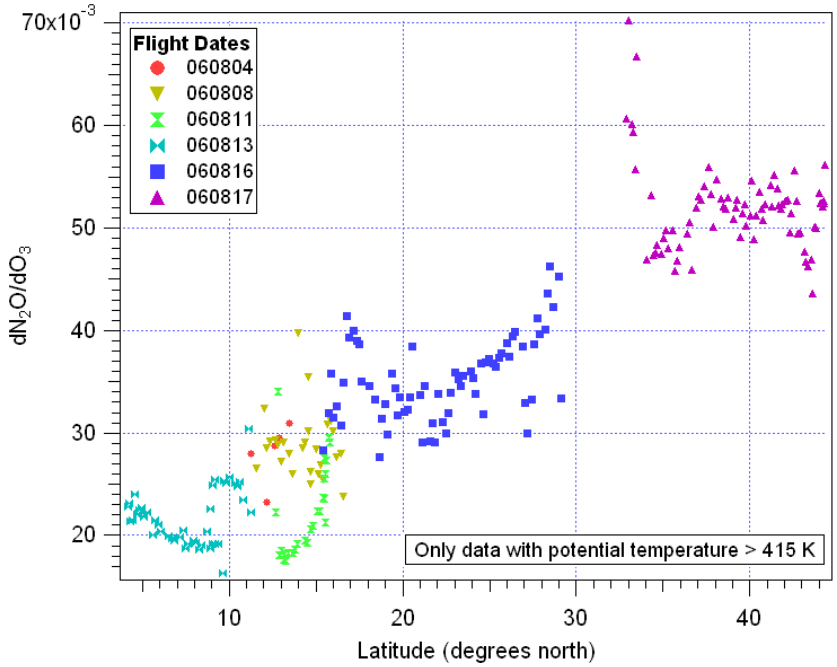

Figure 3.10: Slope dN_2O/dO_3 against latitude for the local AMMA/SCOUT-O3 flights.

AMMA/SCOUT-O3 in the width of the transition between tropical and extratropical tracer values may well be explained by differences in both sampling altitude and season.

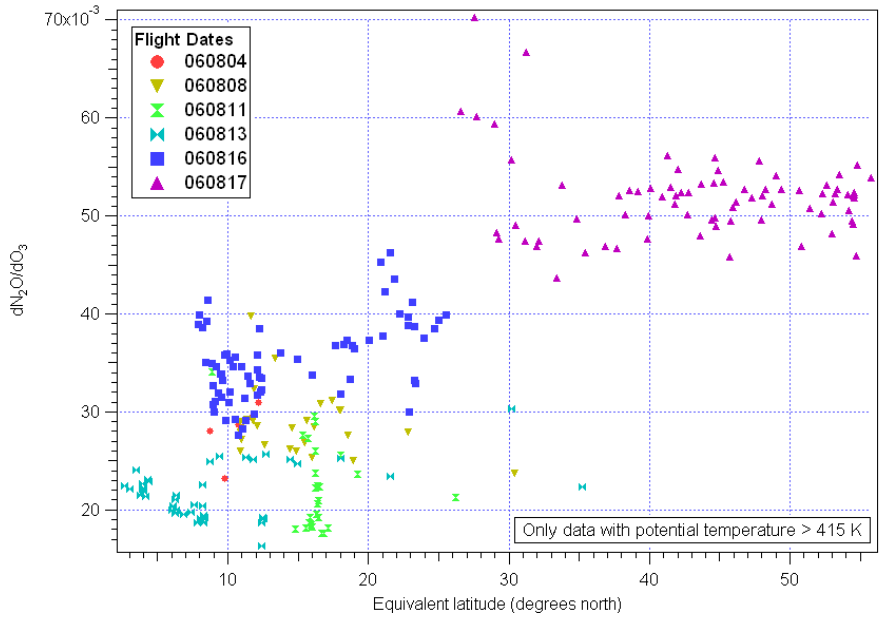

Figure 3.11: Slope dN_2O/dO_3 against equivalent latitude for the local AMMA/SCOUT-O3 flights.

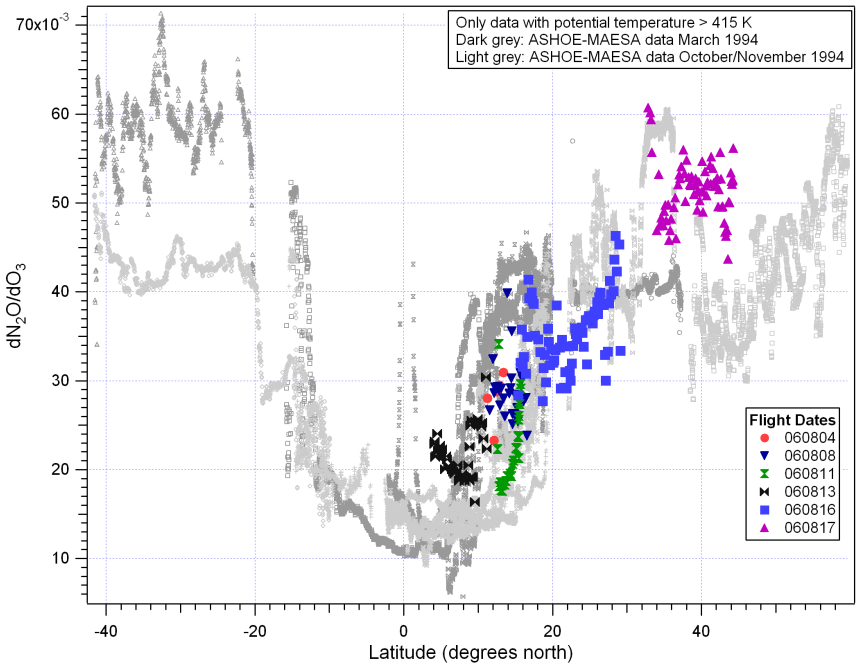

Figure 3.12: Slope of dN_2O/dO_3 against latitude for the local AMMA/SCOUT-O3 flights (coloured) and ASHOE/MAESA (grey).

3.3 Conclusions

The CO_2 profiles (with the exception of August 13) show distinct minima in the TTL, reflecting the outflow of boundary layer air depleted in CO_2. These reductions in CO_2 suggest that i) convective influence in the TTL is quite significant in the sampled air masses and that ii) the main convective outflow was usually located at potential temperature levels up to ∼350-360 K (13-14 km), and for the flight of August 11 even reached up to 370 K (∼15 km). The O_3 profiles, on the other hand, indicate that the larger part of the convective fraction in the sampled air masses must be of rather older origin (several days), as regional boundary layer mixing ratios of 30 ppb are only occasionally found in the TTL (only during the flight of August 4), while average O_3 mixing ratios in the TTL are observed to be 50 ppb or higher. These results agree with those of Law et al. (2010) who find that a large part of the measured air was already residing in the tropical upper troposphere and lower stratosphere when arriving over West Africa and was uplifted over Asia within ten days prior to the measurements. According to their study, regional uplift over Africa above 350 K was only important on 11 August, and potentially on 8 August.

Overshooting convection does not seem to have a large impact on vertical profiles of tracers, which exhibit quite coherent shapes above the maximum level of convective outflow. Only a few small signatures potentially indicative of mixing following overshooting convection were observed in the CO_2 data during the flights of August 4 and 8; another potential signature was observed in CO on August 7. However, similar signatures were not simultaneously observed in other tracers. The absence of frequent high reaching local convection and the lack of major overshooting events impacting the gas-phase composition of the TTL inferred in this study is in accord with the notion that the African region is not a major player in troposphere-to-stratosphere transport (Berthet et al., 2007; Barret et al., 2008), at least not in NH summer.

Stratospheric inmixing of photochemically aged air from the extratropical stratosphere appears to be minimal up to the mean local tropopause at 376 K. The fractions of aged extratropical air in the TTL, as estimated from N_2O profiles is 0.0 ± 0.1 up to 370 K and is increasing above this level up to about 0.3 ± 0.1 at 390 K.

The subtropical barrier does not manifest itself as a sharp boundary in tracer distributions, but rather as a gradual transition region between around 10°N and 25°N where tracer mixing ratios change from characteristic tropical to extratropical values. The subtropical barrier thus appears to be rather permeable to horizontal mixing in the summer subtropics below 20 km altitude.

Chapter 4

Influence of boundary layer pollution, convection and the subtropical jet on the TTL over Darwin during the SCOUT-O3 aircraft campaign

4.1 Introduction

There is considerable evidence that the Indonesian/western Pacific or "maritime continent" is a "hot spot" for air entering the TTL and air crossing the tropopause (Levine et al., 2007; Fueglistaler et al., 2004). The tropical western Pacific, between approximately 100°E to 150°W, contains the warmest water of all the oceans, and is therefore defined as the Tropical Warm Pool. Due to the presence of this latent heat source a lot of high-reaching convection can develop over this region, transporting air up into the TTL.
Fueglistaler et al. (2004) show with an analysis of pathways of trajectories that this region of the tropics is the dominant source region for troposphere-to-stratosphere transport, accounting for about 80% of all trajectories rising from a potential temperature level of 340 K to 400 K.
Therefore, in November and December 2005 the SCOUT-O3 campaign was set up to study transport processes in the TTL over this region (see Section 2.4.1). During the eight local flights on board the M55 Geophysica in situ and remote sensing instruments measured water vapour, particles, reactive chemical species and tracers from the anvil top through the TTL to the lower stratosphere (up to 20 km) both in the anvils of convective systems and in the more quiescent "background" TTL.
This chapter will show the measurements of the tracer data CO_2, N_2O, CO and O_3 obtained by the HAGAR, COLD and FOZAN instruments on board of the aircraft. With help of the tracer data the influence of deep convection, of the subtropical jet and of biomass burning on the TTL above North Australia will be studied. Data from the first four flights, when air originated from the western Pacific and experienced little continental influences (Brunner et al., 2009), are compared with data from the last four flights, when the air originated from

the Indonesian region and travelled along the subtropical jet. In addition to the tracer data, the study will be supported with backward trajectories.

4.2 Measurements

A description of the flights, the measurement methods of HAGAR, COLD and FOZAN and the measurement precisions was already given in Section 2. Additionally, the analysis of the in situ measurements is aided by ECMWF 10-days backward trajectories started from the flight paths (provided by D. Brunner). The 10-day backward trajectories were started every 10 seconds (∼2 km) along the M55 flight track, using the trajectory tool Lagranto (Wernli and Davies, 1997), based on 3-h ECMWF three-dimensional winds (6-h analyses plus 3- and 9-h forecasts in between). In addition to the trajectory position, temperature, humidity and potential vorticity were traced along the trajectories to characterize the physical air mass histories.

4.3 Prevailing meteorology

Darwin is located at the northern tip of Australia, at the border of the Tropical Warm Pool and the so called "maritime continent". Its climate consists of a dry season from roughly May to October, and a wet season from October until April. The wet season is divided into a pre-monsoon or build-up period from October until end of December/beginning of January, and the monsoon period from end of December until April.
During the pre-monsoon period winds are easterly below 300 hPa and convection is mostly initialized by sea breezes. This land based convection occurs usually in the late afternoon or in the evening and can reach and sometimes penetrate the synoptic tropopause at 17 km (Vaughan et al., 2008). The passage of the monsoon through ends this pre-monsoon period and marks the onset of the monsoon period, when the easterly regime changes to a westerly regime and convection becomes more maritime and less deep.
The SCOUT-O3 campaign took place during the pre-monsoon period of the wet season and was aimed to study the deep convection during this period. Especially the Hector storms, occurring almost daily above the Tiwi islands, about 100 km north of Darwin, were of interest. Hectors were probed on 16, 19, 25 and 30 November, although Hector was relatively weak during the first three flights (Brunner et al., 2009). A strong Hector developed on 30 November, and measurements were made before, during and after the onset of the storm. Survey flights in a rather quiescent TTL were made on 23 and 29 November and on 5 December.
As described in Brunner et al. (2009) the origin of air masses sampled in the tropopause region depended on the position of the upper level ridge axis. This led to a distinct separation in origin between the first four (16, 19, 23 and 25 November) and the last four local flights (29 Nov, 2x30 Nov, 5 Dec). During the first four flights air masses in the TTL primarily originated over the equatorial and Northern Hemisphere western Pacific and approached Darwin from the northeast. These air masses often experienced substantial upward trans-

port, potentially from the marine boundary layer. During the last four flights the air in the TTL originated over the equatorial Indian Ocean as well as over southern subtropical latitudes. These air masses typically followed an anticyclonic path over the Indian Ocean and approached Darwin from the south thereby passing over the Australian continent.
The mean position of the Southern Hemisphere subtropical jet stream was unusually close to the equator in November 2005 due to a series of Rossby wave breaking events (Brunner et al., 2009). A breaking Rossby wave between 19 and 23 November caused weak westerlies, resembling monsoon conditions. During this period convection was only moderate over northern Australia.
In November, biomass burning was still prevalent in Indonesia and in northern Australia. Allen et al. (2008) and Heyes et al. (2009) show fire maps of the Moderate Resolution Imaging Spectroradiometer (MODIS) instrument on NASA's TERRA satellite and show the presence of biomass fires above Indonesia and northern Australia in November 2005. As the season progressed, the burning sources abated and the fire maps show a marked decrease in the number of fires both close to Darwin and over Indonesia between October and December. Allen et al. (2008) and Heyes et al. (2009) define the period between approximately 13 and 30 November as the biomass burning period and the period between 30 November and 5 December as the pre-monsoon period, with the same meteorological regime, but an absence of biomass burning sources.

4.4 Results

4.4.1 Vertical profiles of O_3, CO, CO_2 and N_2O

The mean vertical profile of any chemical tracer and the correlation between two different tracers in the tropics should reflect an approximate balance between the different TTL processes of in situ chemistry, vertical advection, convective detrainment, stratospheric isentropic mixing as well as other possible influences. The comparison of different tracers and the correlations between tracers can be used to differentiate between these different processes.
O_3 is a good tracer to study convective activity as deep convection transports air with low O_3 mixing ratios from the boundary layer into the TTL. There, as long a no new convective detrainment occurs, the mixing ratio will steadily increase by photochemical production until it reaches steady state. Therefore, the O_3 profile gives an indication of the frequency of convection. However, in regions with biomass burning or high boundary layer pollution, convection can also transport O_3 precursors, like for example CO and NO, into the TTL and thus increase the O_3 concentrations in the TTL. Also other processes, for example in situ production of O_3 due to lightning (NOx), or horizontal isentropic transport from the extratropical stratosphere can alter the O_3 profile.
CO can be used to study the influence of biomass burning since its primary source in the southern hemisphere is biomass burning. CO is primarily destroyed in the troposphere by reaction with OH and has a chemical lifetime in the TTL of several weeks. Since the sources of CO are mainly at the surface, one would expect deep convection to maintain high concentrations of CO near the convective outflow maximum, which decrease toward the tropopause

as the convective source weakens. Horizontal inmixing from the extratropical stratosphere would reduce the concentrations in the TTL by mixing in air with lower stratospheric CO mixing ratios.
CO_2 does not have a sink in the TTL, and therefore its concentration is dependent on dynamical processes only. CO_2 can often be used as a tracer for continental convection, because its mixing ratio is reduced in the boundary layer due to uptake by the vegetation during daytime (see Section 3.2.1). These low CO_2 values can be transported upwards by convection and are then found around the level of main convective outflow. However, biomass burning or other pollution can enhance CO_2 concentrations in the boundary layer and thus enhance CO_2 concentrations in the TTL after deep convection.
Finally, N_2O is a good tracer to study horizontal isentropic inmixing into the TTL. N_2O has a near uniform mixing ratio in the troposphere due to its long lifetime and the absence of sinks and a rapidly declining mixing ratio in the extratropical stratosphere due to photochemical destruction at higher altitudes. Isentropic horizontal inmixing from the extratropical stratosphere will decrease the N_2O concentration in the TTL. Also a negative correlation with O_3 is an indication of stratospheric influence.
Figure 4.1 shows the vertical profiles of O_3, CO, CO_2 and N_2O for the 8 local flights. The average location of the cold point tropopause during the campaign was located at 17 km ($\sim$380 K).
The O_3 profile shows the typical S-shape, with typical low O_3 mixing ratios between 5 and 50 ppb over the marine boundary layer, increasing concentrations in the free troposphere, again low O_3 mixing ratios at the level of main convective outflow, and above that increasing mixing ratios due to the photochemical production of O_3.
The distinction of two different periods as described in the previous section is clearly observed. The first four flights of the campaign (16, 19, 23 and 25 November) show a strong S-shape, with high mixing ratios of O_3 in the free troposphere between 5 and 9 km, with a maximum of almost 100 ppb found on November 25. The high mixing ratios at this level on 23 and 25 November can be explained by the Rossby wave breaking event, which caused an intrusion of dry, O_3-rich stratospheric air (Allen et al., 2008). In the TTL these flights show very low values, with a minimum on November 16, where mixing ratios as low as 5 ppb were found between 11 and 15 km, indicating that very clean maritime air was sampled.
The flights during the second half of the campaign show a less pronounced S-shape, and profiles are more coherent. Mixing ratios found in the TTL are not as low as during the first part of the campaign, and cannot be directly related with those observed in the boundary layer.
The CO profiles also show a lot of variation in the free troposphere during the first half of the campaign, and more coherent profiles afterwards. Enhanced CO mixing ratios were measured during the second half of the campaign between 13 and 17 km.
The CO_2 profiles are less coherent than the O_3 and CO profiles. They show mixing ratios between 378 and 380 ppb in the lowest 14 km, followed by a steady decrease above reflecting the expected coherent "tape recorder" signal due to the monotonic aging of the slowly ascending air and the progressing CO_2 seasonal cycle in the tropospheric boundary layer (Boering et al., 1996; Park et al., 2007a). Enhanced mixing ratios in the TTL during the second part of the campaign are also observed.

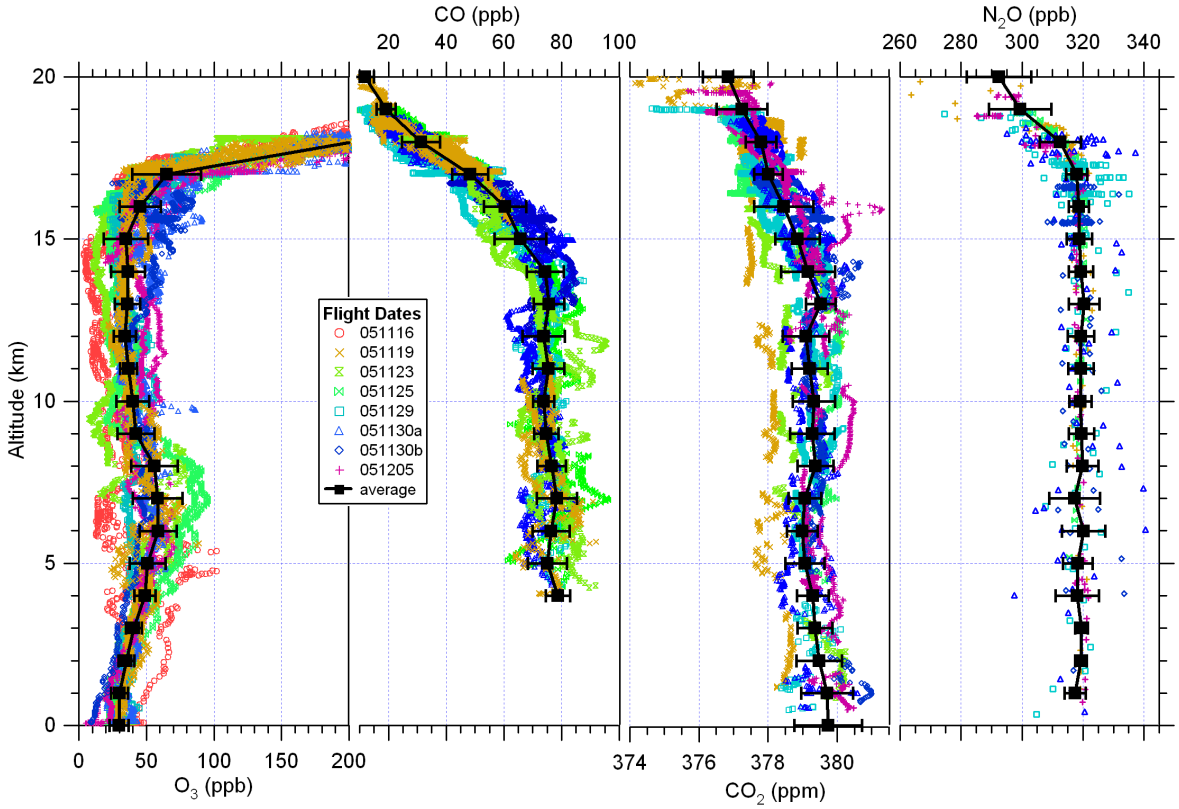

Figure 4.1: Vertical profiles of O_3, CO, CO_2 and N_2O for all local flights. The average profile is indicated by the black line. Error bars indicate one standard deviation of the measurements in the given 1 km bin.

The N_2O profiles show a mixing ratio of around 320 ppb up to 17 km, above which the mixing ratio starts to decrease. The higher scatter of the data during the flights of 29 and 30 November is due to the lower precision caused by an instrumental problem (cf. Section 2.4.1).

The differences between the first four and the last four flights become even clearer when the tracers are plotted against potential temperature. Figures 4.2 and 4.3 show the data from the four last flights compared with the average profile of the first four flights.

The figure shows clearly enhanced O_3 mixing ratios between 350 and 380 K, especially for the two flights on 30 November and the flight on 5 December. The flight of 29 November shows only a few enhanced values at 350 K and 380 K, but is more similar to the background profiles of the first four flights.

The CO profile also shows enhanced mixing ratios between potential temperatures of 355 and 380 K during the two flights on 30 November. Again, the flight of the 29th shows less enhancement (only at 355 K). For 5 December, CO data are not available. The CO_2 data show enhanced values over the whole profile, but during the flights of 30 November most

pronounced between 360 and 380 K. The flight on 29 November only shows enhanced values at 350 and 390 K.
The N_2O profiles are very similar for the first and the second part of the campaign. Although the scatter during three of the last four flights is large due to the high imprecision, the average profiles agrees well up to 390 K. The stronger decline above 390 K in the second half of the campaign is owed to the flight on 5 December, which was the only survey flight leaving the tropics towards southern latitudes (cf. Figure 2.3).
To conclude, the first four flights show overall higher variability in mixing ratios than the last four flights, but in general exhibit very low O_3 mixing ratios in the TTL, indicating that very clean air was sampled. The last four flights show higher mixing ratios, with some enhancements in the TTL on 29 November and 5 December, and with even higher enhancements during the two flight of 30 November.

4.4.2 Tracer-tracer correlations

In addition to the mean profiles of tracers, the correlation plot between two long-lived tracers (tracer-to-tracer correlation) is also very useful for studying transport and mixing processes in the TTL. Specific tracer pairs form compact and often distinct correlation curves in the troposphere and stratosphere (Plumb and Ko, 1992). Deviations from these climatological correlations may be caused by mixing between the regions as was discussed in more detail in Section 1.3.

Figure 4.4 shows the scatter plots between O_3 and CO and between O_3 and CO_2. The background (first four) flights show the expected L-shape (cf. Section 1.3), with increasing O_3 and decreasing CO in the stratosphere, and high CO and low O_3 in the troposphere. The average correlation of these flights is indicated by the black line. The coloured symbols indicate the last four flights. The two flights on 30 November, and the flight on 5 December show deviations from this background correlation, which might be an indication of mixing. Mixing would mean that air with a certain potential temperature on one branch of the L-profile mixes with air of the other branch (with presumably different potential temperature) along a mixing line. Hypothetical potential mixing lines are drawn in red in Figure 4.4. The possibility of mixing causing the observed signatures will be investigated in detail in Section 4.5.3.

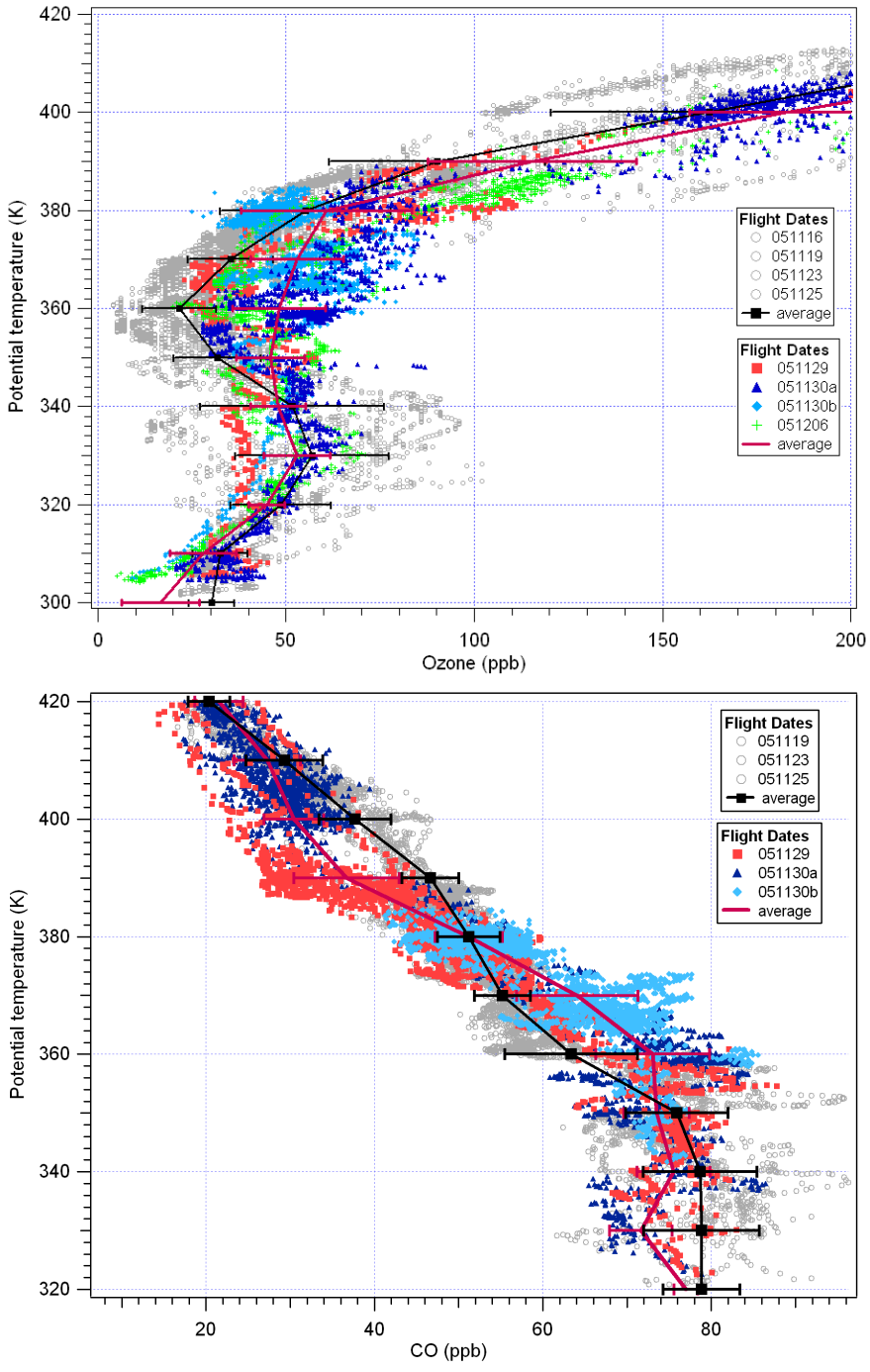

Figure 4.2: Vertical profiles versus potential temperature for O_3 (top) and CO (bottom). The grey points indicate the flights of 051116, 051119, 051123 and 051125. The coloured points are the four last flights. The averages for the first four (three in case of CO) and the last four flights (three in case of CO) are indicated with the black and purple line, respectively. Error bars indicate one standard deviation of the measurements in the given 10K potential temperature bin.

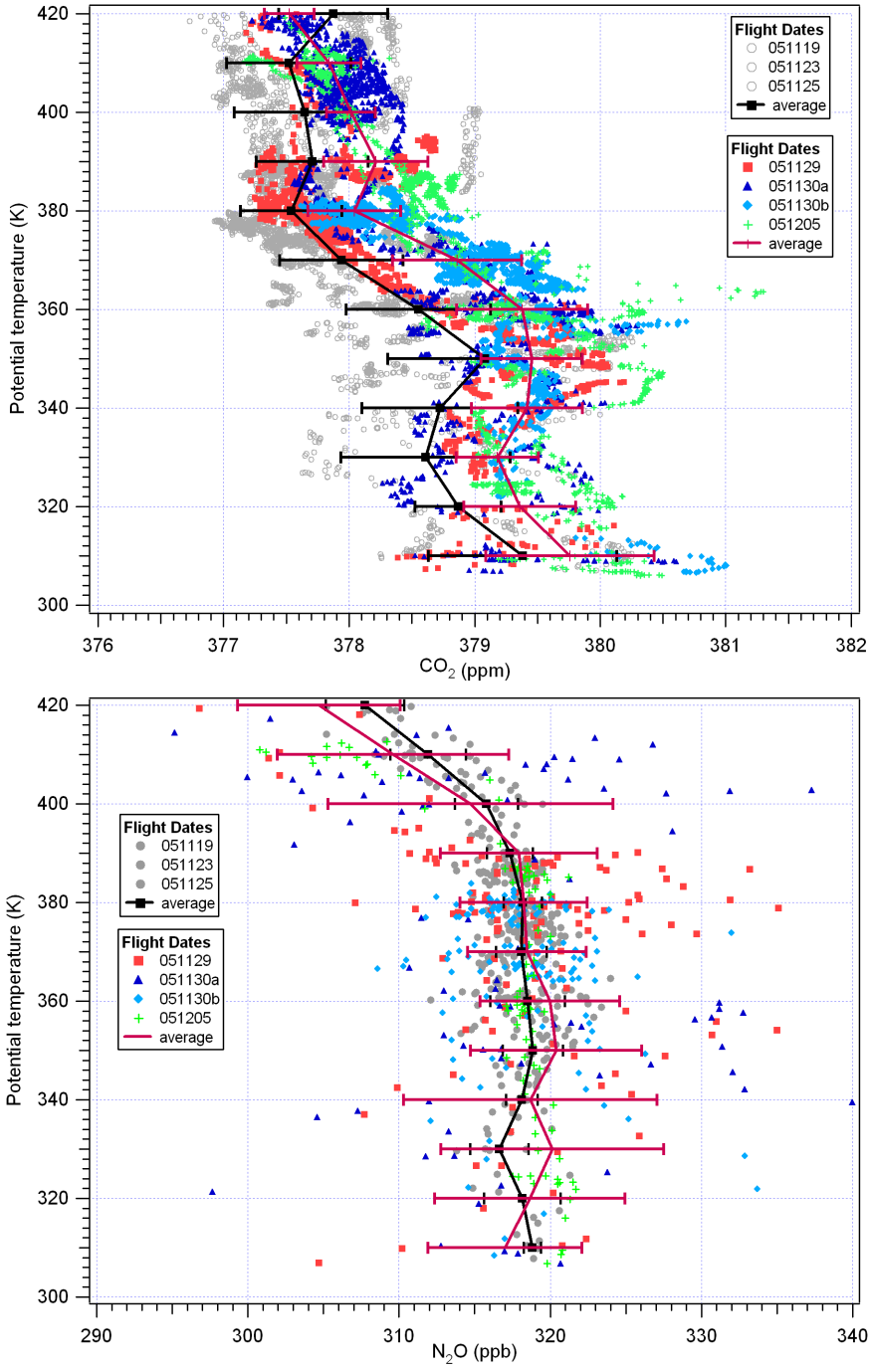

Figure 4.3: Vertical profiles versus potential temperature for CO_2 (top) and N_2O (bottom). The grey points indicate the flights of 051119, 051123 and 051125. The coloured points are the four last flights. The averages for the first three and the last four flights are indicated with the black and purple line, respectively. Error bars indicate one standard deviation of the measurements in the given 10K potential temperature bin.

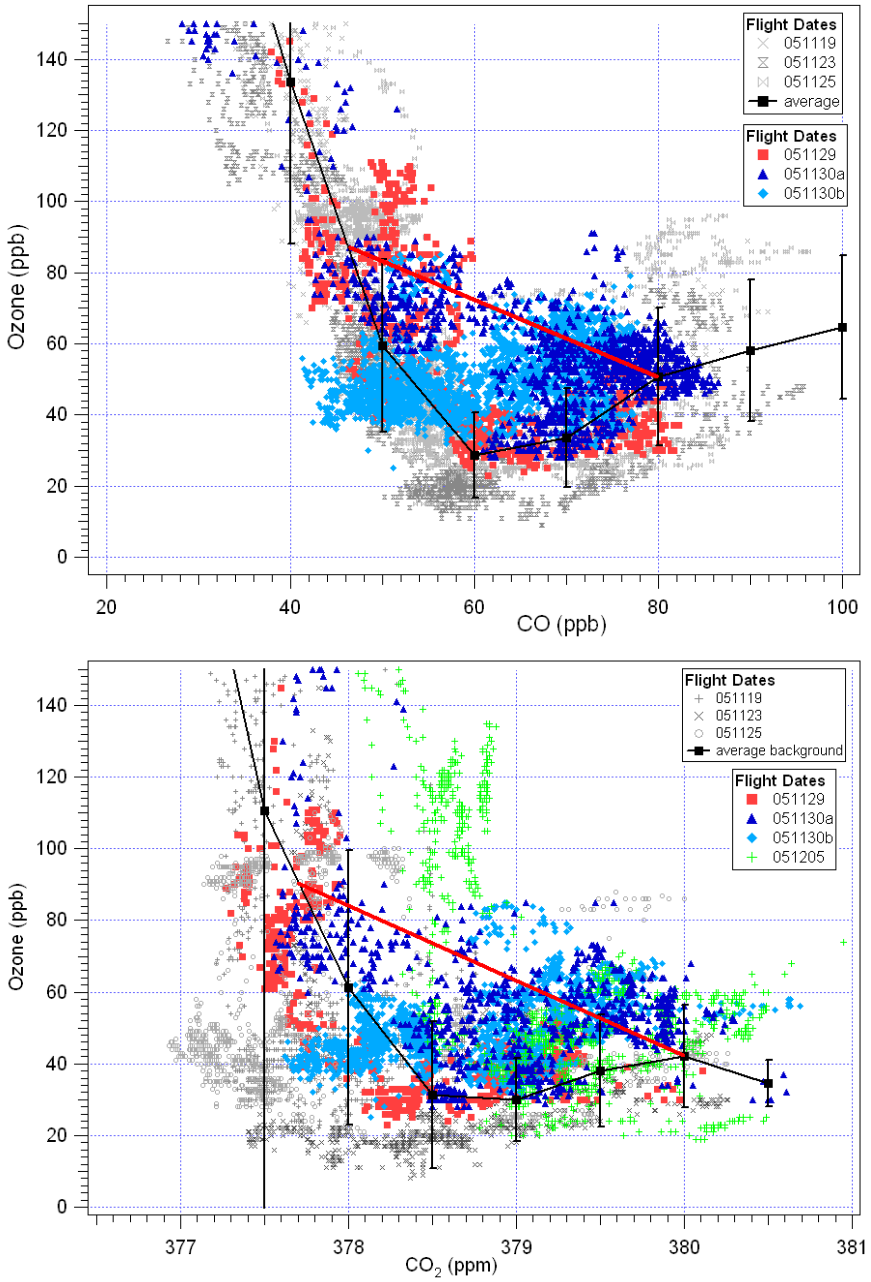

Figure 4.4: Correlation between CO and O_3 (top) and between CO_2 and O_3 (bottom). The first three flights are indicated with the grey dots, and their average with the black line. The error bars indicate one standard deviation of the measurements in the given bin. The coloured points are the last three (CO) or four (CO_2) flights.

4.4.3 Backward trajectories

In order to find explanations for the enhanced tracer mixing ratios during the last flights of the campaign, it is important to know the origin of the air masses. In Section 4.3 it was already mentioned that the origin of the air was different for the second half of the campaign in comparison with the first half, when air originated over the Pacific and was observed to be very clean. The backward trajectories for the first four local flights are shown in Brunner et al. (2009). Figures 4.5, 4.6, 4.7, and 4.8 show the 10-day backward trajectories for the flight of 29 November, the morning and evening flight of 30 November and the flight of 5 December between potential temperatures of 340 and 380 K, respectively. In each case the upper plot shows all backward trajectories starting on the flight track in the complete potential temperature range, the second plot those starting between 350 and 360 K, the third plot those between 360 and 370 K, and the bottom plot between 370 and 380 K. The backward trajectories are coloured according to the potential temperature of the air parcels. The black dots are spaced at 1-day intervals.
The overall pattern of the trajectories shows that the air originated in the region around Indonesia, travelled westward over the Indian Ocean, and then turned around and approached Darwin from the southwest, travelling over the Australian continent for two days. However, small differences are observed.
On 29 November the air with potential temperatures between 350 and 360 K originated from the Pacific region and travelled across Java towards Australia. Most of the trajectories at higher levels did not cross any land area for the last ten days and originate just west of Indonesia.
The trajectories of both flights of 30 November crossed a large part of Indonesia in the first three days. Only above 370 K the air travelled only over the Indian Ocean in the past ten days.
On 5 December, the air up to a potential temperature level of 370 K also originated above Indonesia but further southwards. Part of the air also travelled directly from Papua New Guinea towards Australia, thereby not approaching Darwin from the southwest, but directly from the northeast. Above 370 K a part of the trajectories took that latter path and another part originates from the west, from the Indian Ocean and from Madagascar.
The trajectories are coloured according to their potential temperature along their path. For all four flights not much change is seen during the ten days; in particular the backward trajectories do not experience any strong large-scale uplift.
Heyes et al. (2009) also studied backward trajectories during the ACTIVE campaign (November 2005 to February 2006) of which the first part took place at the same time as the SCOUT-O3 campaign. They show with backward trajectories and ozonesonde data that air uplifted over Indonesia, west of 140°E, exhibits high O_3 concentrations, in contrast to the air uplifted over the remote marine Pacific region, which exhibits far lower O_3 concentrations. They also show that during the pre-monsoon phase, only 18% of the backward trajectories between 200 and 100 hPa (∼350-375 K) experienced uplift over the previous ten days, suggesting that very long-range or diffuse sources dominated the TTL composition at this time.
However, the apparent lack of uplift of the backtrajectories for the second half of the SCOUT-

O3 campaign does not prove that the sampled air parcels were not affected by convection at all over the past ten days. Convection takes place on smaller spatial and temporal scales than are resolved by trajectory calculations. Therefore convection on these smaller scales may well have occurred without being reflected as large-scale uplift in the back trajectories.

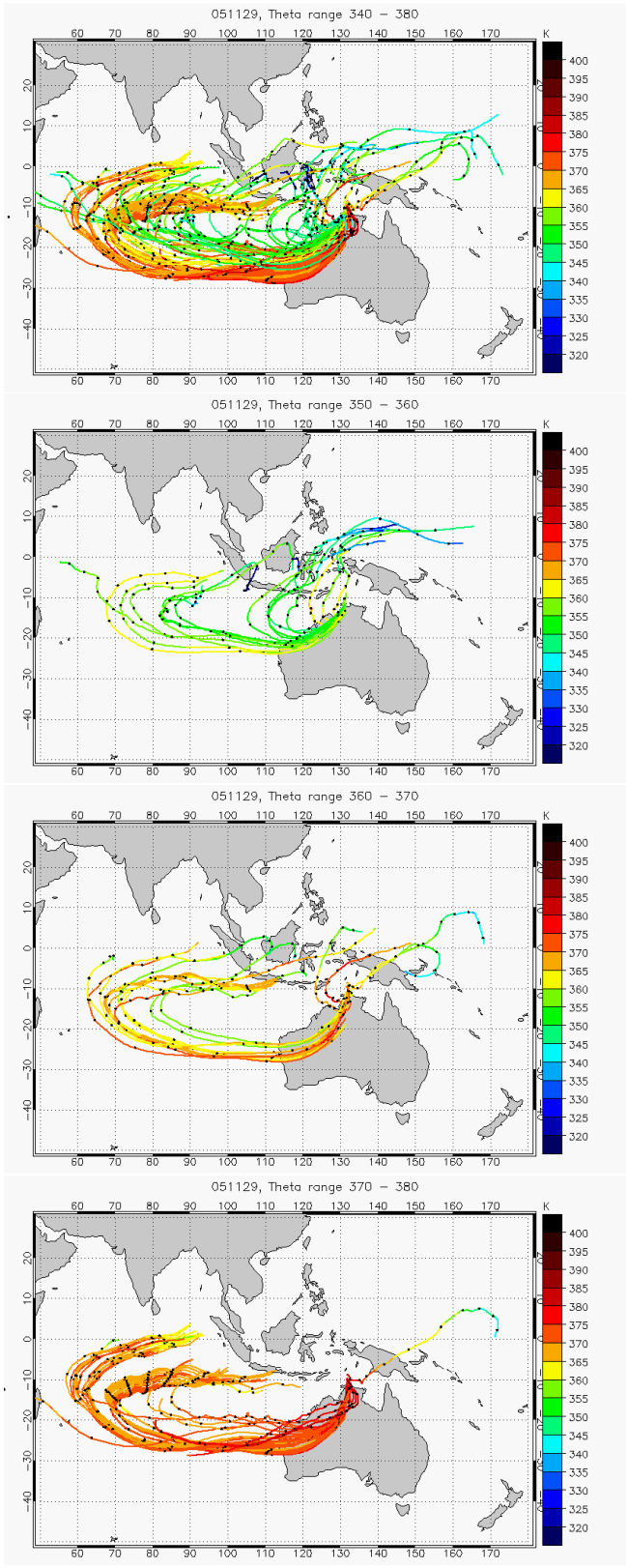

Figure 4.5: Backward trajectories for the air measured between potential temperatures of 340 K and 380 K during the flight of 29 November, colour coded by potential temperature. Black dots are spaced at 1-day intervals along the trajectories.

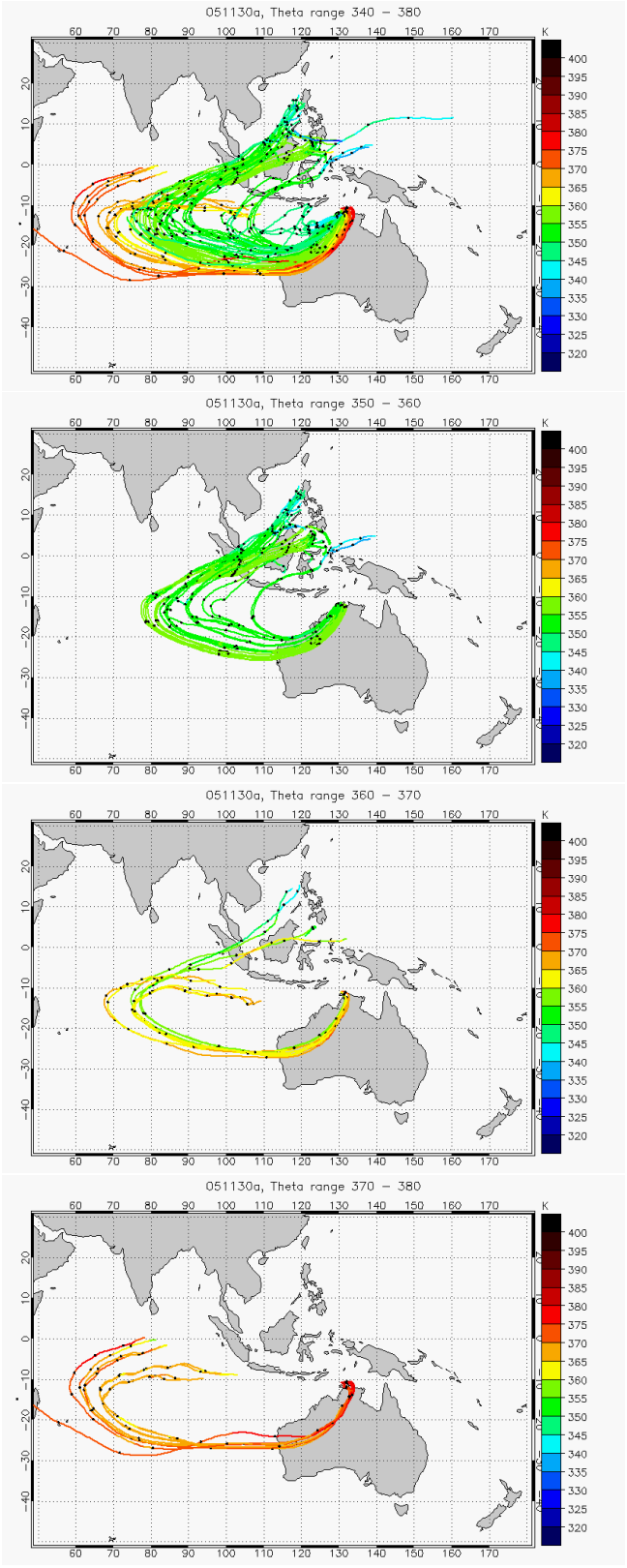

Figure 4.6: Backward trajectories for the air measured between potential temperatures of 340 K and 380 K during the morning flight of 30 November , colour coded by potential temperature. Black dots are spaced at 1-day intervals along the trajectories.

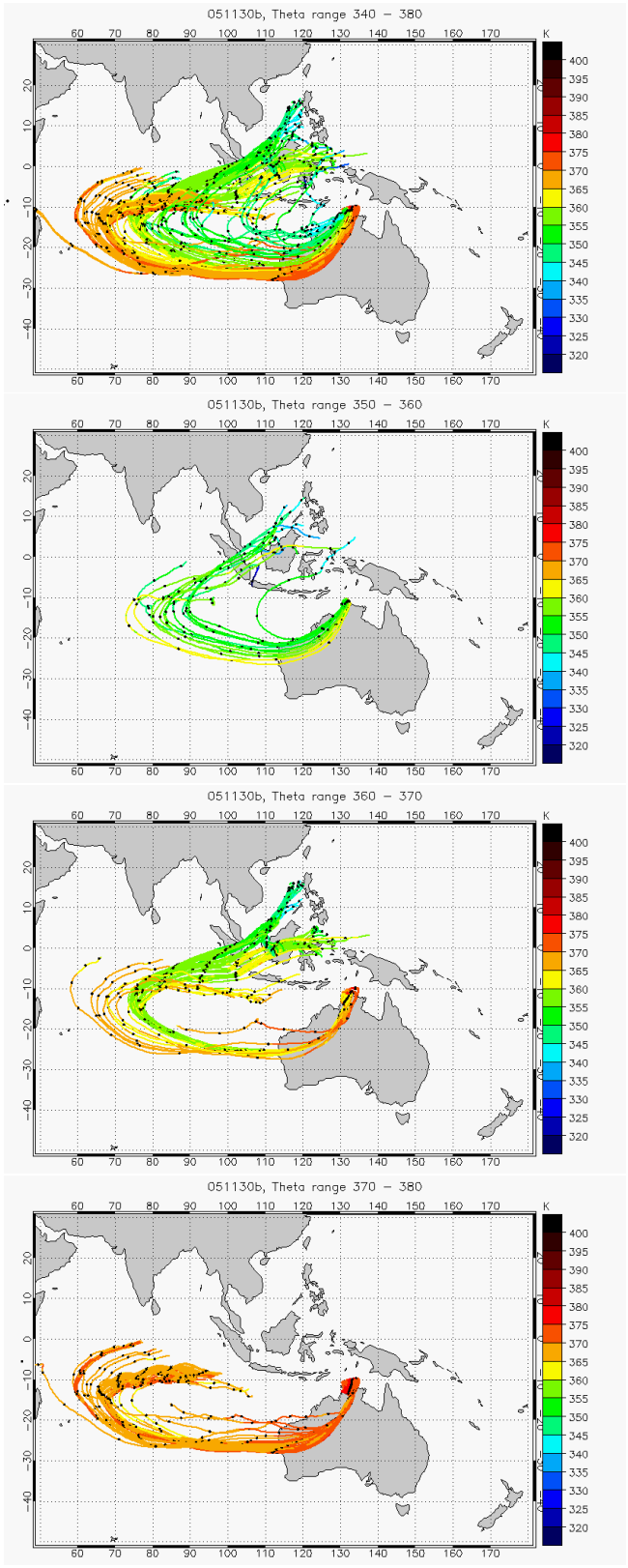

Figure 4.7: Backward trajectories for the air measured between potential temperatures of 340 K and 380 K during the afternoon flight of 30 November, colour coded by potential temperature. Black dots are spaced at 1-day intervals along the trajectories.

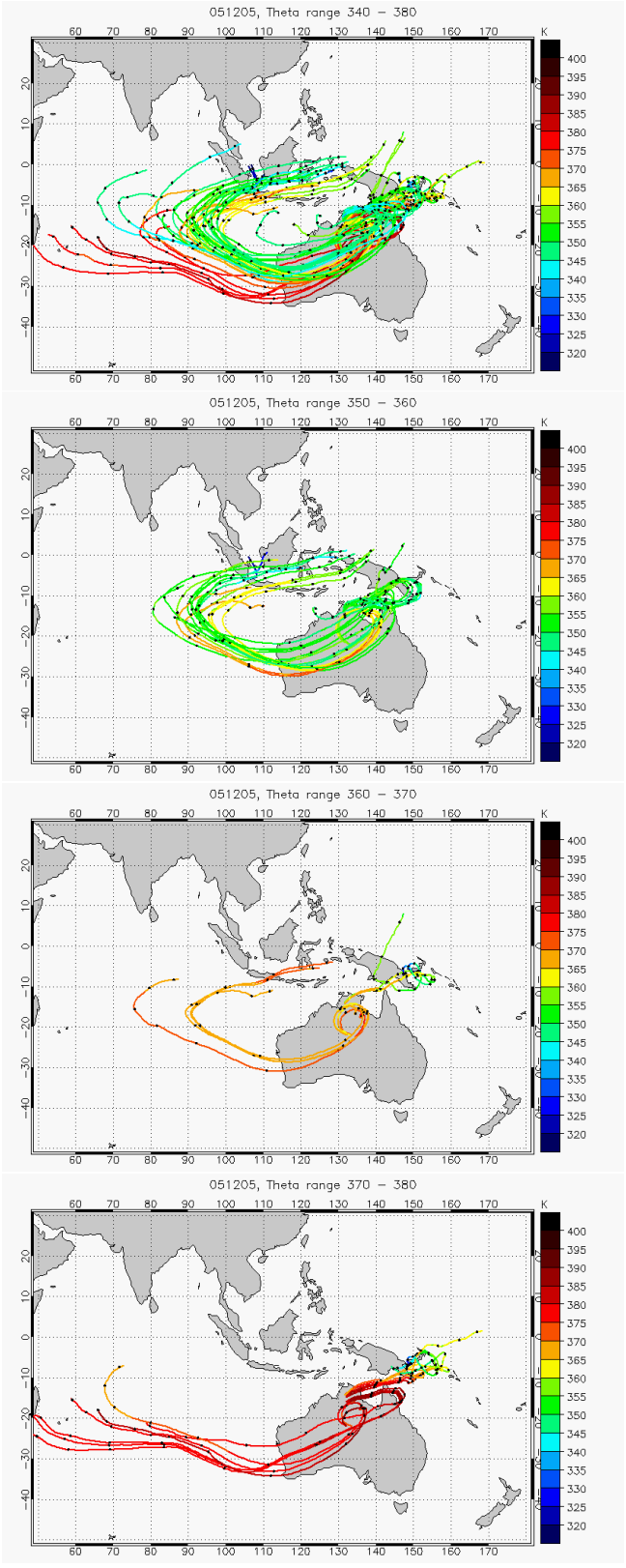

Figure 4.8: Backward trajectories for the air measured between potential temperatures of 340 K and 380 K during the flight of 5 December, colour coded by potential temperature. Black dots are spaced at 1-day intervals along the trajectories.

4.5 Interpretation

This section will discuss four different processes that could explain the enhanced values of O_3, CO and CO_2, namely horizontal inmixing, the influence of the convective system Hector, vertical mixing along the subtropical jet, and the influence of biomass burning and polluted boundary layer air over Indonesia.

4.5.1 Horizontal isentropic inmixing

As the air during the last four flights approached Darwin from the south and travelled as far as 30 degrees south, horizontal inmixing from the extratropical stratosphere could have occurred. Such inmixing would bring in air with higher O_3 mixing ratios. However, it would also cause lower CO mixing ratios in the TTL, since stratospheric mixing ratios of CO are lower than mixing ratios in the TTL. This is in contrast with the enhanced mixing ratios seen in Figure 4.2, which are not likely to be of extratropical origin.
Horizontal inmixing would also be observed in the correlation between O_3 and N_2O. If a significant fraction of the O_3 is of stratospheric origin, the correlation with N_2O is negative, since in the stratosphere N_2O decreases with height and O_3 increases, whereas in the troposphere N_2O is well-mixed and does not show any correlation with variations in O_3. The correlation between O_3 and N_2O during three of the last four flights is shown in Figure 4.9. The figure does not indicate any significant horizontal inmixing in the upper troposphere below 385 K. A significant negative correlation only exists above 385 K, i.e. in the stratosphere. The correlation plot thereby confirms that there is not a large influence of extratropical stratospheric inmixing into the TTL during the second half of the campaign.

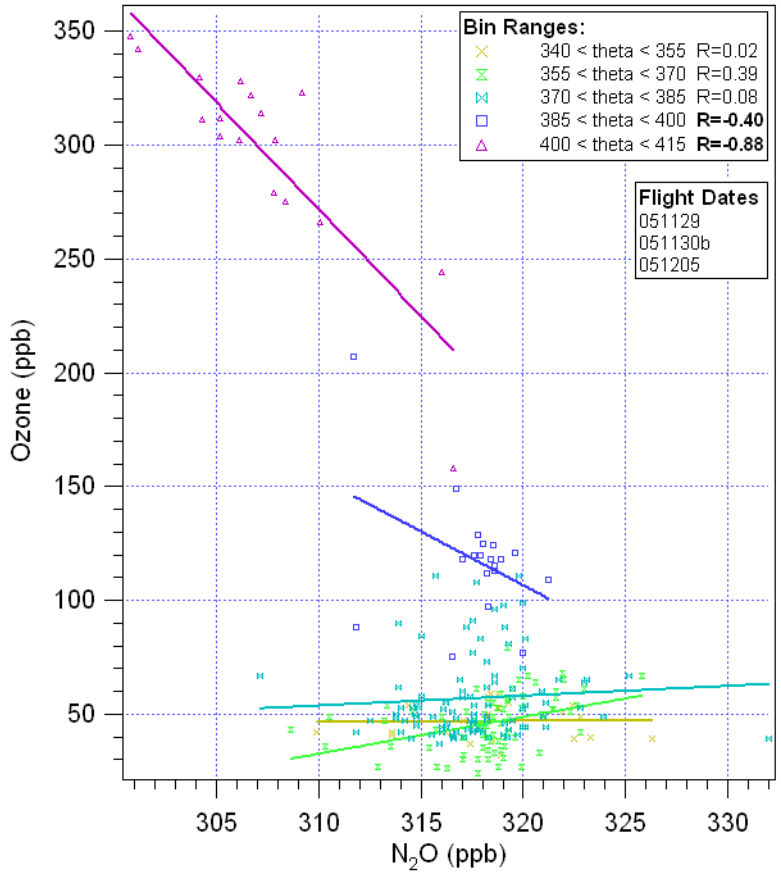

Figure 4.9: Correlation between O_3 and N_2O for the flights 051129, 051130b and 051205. Data are divided into theta-bins of which the correlation coefficient is calculated. Correlation coefficients R printed in bold are significant (95% confidence level).

4.5.2 Hector

Since the flights on 30 November were dedicated to probe the local convective system Hector, it is plausible to suspect the Hector storm to have caused the elevated levels of O_3, CO and CO_2. Overshooting of convection would mix air with higher potential temperatures with air parcels with a potential temperature around the level of main convective outflow. Given the shapes of the background vertical profiles of O_3, CO and CO_2 (cf. black lines in Figures 4.2 and 4.3) this process would yield to enhancement of these species in the mixed air, compared to the background as described in Section 1.2.2. The correlations shown in Figure 4.4 also promote the idea of mixing due to overshooting convection. The mixing would result in data points along the hypothetical mixing line shown in Figure 4.4, which are indeed observed mostly for the flights of 30 November.
The first flight of the Geophysica took place in the early afternoon, before and during the onset of Hector. The Geophysica flew around the system and spent most of its time above the anvils, or near anvil tops, in order to sample convective overshoots. The downward pointing Lidar MAL onboard the airplane showed a mean anvil deck at 17 km and overshoots reaching up to 18 km. De Reus et al. (2008) observed ice clouds up to 1.4 km above the local tropopause, indicating direct transport of cloud particles from the troposphere to the stratosphere.
On the evening of 30 November, 4 hours after the first flight, the Geophysica took off again to re-sample the air masses lofted by Hector. The aircraft performed zig–zag manoeuvres close to the Tiwi islands to measure aged anvil outflow. Figure 4.10 shows the satellite pictures during the first flight, and superimposed the flight track (white) and the part of the flight taking place at the time of the image (dark green). The first three pictures show the first flight of the day. The airplane took off before the development of Hector, and then flew above and to the northwest of the system. The last picture shows the evening flight when the airplane sampled the whole area of the already disappeared Hector system.
Figures 4.11 and 4.12 show the flight tracks with the parts of the flights between 360 and 375 K colour coded with the CO and O_3 mixing ratios. Enhanced mixing ratios were already found before the onset of the system, and both to the east and to the west of the system. During the second flight, enhanced values were also found over the whole region, and not just in the outflow region. Therefore, Hector itself cannot explain these high values.

The study of Heyes et al. (2009) also concludes that localised convection does not significantly perturb the background TTL during that period. They observed highly variable O_3 profiles in the TTL while low-level concentrations were hardly changing.

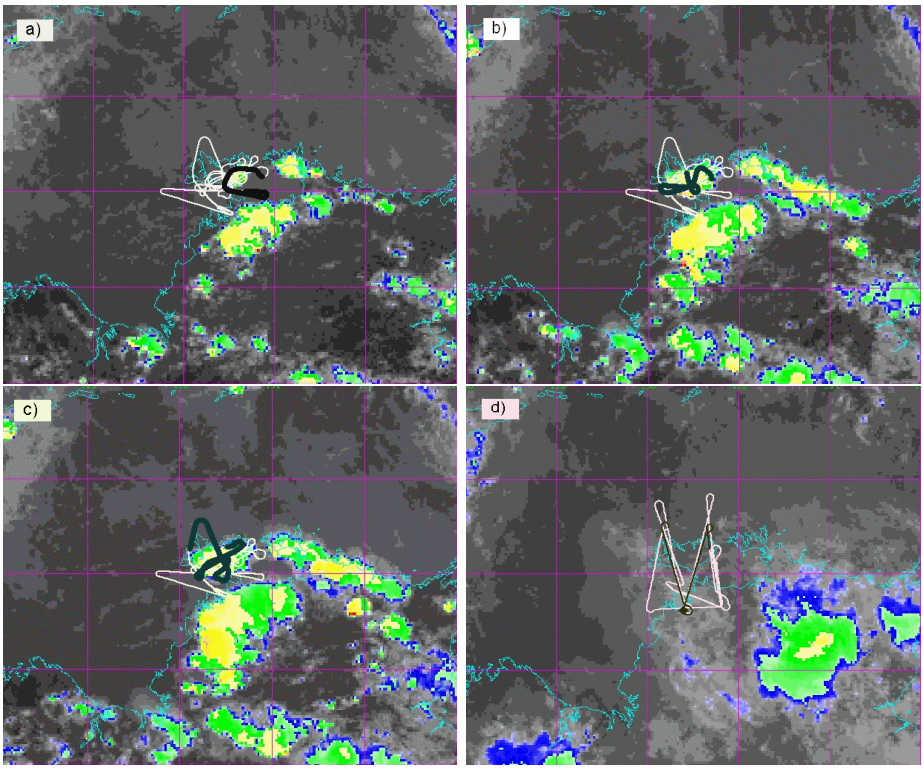

Figure 4.10: GMS-5 satellite pictures of the two flights of 30 November a) 4.33 UTC b) 6.00 UTC c) 6.33 UTC and d) 13.33 UTC (evening flight). Local time Darwin is UTC + 9.5 hours. Superimposed are the flight track (white) and the part of the flight taking place at the time of the image (dark green). Colours indicate the cloud top height (red = highest, followed by yellow)

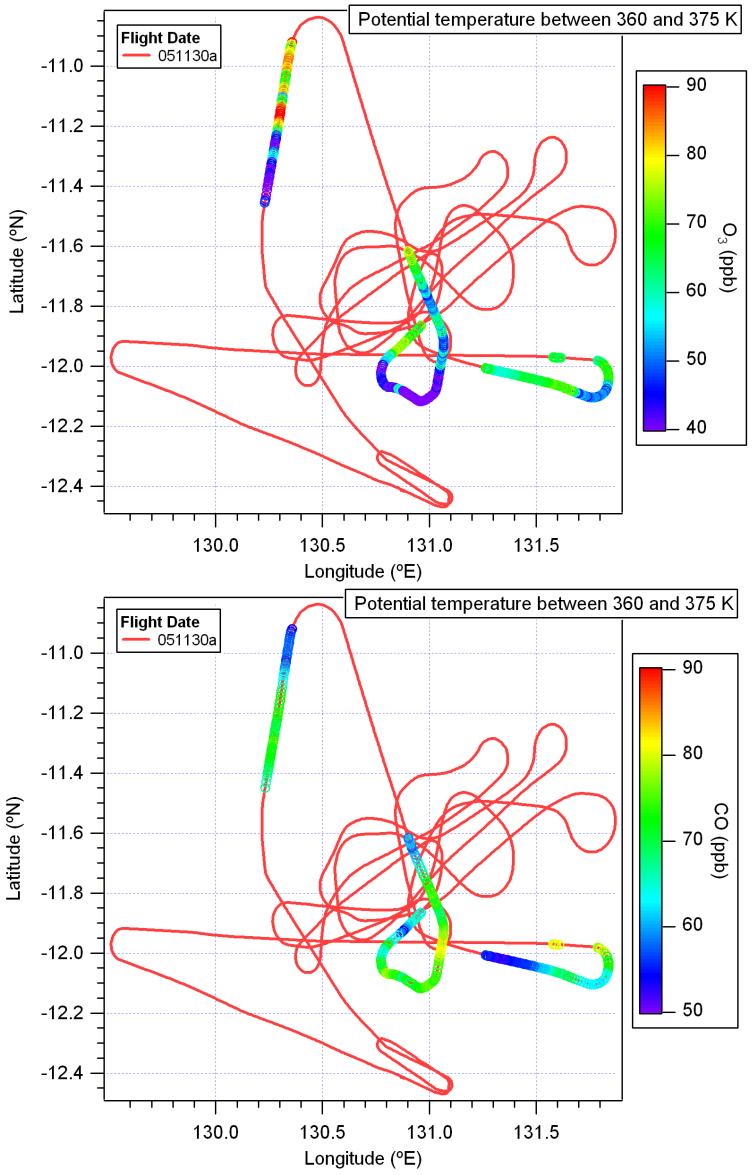

Figure 4.11: Flight path for 051130a. Coloured are the parts of the flight where air was measured with a potential temperature between 360 and 375 K. The colour scales indicate the measured O_3 (top) and CO (bottom) mixing ratios.

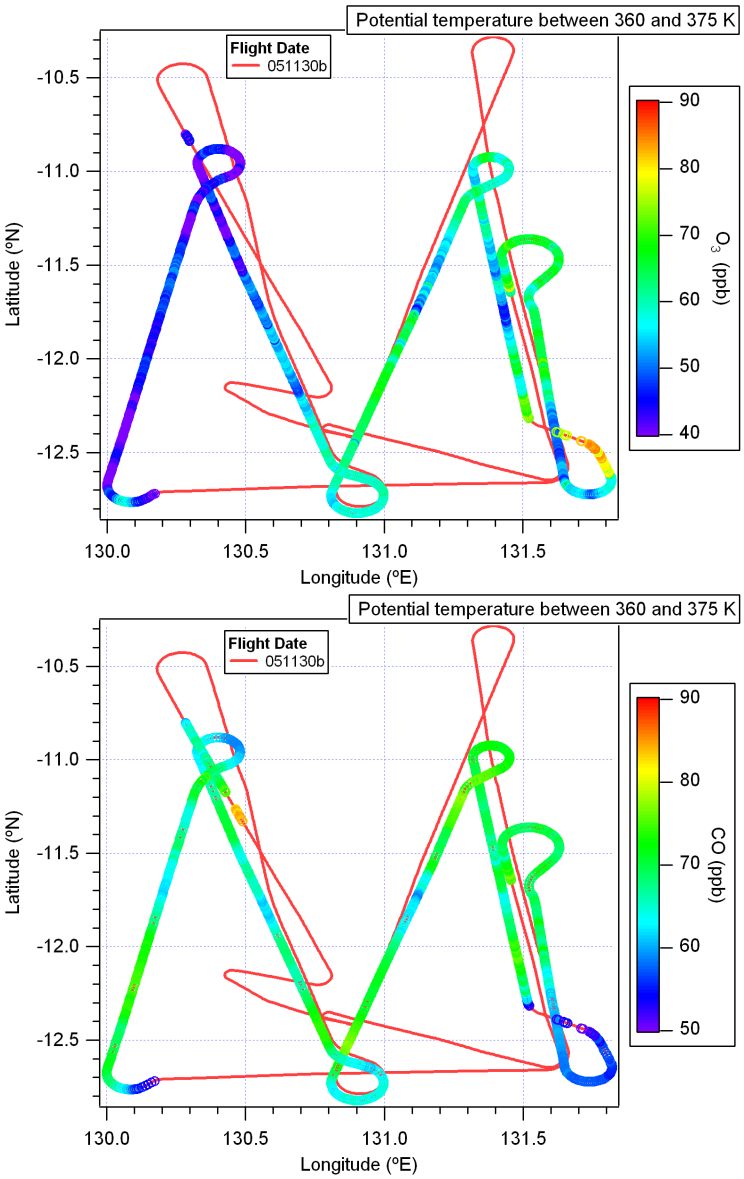

Figure 4.12: Same as previous figure, but now for the 051130b flight.

4.5.3 Influence of the subtropical jet

The third possible explanation is mixing along the subtropical jet. The subtropical jets (STJ) confine the TTL laterally and vary seasonally in both their intensity and meridional position with a strong, equatorwards shifted jet in the winter hemisphere and a weak, meandering, poleward shifted STJ in the summer hemisphere. They form an effective transport barrier for the meridional quasi-isentropic transport between the TTL and the mid latitudes with highest permeability during the weaker summer jet (Haynes and Shuckburgh 2000).
In addition to this quasi-isentropic transport, Konopka et al. (2007) show with simulations of CLaMS (Chemical Lagrangian Model of the Stratosphere) that the tropical flank of the subtropical jet also provides a region with high vertical shear and a resulting deformation of the flow field, thereby causing strong vertical mixing.

The backward trajectories in Figures 4.6 and 4.7 show that the air measured on 30

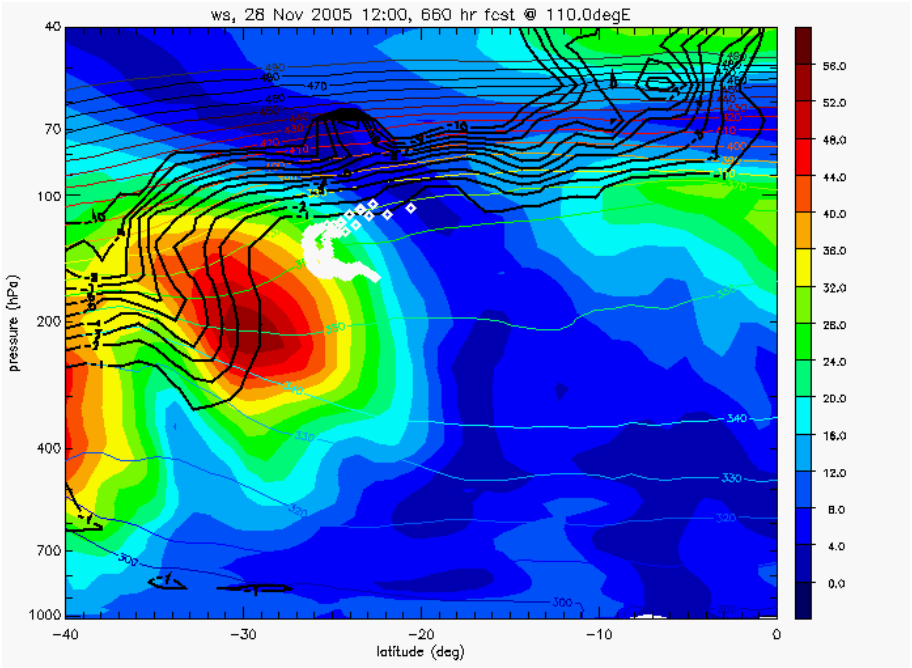

Figure 4.13: Vertical cross section at 110° E of the wind speed (colour contours), PV (black contours) and potential temperature isentropes (thin lines). White squares indicate crossing of the backward trajectories from the Geophysica flight.

November had originated in the Indonesian equatorial region 10 days before, had passed convective systems at various places and travelled for several days along the subtropical jet stream. Figure 4.13 shows the position of the backward trajectories of the second flight in a vertical cross section at 110°E. The wind speed is indicated by colour, with red indicating the highest windspeed. The core of the subtropical jet is observed around 30°S and at 200

hPa or around 360 K. Both potential temperature and potential vorticity show a strong change between both sides of the jet. The location where the backward trajectories cross the vertical cross section is indicated by the white squares. The backward trajectories travelled along the tropical flank of the subtropical jet. The high wind speeds and shear at this flank may promote vertical mixing of the air masses in this area (Konopka et al., 2007). This vertical mixing would then be observed in the correlation plot between the long-lived tracers.

Figure 4.14 shows the correlation between CO and O_3 and CO_2 and O_3 as already shown in Section 4.4.1, but now coloured by potential temperature. In the troposphere, the CO mixing ratio is variable and the O_3 concentration is low. In the stratosphere the opposite is true. Therefore, without mixing of air masses, the correlation plot would show an L-shape. If mixing between the two air masses occurs it will manifest itself as a mixing line connecting the two air masses, as already shown in Section 4.4.2.

The grey dots indicate the first four flights of the campaign. The average correlation is displayed as the black line, and shows the L-shape profiles. Shown in colour are the last four flights, coloured by their potential temperature. The data of both flights on 30 November are consistent with mixing between a potential temperature of about 350 and 390 K as indicated by the hypothetical mixing line (red). This is exactly the height where the subtropical jet is observed. On 5 December no CO was measured, but possible signatures of mixing are also observed in the correlation between CO_2 and O_3, albeit much higher (above 380 K).

Vertical mixing along the flanks of the subtropical jet could therefore be an explanation for the enhanced values of O_3, CO and CO_2 on 30 November and maybe even on 5 December. However, if the subtropical jet caused the enhanced mixing ratios one would also expect to observe enhanced mixing ratios during the flight of 29 November, as the air measured during this day was also transported along the same pathway during at least the previous five days (see Figure 4.5). As this is not the case, the subtropical jet cannot be the only factor influencing the mixing ratios of the probed air.

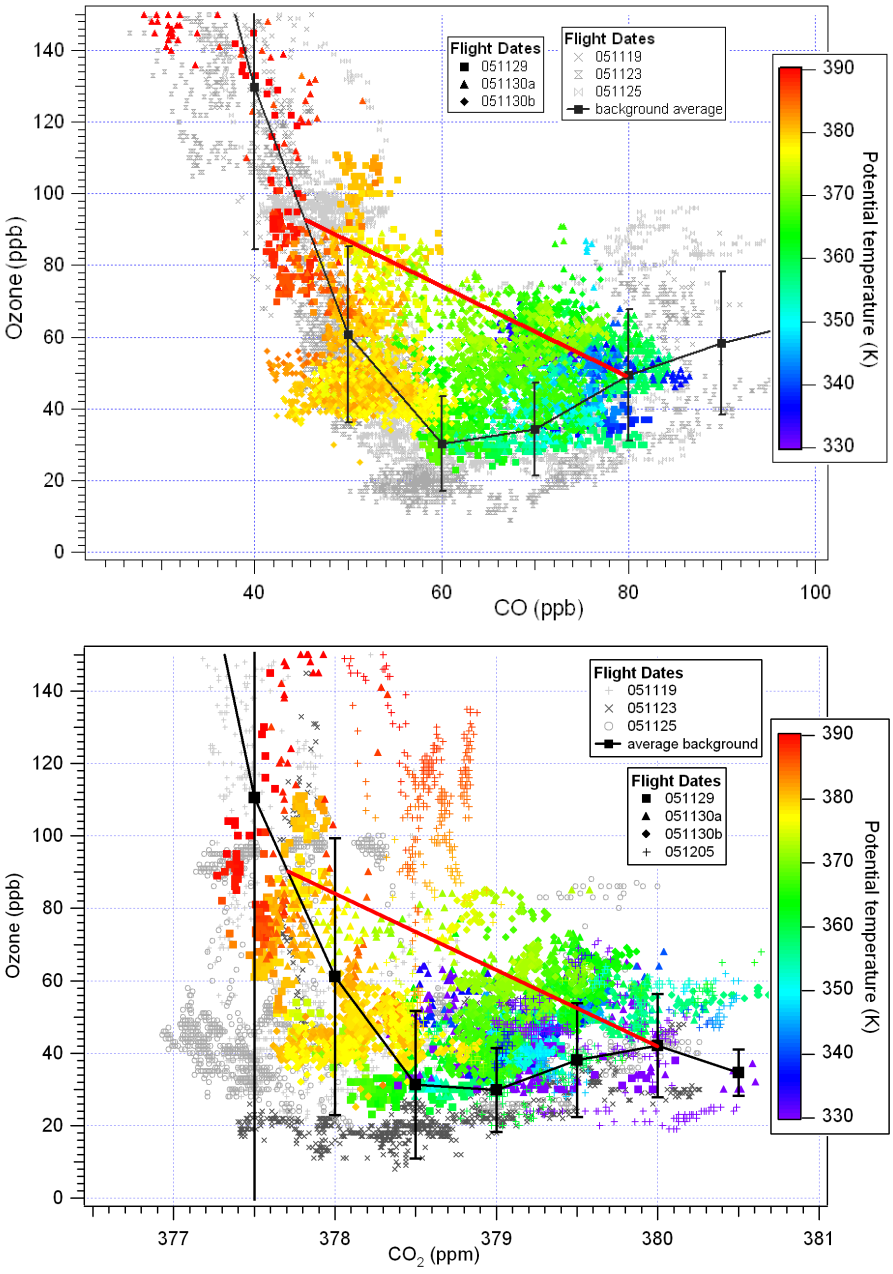

Figure 4.14: Correlation between CO and O_3 (top) and between CO_2 and O_3 (bottom). The first four flights are indicated with the grey dots, and their average with the black line. Error bars indicate one standard deviation of the measurements in the given bin. The coloured points are the last four flights. Data are coloured according to their potential temperature.

4.5.4 Influence of boundary layer pollution over Indonesia

A fourth possible explanation of the enhancements is the influence of boundary layer pollution in the region of uplift of the measured air masses. In Section 4.4.3 it was already discussed that the air masses measured during the last four local flights originated in the region around Indonesia ten days earlier. Especially both flights of 30 November crossed large parts of Malaysia, Borneo and Sumatra (cf. Figures 4.6 and 4.7). The air sampled during the flights of 29 November and 5 December had crossed the region more southwards (Figures 4.5 and 4.8). Boundary layer trajectories during the second half of November 2005 (Fig. 4.15) show a sharp boundary between the origin of boundary layer air masses over Malaysia/northern Indonesia and southern Indonesia. In the north air masses originate over East Asia and from the west. The southern region receives air masses from the Indian Ocean to the west and south. These different air masses converge just south of the equator.

Satellite images indicate that there is more pollution over Malaysia, the northern region

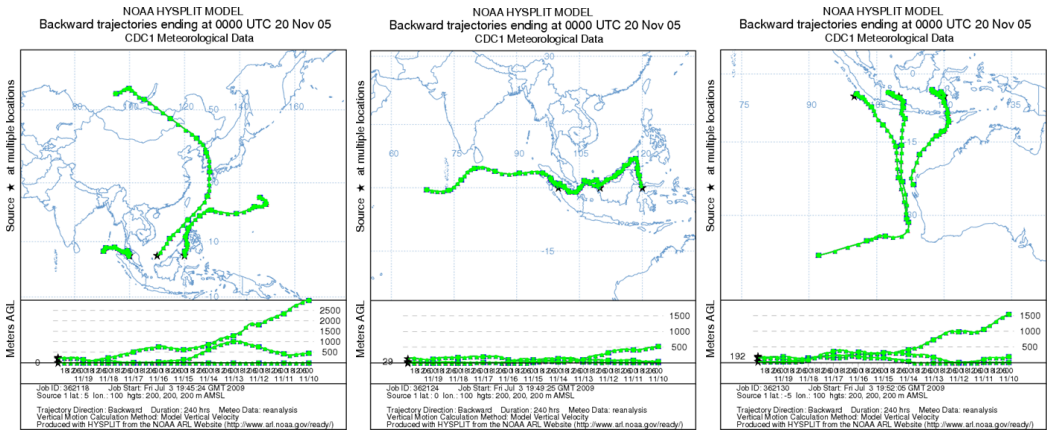

Figure 4.15: NOAA HYSPLIT 10-day backtrajectories ending 20 November 2005 at 5°N (left), 0°N (middle) and 5°S (right) at 200m height.

of Indonesia and the rest of South East Asia where boundary layer air may originate from than over the more southern regions of Indonesia. Figure 4.16 shows CO at the surface for November 2005 from the MOPITT satellite which observes high mixing ratios above Sumatra and Borneo. Figure 4.17 shows the column average CO_2 mixing ratios on 21 November as measured by NOAA ESRL's Carbon Tracker Model. Mixing ratios are high in the Northern Hemisphere and in the biomass burning regions of Africa and South America. A band of high CO_2 mixing ratios is also found reaching from China down to Malaysia and northern Indonesia.

These high mixing ratios could be due to boundary layer pollution from anthropogenic sources or biomass burning. High CO emissions occur from traffic, especially in Malaysia, southern Sumatra and western Java (World Bank Indonesia Office, 2003). Traffic also emits VOCs (Volatile Organic Compounds) which in combination with emissions of NOx could lead to the production of O_3. Cities such as Jakarta have been recognized by the World

Health Organization (WHO) and others as having heavily polluted air. Biomass burning is a large source of O_3 precursors (nitrogen oxides, carbon monoxide, and hydrocarbons) over Malaysia and Indonesia between September and November. In strong biomass burning years, biomass burning is the major source of CO and other O_3 precursors (Duncan et al., 2007). In weaker years, and at the end of the season, which was the case during the SCOUT-O3 campaign, anthropogenic sources may have a similar or stronger impact.

Figures 4.18 and 4.19 show METEOSAT satellite cloud images of November 22 (21.00

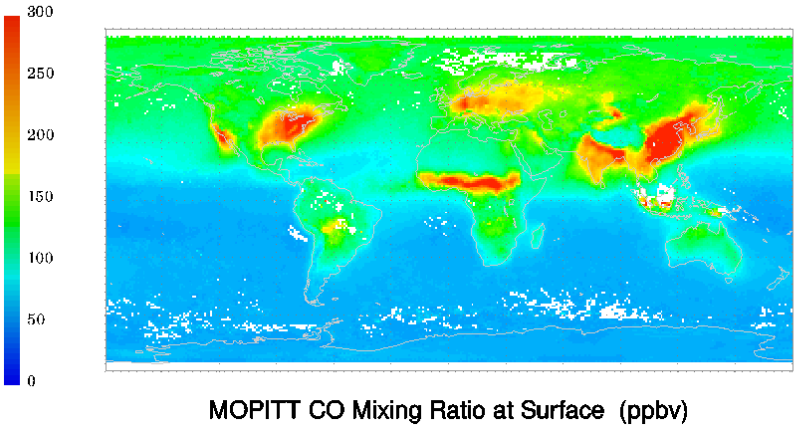

Figure 4.16: Surface CO November 2005. Source: NASA

UTC) and 23 (2:00 UTC), i.e. about 7.5 days before the flights of 30 November, respectively. They show that the deepest convection mostly took place above the northern part of the region and less above the southern part.

The marked convective regions (red circles) correspond with the backward trajectories of the flights of 30 November. The red circle in Figure 4.18 marks a convective region which corresponds in space and time with the backward trajectories of the first flight, the red circle in Figure 4.19 similarly corresponds with the backward trajectories of the second flight.

Strong uplift over this northern Indonesian region of polluted boundary layer air could be an explanation for the higher O_3 and CO mixing ratios found on 30 November, in contrast to the flights of 29 November and 5 December when air originated from regions more to the south and from above the Indian Ocean with cleaner boundary layer air.

Polluted boundary layer air can significantly elevate O_3 in the upper troposphere when large amounts of O_3 precursors are quickly transported upwards by deep convection followed by production of O_3 in cloud outflows (Chatfield and Delany, 1990; Pickering et al., 1996). Pickering et al. (1996) show with a case study over Brazil that initially O_3 production can be up to 7-8 ppb/day, with a total increase of 30 ppb after 3-4 days. Kita et al. (2003) show that during the BIBLE-A (Biomass Burning and Lightning Experiment) campaign in Darwin in September/October 1998 active convection over Indonesia carried polluted air upward from the surface and had a discernible influence on the distribution of O_3 in the up-

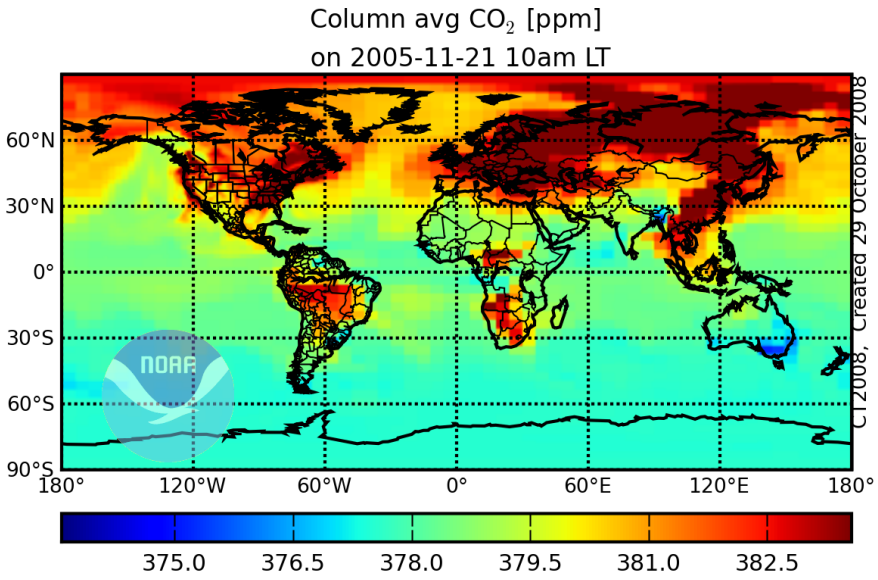

Figure 4.17: Column average CO_2 21 November 2005. Source: CarbonTracker, NOAA-ESRL

per troposphere (up to 13.5 km) over the Indian Ocean, northern Australia, and the south subtropical Pacific Ocean, combined with NO production by lightning. They observed a photochemical production of O_3 of about 15 ppbv in Indonesian air during the week-long transport from Indonesia to Australia.
Folkins et al. (1997) use in situ measurements of NO, NOy, CO and O_3 in the TTL on board of the ER-2 aircraft to demonstrate that deep convection in southeast Asia can inject emissions from biomass burning to near tropical tropopause altitudes. They state that long residence times of chemical species in the upper tropical troposphere could give rise to hemispheric-wide dispersal of these biomass burning plumes and other anthropogenic emissions.
Duncan et al. (2007) show with a modelling study the influence of the biomass burning period in Indonesia on the TTL in the strong El Nino year 1997. They describe that deep convection mixed the wildfire's pollution throughout the troposphere over the tropical Indian Ocean. From there, cross-tropopause transport of the pollution occurred by slow ascent in the TTL to the lowermost stratosphere. The pollution was transported away by the subtropical jets, especially the southern jet, from the main plume over the Indian Ocean, and rapidly circled the globe. They show that CO increased in the entire TTL by more than 40%. The monthly averaged CO perturbation of the TTL in November 1997 over Indonesia and northern Australia was calculated to be 100%. To the northeast of Australia, where the air of the first flights of the SCOUT-O3 campaign originated, the perturbation was much smaller, between 20 and 50 %.
Although the biomass burning over Indonesia in the neutral to weak La Nina year 2005 was much smaller than in 1997 (see http://rapidfire.sci.gsfc.nasa.gov/firemaps for firemaps

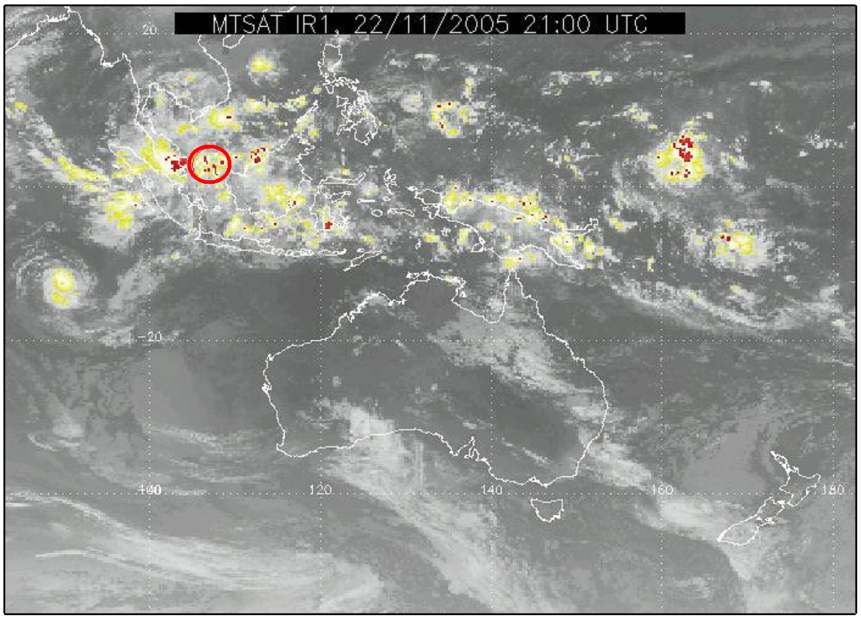

Figure 4.18: METEOSAT satellite IR image of convection over Indonesia on November 22 21.00 UTC. The colour indicates the cloud top temperature, with red the coldest temperature indicating the highest convection.

of 2005), the pathways of biomass burning and other pollution will be comparable, and pollution from the Indonesian region will approach Australia from the west travelling along the subtropical jet.

Analysis of enhancement signatures

To analyse the possible influence of polluted boundary layer air on the vertical profiles measured during the last four flights, enhancement ratios of CO, CO_2, and O_3 are calculated. Enhancement ratios and the progression of these ratios in time and space are mostly used to diagnose the emission, formation, and loss of species in biomass burning (BB) plumes. However, the concepts developed for BB plumes are more generally applicable for BL pollution plumes in the UT. Like in BB, the issue is a localized plume (here generated by convection into the TTL) that exhibits pronounced enhancements of CO, CO_2, O_3 and evolves photochemically and by dilution with a cleaner background. The ratios of enhancements are unchanged by dilution and evolve according to photochemistry (here mainly O_3 production) alone.
Enhancement ratios are defined as $\Delta y/\Delta x$, where Δ indicates the enhancement of a compound in the plume above the local background mixing ratio, y is a compound either emitted directly or produced in the plume, and x is a reference tracer assumed to be conserved in

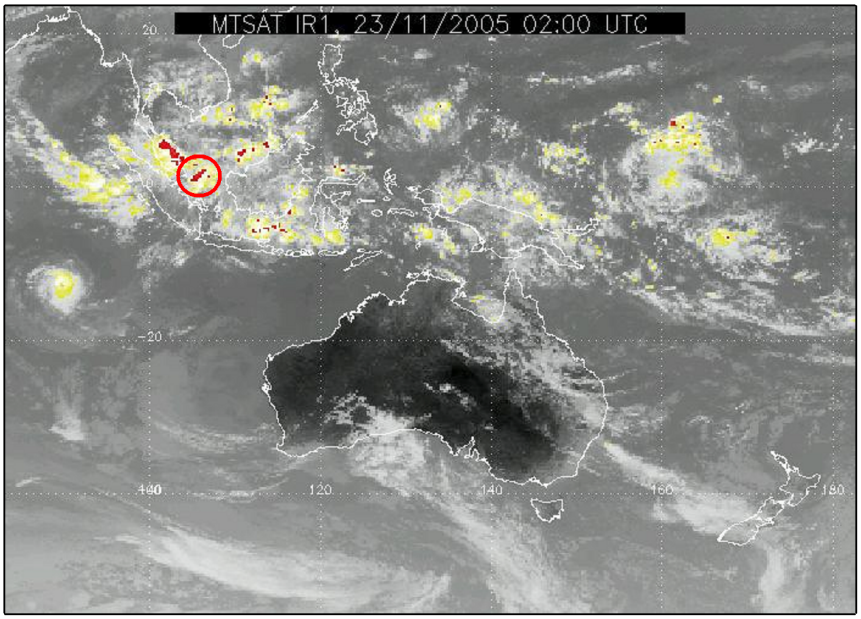

Figure 4.19: METEOSAT satellite IR image of convection over Indonesia on November 23 2:00 UTC. The colour indicates the cloud top temperature, with red the coldest temperature indicating the highest convection.

the plume (usually CO or CO_2) (Mauzerall et al., 1998). The temporal evolution of enhancement ratios is a function of both photochemistry and plume dilution (McKeen and Liu, 1993). The main advantage of enhancement ratios is that they only require simultaneous measurements of the species of interest and the reference species in the plume and the background air. No knowledge of the composition or the amount of emitted pollution at the source is necessary. This is particularly useful in aircraft studies, where this information is usually not available.
Enhancement ratios of this type have been used in combination with estimates of the amount of biomass burned to quantify the contribution of biomass burning to trace gas budgets for CO, CH_4, NOx, and other gases (Crutzen et al., 1979; Crutzen and Andreae, 1990; Laursen et al., 1992). A similar approach has also been employed to estimate photochemical production of O_3 by assuming that $\Delta O_3/\Delta CO$ indicates the number of O_3 molecules produced per CO molecule emitted during combustion (Parrish et al., 1993; Andreae et al., 1994). Most studies however focus on the mid-troposphere, and few data are available for the TTL.
In this study, enhancement ratios of O_3 versus both CO and CO_2 are used. CO_2 is chemically inert in the atmosphere but has large background concentrations and natural variability which can make small enhancements difficult to detect. CO, emitted primarily during smouldering combustion, is an attractive reference tracer because it is not taken up by vegetation, and its background mixing ratio is 3 orders of magnitude lower than CO_2, making detection

of boundary layer pollution plumes easier (Mauzerall et al., 1998). CO is not chemically inert, but above 360 K, oxidation by OH will be slow and CO loss is assumed to be negligible over a period of 10 days.
In order to calculate the enhancements in the observed data the average of the first four flights (05116, 051119, 051123 and 051125) is used as a proxy for the clean background TTL into which the plume gets gradually mixed. Indeed the lowest mixing ratios observed during the last 4 flights agree fairly well with this choice. Enhancements during the last four flights (051129, 051130a, 051130b and 051206) are calculated as the difference between the observed mixing ratios and this background profile.
The enhancement ratios $\Delta y/\Delta x$ are evaluated as the slope of a regression of Δy versus Δx over the whole vertical range of interest. This regression slope is only weakly sensitive to the specific choice of background mixing ratios. The theta range included here is 340-380 K (i.e. the whole TTL) as the region over which convective detrainment could have occurred and within which the enhancements of CO, CO_2, and O_3 are observed.

Figure 4.20 shows the correlation plots between ΔO_3 and ΔCO, ΔO_3 and ΔCO_2 and

Table 4.1: Correlation factors (R) and the slopes of the regressions between ΔO_3, ΔCO and ΔCO_2 between 340 and 380 K for the last four flights separately and together. Units are ppb/ppb for $\Delta CO/\Delta O_3$ and ppb/ppm for $\Delta O_3/\Delta CO_2$ and $\Delta CO/\Delta CO_2$.

Flight date	**slope $\Delta O_3/\Delta CO$**	**R**	**slope $\Delta O_3/\Delta CO_2$**	**R**	**slope $\Delta CO/\Delta CO_2$**	**R**
20051129	-0.04	-0.01	25.2	0.30	3.7	0.25
20051130a	1.02	0.67	16.7	0.69	10.3	0.67
20051130b	1.26	0.52	31.8	0.75	10.3	0.56
20051205	-	-	9.69	0.39	-	-
together	1.14	0.51	16.1	0.51	8.84	0.60

between ΔCO and ΔCO_2 for the last four flights. The line indicates the regression slope with the correlation coefficient R for all four flights together. Table 4.1 gives the slope of the regression and the correlation coefficient R for the last four flights separately and for all four flights together. A clear correlation between O_3, CO_2 and CO exists for the four flights together, which supports the hypothesis that boundary layer pollution is responsible for the enhancements. When observing each flight separately it turns out that especially the two flights on 30 November are influenced by boundary layer pollution. These two flights show positive correlation coefficients between all three trace gases. This is what is expected in case of pollution, as due to an increase of CO and CO_2, and consecutive production of O_3, also the O_3 mixing ratio will increase. The flight of 29 November shows no correlation between O_3 and CO, and only a correlation of 0.3 and 0.25 between O_3 and CO_2 and CO_2 and CO, respectively. This is much lower than the correlation coefficients for the flights on 30 November. For the flight on 5 December only the enhancement ratio of $\Delta O_3/\Delta CO_2$ could be calculated, but this enhancement ratio also shows a lower correlation factor than for the flight on 30 November. These results confirm the hypothesis that there is less influence of boundary layer pollution on the measurements of 29 November and 5 December because the

uplift occurred over a region more southwards and less polluted than the region where air measured on 30 November originated from.

To confirm that the enhancements in the plume originate from uplift from the Indonesian

Table 4.2: Enhancement ratios as published in Mauzerall et al. (1998). Units are ppb/ppb for $\Delta CO/\Delta O_3$ and ppb/ppm for $\Delta O_3/\Delta CO_2$ and $\Delta CO/\Delta CO_2$.

Age of plume	$\mathbf{\Delta O_3/\Delta CO}$	$\mathbf{\Delta O_3/\Delta CO_2}$	$\mathbf{\Delta CO/\Delta CO_2}$
fresh (< 0.2 days)	0.15 ± 0.37	5.1 ± 2	47.4 ± 6.4
recent (0.5 - 1 day)	0.32 ± 0.76	8.6 ± 1.1	23.2 ± 2.0
aged (2 - 5 days)	0.71 ± 0.12	12.4 ± 1.7	21.3 ± 1.2
old (> 6 days)	0.74 ± 0.9	12.5 ± 2.6	16.1 ± 1.9

region more than a week before, it is also important to define the age of the plume. Mauzerall et al. (1998) give an indication of the enhancement ratios found in biomass burning plumes of different age. They divide the plumes into four categories, defining plumes younger than 0.2 days as fresh, between 0.5 and 1 day as recent, between 2 and 5 days as aged, and older than 6 days as old. The enhancement ratios relevant for this study as published in Mauzerall et al. (1998) are summarized in Table 4.2. The $\Delta O_3/\Delta CO$ ratio increases due to O_3 production as the plume ages. Old plumes have an enhancement ratio of 0.74 ± 0.9. The flights on 30 November have enhancement ratios of 1.02 and 1.26, indicating a plume of at least six days old.

The $\Delta O_3/\Delta CO_2$ ratio also increases over time. Mauzerall et al. (1998) give a ratio of 12.5 ± 2.6 for old plumes. The $\Delta O_3/\Delta CO_2$ ratio measured during the first flight on 30 November is 16.7 and during the second flight 31.8. These enhancement ratios are both higher than the ratios given by Mauzerall et al. (1998), and may indicate old to very old plumes.

In contrast to the other enhancement ratios, the $\Delta CO/\Delta CO_2$ ratio decreases over time. The SCOUT-O3 measurements show a $\Delta CO/\Delta CO_2$ ratio of 10.3 for both flights. Again, this supports the idea of a very old plume (Mauzerall et al. (1998): 16.1 ± 1.9 for old plumes). It has to be taken into account however, that it is impossible to differentiate between biomass burning and other sources of pollution in this study, and therefore enhancement ratios may differ from studies where only biomass burning plumes were measured, as in Mauzerall et al. (1998). However, the dynamical mechanisms of dispersal of biomass burning plumes would also apply to other types of emissions and the result of an “old or very old” plume is consistent with the actual circumstances of this case and with the results of Heyes et al. (2009).

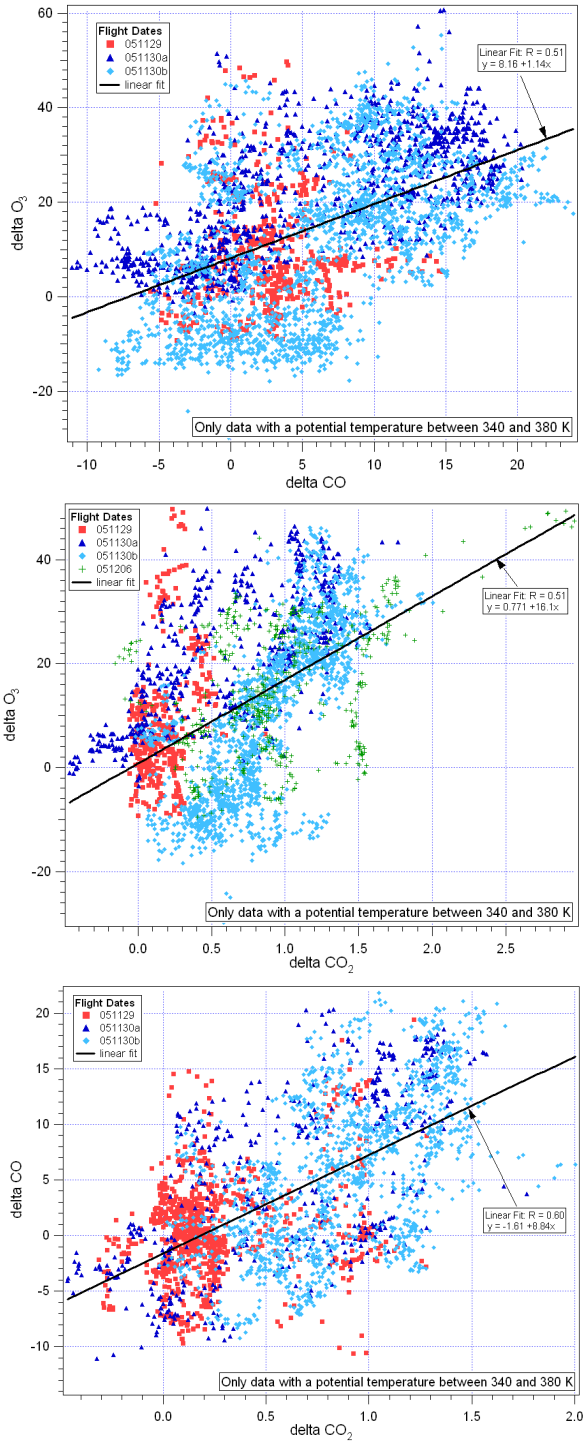

Figure 4.20: Correlation between ΔO_3 and ΔCO, ΔO_3 and ΔCO_2 and between ΔCO and ΔCO_2 for the last four flights. The line indicates the regression and the correlation coefficient R for all flights together. Units are ppb for CO and O_3 and ppm for CO_2.

4.6 Conclusions

The last four flights of the SCOUT-O3 campaign (051129, 051130a, 051130b, 051206) show enhanced mixing ratios of O_3, CO and CO_2 between 355 and 380 K potential temperature in comparison with the first four flights (051116, 051119, 051123, 051125). This suggests vertical mixing through the TTL, influence of polluted boundary layer air or stratospheric influence. Especially the two flights on 30 November, which focused on measuring the local convective storm Hector showed enhanced mixing ratios.
However, this local storm cannot explain the enhanced mixing ratios. Satellite pictures were compared with the flight paths and the part of the flights where the enhanced mixing ratios were found. It turned out that the elevated mixing ratios were already found before the onset of the convective system, and at all sides of the system. Therefore, Hector alone cannot explain the enhanced mixing ratios, and other possible explanations were studied.
The influence of horizontal isentropic inmixing from the extratropical stratosphere was also found to be not relevant. Horizontal inmixing is not consistent with the elevated CO concentrations, and the correlation between N_2O and O_3 showed no influence of aged stratospheric air below the tropopause.
Backward trajectories showed that the air during the last four flights travelled along the subtropical jet for a few days and originated from the Indian Ocean or Indonesia ten days earlier, in contrast to the first four flights, when air approached Darwin from the West Pacific. A study by Konopka et al. (2007) shows that the subtropical jet provides a region with high vertical shear and a resulting deformation of the flow field, thereby causing strong vertical mixing. Such mixing would tend to increase O_3, CO, and CO_2 mixing ratios in the TTL. Correlations between O_3 and CO confirm the possibility of vertical mixing. Vertical mixing due to strong wind shear in the vicinity of the subtropical jet could therefore provide an explanation for the enhanced mixing ratios. However, it would not explain differences between the flights of 29 November and 5 December and the two flights on 30 November. Only small enhancements were found during the first two flights, although the air also travelled along the jet.
The most reasonable explanation for the enhanced mixing ratios which agrees with our measurements is therefore convective uplift of polluted boundary layer air over Indonesia and Malaysia. Air samples during the flights of 30 November had crossed over large parts of Indonesia and Malaysia where pollution was present and deep convection occurred. In contrast, the backward trajectories of 29 November and 5 December cross the region more to the south or originate more over the Indian Ocean where the boundary layer was cleaner. Enhancement ratios, used to assess the influence of biomass burning and pollution plumes, is consistent with the hypothesis that plumes older than 6 days were observed, which does agree with the trajectories.

Chapter 5

Residence times and vertical transport rates in the background TTL

5.1 Introduction

The vertical net transport in the TTL is controlled by three processes: deep convection, vertical mixing and slow diabatic ascent. Vertical profiles of ozone, CO and other trace gases in the previous chapters and other studies (e.g. Folkins et al. 2002) show that convection contributes significantly to the vertical transport in the lower TTL, but that this influence declines rapidly with height in the upper TTL. In the upper TTL, above the level of zero radiative heating, slow ascent over the tropics is probably the most dominant factor. This slow ascent is forced by the wave-driven stratospheric Brewer-Dobson circulation that is balanced by radiative heating (Holton et al., 1995).
The quantification of the net vertical transport is important to determine the time air parcels reside in the TTL. The residence time allows to assess which compounds can reach the stratosphere chemically unaltered and which species will be chemically processed before reaching the stratosphere (Holton et al., 1995). This is especially important for short-lived chemical compounds which can reach the stratosphere and thus can have a major impact on stratospheric chemistry (WMO, 2007). Due to the weaker Brewer-Dobson circulation in NH summer than in NH winter (Bonazzola and Haynes, 2004), it is expected that in NH summer the residence times of the parcels are longer than in NH winter.
Different studies to define the net vertical ascent rate in the TTL have been performed over the past years.
Fueglistaler et al. (2004) used trajectory calculations to analyze pathways of air parcels between 340 and 400 K. They observed an average time for an air parcel to ascend from 340 to 400 K of about a month in both January/February and July/August 2001. The residence time was highest for trajectories starting at 360 K. At this level an air parcel needed on average 13 days for a change in potential temperature of $\pm$ 10 K. Trajectories starting at 370 K needed on average 9 days to ascend or descend 10 K. However, these results are most

probably an underestimate, since it is expected that the use of vertical winds from meteorological datasets causes an overestimation of vertical transport rates in the TTL (WMO, 2007; Wohltmann and Rex, 2008).
In order to reduce the influence of the uncertainty of the vertical wind fields, Krüger et al. (2009) used a reverse domain filling trajectory model coupled with a radiative transfer model. They deduce a mean residence time of 34 days for the layer between 360 and 380 K (lower TTL), 38 days for the layer 380 - 400 K (upper TTL) and 70 days for the layer 360 - 400 K for the 1962 - 2001 period. They show that there is large interannual variability for the residence time varying up to ± 20% from the long-term mean, due to ENSO variations, with strongest variability seen in the lower part of the TTL.
Kremser et al. (2009) also compared calculations of residence times in a CCM for northern hemisphere winter (1995/1996). They found a residence time of 9-10 days between 385 and 395 K when they used reference trajectories based on ERA 40 heating rates (diabatic trajectories), and residence times of mostly shorter than 5 days when transport was only based on vertical winds (kinematic trajectories).
Folkins et al. (2006) used ozonesonde O_3 data and satellite CO measurements and tried to reproduce the observed seasonal cycles of O_3 and CO at the tropical tropopause between 20°N and 20°S with a simple model driven by radiative mass fluxes. They calculated "an elapsed time since convective detrainment" at the altitude of 17 km, which can be interpreted as the age of air. The estimate of age was 40 days at 17 km during NH winter, but it was reduced to 25 days when modeled with correction for air mass export to the extratropics.
A residence time of about 80 days to cross the 360-380 K layer has been inferred from a onedimensional tropical-mean model of Folkins and Martin (2005). This is almost certainly an overestimate, since it neglects the dispersive effects of geographical variation in vertical velocity (WMO, 2007).
The large spread in the residence times indicates that there are still large uncertainties in the processes influencing the net vertical transport rates and large uncertainties in vertical wind profiles in the tropics. Also, satellite and radar observations may tend to underestimate other factors influencing the transport rates, like water vapor, clouds and ozone (Corti et al., 2005, 2006; Fueglistaler and Fu, 2006). Large interannual and seasonal differences and different geographical locations should also be studied in more detail.
Therefore, a comparison with in situ observations is indispensable to validate the models. Until now, only few analyses with in situ data have been made.
A useful tracer to define ascent rates is CO_2. The CO_2 mixing ratio in the tropical lower troposphere has a well characterized trend over time, upon which is superimposed a pronounced seasonal cycle. This seasonal signal, together with slow vertical transport gives rise to a "tape recorder" signature in the tropical UTLS, which may be used to trace the time since air left the near-surface environment and entered the TTL. Boering et al. (1996) observed that the seasonal cycle of CO_2 occurring in the planetary boundary layer can be found with little damping at 390 K and 420 K with a time lag of 60 ± 20 days and 110 ± 30 days, respectively.
Park et al.(2007) used the same CO_2 clock model as Boering et al. (1996) but focussed on mean ascent rates in the TTL instead of the lower stratosphere. They used measurements made during the CR-AVE and TWP-ICE campaigns in January/February 2006 above Costa

Rica and Australia, respectively, and could therefore compare data from the Northern Hemisphere with the Southern Hemisphere. The data confirm that air entering the upper TTL has been efficiently mixed between the hemispheres and has a CO_2 mixing ratio very similar to the average of surface stations close to the ITCZ. They also observe limited impact of mixing and convection at altitudes above 360 K and therefore consider the level of 360 K as the average top of convection in the deep tropics for NH winter and as the level where the air has near zero age. Using the near-linear increase of tropical tropospheric CO_2 during winter, they calculate for the upper TTL during NH winter a mean vertical ascent rate of 1.5 +/- 0.3 mm s^{-1} and a residence time of 26 $\pm$ 4 days in the 360 - 390 K layer. Schoeberl et al. (2008) argue that these vertical ascent rates are an overestimate. They show that the assumption that all the CO_2 transport above 360 K is due to mean upward advection cannot be justified. With help of CO_2 simulated by the Global Modeling Initiative-Chemical Transport Model (GMI-CTM) they calculate that vertical and horizontal eddy transport of CO_2 accounts for nearly half the tendency, especially in the lower TTL.
The measurements of the HAGAR instrument provide a unique set of CO_2 data, in combination with long lived tracers, measured in different seasons and at different hemispheres, to extend the knowledge of vertical ascent. In this chapter time scales and residence times from four different regions will be estimated: the Indian Ocean (APE-THESEO, 2/1999), Brazil (TROCCINOX, 2/2005), the Maritime Continent (SCOUT-O3 11-12/2005) and West Africa (AMMA/SCOUT-O3 8/2006). This is the first study in which both the NH winter and summer can be compared and where long-lived tracers are used to exclude data originating in or influenced by the extratropical stratosphere.

5.2 Measurements and method

The base of this study is the work of Boering et al. (1996) and Park et al. (2007). Boering et al. (1996) suggest that the average data for CO_2 at Mauna Loa (19°N, 155°W) and Samoa (14°S, 170°W) is a suitable approximation of the air lofted into the upper troposphere ("CO_2 Index", data updated by T. Conway). The seasonal rates of change of the Index appear capable of providing a very sensitive "CO_2 clock" for tracing the time since air left the near-surface environment and entered the TTL.
This study will make use of this CO_2 index. Figure 5.1 shows the average CO_2 mixing ratio of Mauna Loa and Samoa at the surface. The four campaigns on this timeline are indicated by the arrows. CO_2 data from the APE-THESEO, TROCCINOX, SCOUT-O3 and AMMA/SCOUT-O3 campaigns are used. The data cover the Southern Hemisphere (APE-THESEO, TROCCINOX and SCOUT-O3) and the Northern Hemisphere (AMMA/SCOUT-O3) and both Northern Hemisphere winter (APE-THESEO, TROCCINOX and SCOUT-O3) and summer (AMMA/SCOUT-O3).
It is assumed that at a level of 360 K the air is well mixed between the hemispheres and the air has an age of near zero, as confirmed by Park et al. (2007) and Sherwood and Dessler (2003) so that the CO_2 mixing ratios of the CO_2 index can be used as a proxy for the mixing ratios at 360 K. In order to assemble typical TTL background tracer profiles from the observed data, data were selected according to the following criteria: firstly, samples

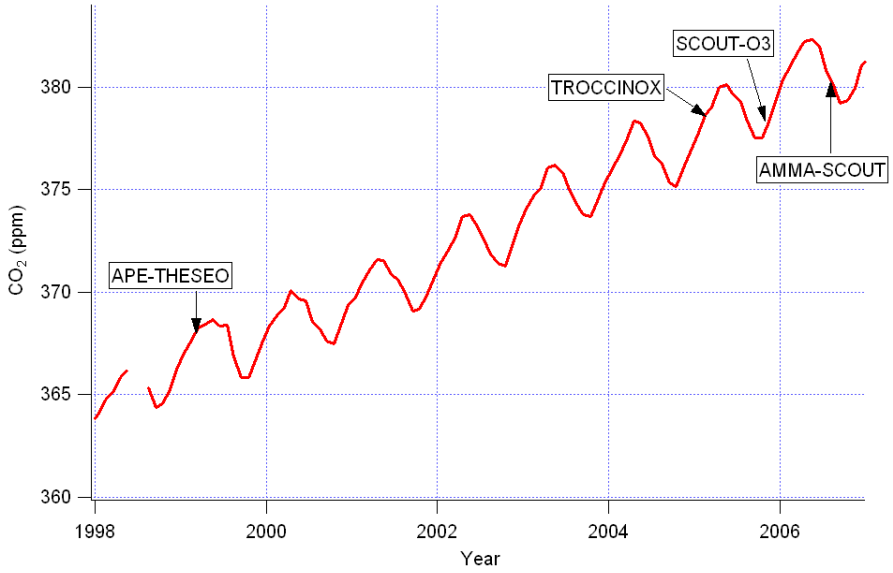

Figure 5.1: Average CO_2 surface mixing ratio at Mauna Loa and Samoa.

exhibiting CFC-12 mixing ratios significantly below the well-defined observed tropospheric value of 540 ppt, i.e. samples with values of CFC-12 smaller than 532 ppt, were excluded because such low values are almost certainly due to horizontal inmixing from the extratropical stratosphere. For APE-THESEO samples with values of CFC-12 smaller than 528 ppt were excluded since in 1999 global CFC-12 mixing ratios were lower than in 2005/2006. In this study CFC-12 is used instead of N_2O (used in the previous two chapters) to exclude stratospheric influences, because CFC-12 was more precisely measured during TROCCINOX. Furthermore, to examine only tropical profiles, only data between 14°N and 14°S are included for this analysis. For TROCCINOX most flights were made south of 14°S, so in this case all data northwards of 23°S are used. Lastly, since only average ascent rates are of interest, relatively undisturbed profiles are needed: flights which focused on measuring convective systems are not used. The flights which are used for each campaign are displayed in the relevant figures.
After the selection of the data, the net vertical mean ascent is calculated following two different methods. As a first approach the slope of the CO_2 index is used to calculate ascent rates. The different slopes are obtained from the linear part of the index around the time of the campaign. This slope is used to calculate the mean vertical ascent rate and the residence time. The residence time is calculated by dividing the difference in CO_2 mixing ratio between the 390 and 360 K potential temperature level with the slope value (5.1).

$$t_{res} = ([CO_2(390K)] - [CO_2(360K)])/(\Delta CO_{2index}/\Delta t_{index}) \quad (5.1)$$

where t_{res} is the residence time in days, [CO_2(390K)] is the average CO_2 mixing ratio at 390 K, [CO_2(360K)] the average mixing ratio measured at 360 K, and $\Delta CO_{2index}/'\Delta t_{index}$ the slope of the CO_2 Index. Subsequently, the ascent rate is calculated by dividing 30 K (390-360 K) by the residence time (5.2):

$$w=(390\text{-}360)K/t_{res} \tag{5.2}$$

where w is the net vertical ascent (K/day).
This first approach, however, can only be used if the timing of the campaign is such that the increase or decrease of CO_2 is more or less linear over time for several months before the campaign. Therefore, when the campaign is just after a change in the seasonal cycle from a positive to a negative slope or vice versa, as is the case during the SCOUT-O3 campaign, this approach is not valid and a different approach to calculate the vertical ascent rate has to be used. In this second approach, the CO_2 index itself is fitted to the measured CO_2 profiles of the different campaigns. The assumption is made that the ascent rates are uniform throughout the TTL. A simple model formula for this approach is:

$$CO_2(\Theta, t) = CO_{2-index}\ (t - [\Theta\text{-}360K]/w) \tag{5.3}$$

where $CO_{2-index}$(t) for an arbitrary time t is derived by linear interpolation of the monthly mean CO_2 index, Θ is the potential temperature (K), t is the time (years) and w is the vertical ascent rate (K/day). This modeled CO_2 profile is then fitted to the observed CO_2 profiles to establish the ascent rate providing the best fit. Both approaches assume that the CO_2 time lag equals the actual transport time between any two theta levels above 360 K. Thus the assumption is made that the constructed "background TTL" profiles are not significantly influenced by transport processes other than slow diabatic ascent above 360 K. The limitations of this assumption will be discussed in Section 5.4.

5.3 Results

Figure 5.2 shows the CO_2 profiles for the four campaigns. The profiles, taken in different years and seasons, all show a different shape. A clear increase in CO_2 mixing ratio between 1999 (APE-THESEO) and 2005/2006 is present. The mixing ratios from the boundary layer up to the lower TTL are very variable, as seen by the large scatter up to 360 K. Up to this level, local processes such as convection and daily cycles of CO_2 uptake by the vegetation dominate. Above 360 K, a more coherent signal is observed, dominated by slow ascent.

In order to get a qualitative idea of this slow ascent through the upper TTL, Figure 5.3 shows the CO_2 index, together with the average CO_2 mixing ratios measured during the campaigns for 10 K steps between 360 K and 390 K. The CO_2 index is also plotted with a delay of 1 month and 2 months, thus giving an indication of the residence time.

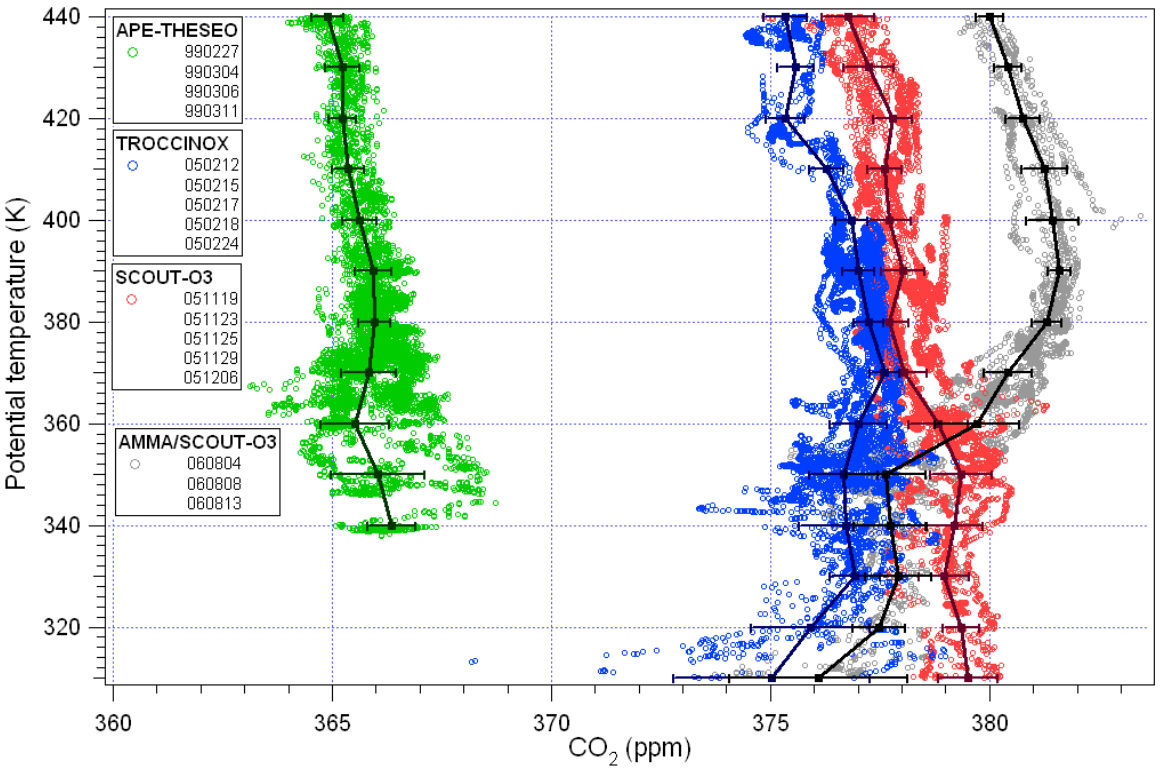

Figure 5.2: CO_2 profiles for the four campaigns. Average profiles in black with error bars indicating one standard deviation of the measurements in the given potential temperature bin.

The mixing ratios measured at 360 K do coincide with the CO_2 index during the SCOUT-O3 and AMMA/SCOUT-O3 campaigns, indicating that the assumption that the air at 360 K has a near zero age is justified for these campaigns. During the APE-THESEO and TROCCINOX campaigns the measured mixing ratios are lower than the average CO_2 index (by 2 and 1.5 ppm respectively). During TROCCINOX a lot of convective activity was measured, and influences of this convection are observed up to 370 K (Baehr et al., in preparation). It is thus likely that the CO_2 mixing ratio at 360 K reflect in part the local boundary layer and are therefore not representative of the global background TTL. Therefore, in this study, the calculations will be based only on aircraft data between 370 and 390 K levels, and whenever a mixing ratio for the background TTL at 360 K is needed in the analysis, it will be set equal to the CO_2 index mixing ratio during TROCCINOX.
The APE-THESEO data do not fit with the CO_2 index at all. The sampling region was largely non-convective, thus convection cannot explain the lower values measured. About 0.5 ppm of the discrepancy can be explained by the fact that the APE-THESEO data were not calibrated on the same calibration scale as the rest of the data used in this study (cf. Appendix A). The remaining discrepancy may partly be explained by a lower accuracy of the APE-THESEO data, and a potential bias due to interference by water vapour (since the

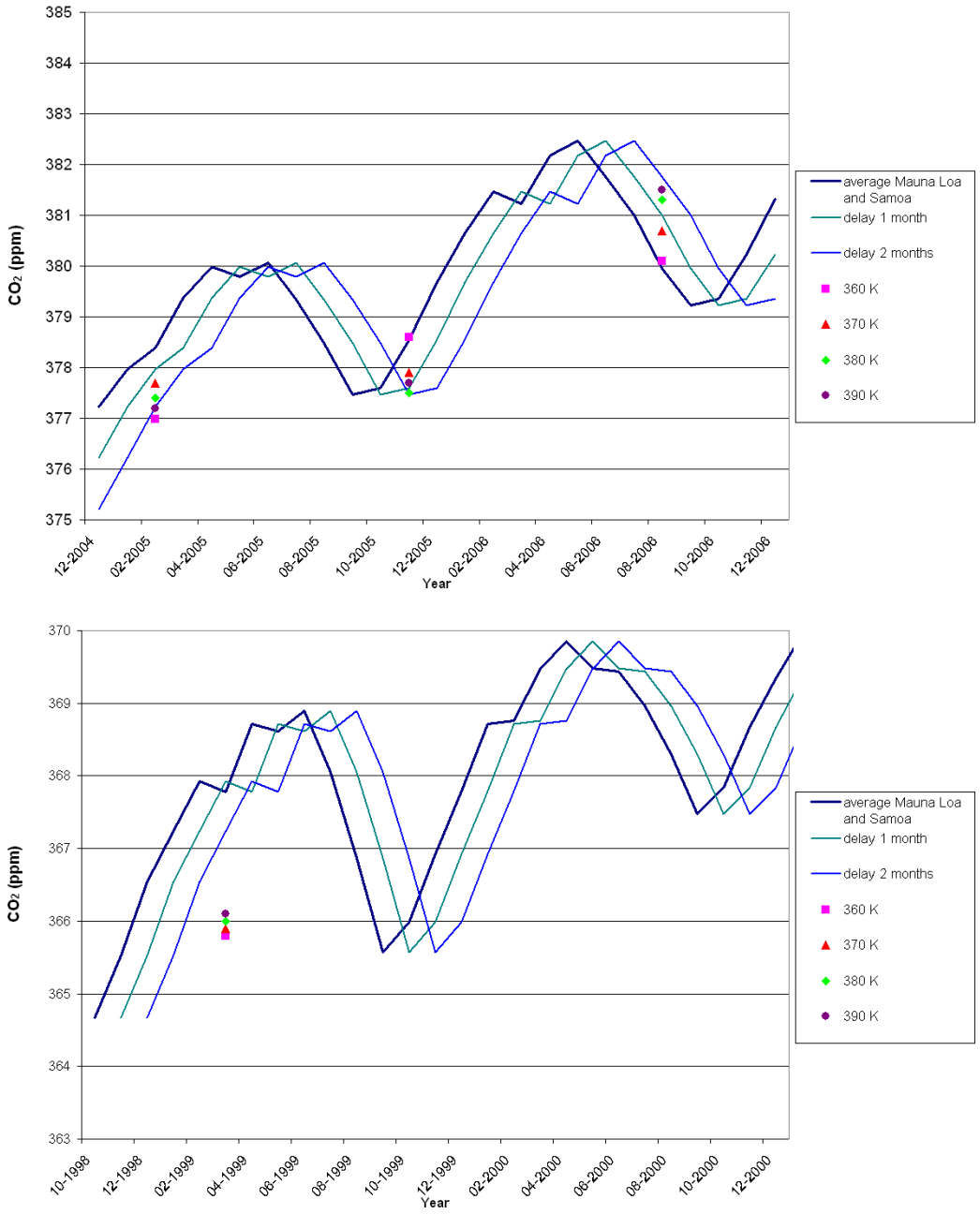

Figure 5.3: CO_2 index (line) compared with measured data (points) during a) TROCCINOX, SCOUT-O3 and AMMA/SCOUT-O3 and b) APE-THESEO. CO_2 index delayed by 1 and 2 months are also plotted.

sampled air was not dried before measurement at that time).
At the 370 K potential temperature level, the data are delayed by less than a month in the case of the last two campaigns, and a bit more during the TROCCINOX campaign, when the CO_2 index mixing ratio is used as the mixing ratio at 360 K. Above 370 K, the ascent rate appears to increase, and the points come closer to each other. This can be most clearly seen during the AMMA/SCOUT-O3 and TROCCINOX campaigns, where the 380 K point is located just past the 1 month delay line, and the 390 K point is not much older. Because the SCOUT-O3 campaign took place just after the change from decreasing CO_2 mixing ratios to increasing CO_2 mixing ratios, it is harder to estimate the residence time from this plot for the higher potential temperature levels, since there is no large change in mixing ratio between the 1 month delay line and the 2 month delay line. Indeed, the 390 K point lies above the 380 K point, indicating that the sign of the slope changes in between these two potential temperature levels.
Table 5.1 gives a more quantitative indication of the residence times. First the residence times are calculated with the first approach using the slopes of the CO_2 index, as described in the previous section. The slopes for the different campaigns are: APE-THESEO 0.019 ppm/day, based on the slope between November 1998 and March 1999, TROCCINOX 0.024 ppm/day based on the slope between November 2004 and February 2005, SCOUT-O3 0.033 ppm/day based on the slope between October and December 2005, and -0.028 ppm/day for AMMA/SCOUT-O3 based on the slope between June and August 2006. The first two columns indicate the potential temperature and the according height. The third column gives the average CO_2 mixing ratio at the respective level. The fourth column lists the number of days the air parcels travelled from the 360 K level to the respective level calculated using equation 5.1, and the fifth column the resulting mean ascent rate between the 360 K level and the respective level calculated using equation 5.2.
Since the mixing ratios during APE-THESEO are not changing much with height, and in fact show a positive instead of a negative slope (see fig. 5.4), the calculated results in the table are unphysical (negative). For the other three campaigns the data give reasonable results for transport times and ascent rates. Note that for the TROCCINOX campaign, the 360 K mixing ratio is taken from the CO_2 index instead of the measured data, since the measured profile is likely too much influenced by local convection delivering regionally CO_2-depleted boundary layer air to the 360 K level. The time the air travelled from 360 K to 370 K is estimated as 30 days during TROCCINOX and 24 days during SCOUT-O3, yielding an average ascent rate of 0.3 and 0.4 K/day, respectively. Transport to the 380 K level took 42 days for TROCCINOX and 35 for SCOUT-O3, yielding an average ascent rate of 0.5 K/day for TROCCINOX and 0.6 K/day for SCOUT-O3. The travel time above 380 K cannot be estimated the same way for the SCOUT-O3 campaign, since the slope of the CO_2 index is changing one month before the campaign. For TROCCINOX the time from the 360 to the 390 K is 47 days. The calculations also suggest an increase with height of the ascent rate for TROCCINOX, but uncertainties are likely at least as large as the suggested height variation.
For AMMA/SCOUT-O3 the transport to the 370 K level took 15 days, faster than during SCOUT-O3 and TROCCINOX. Above that level ascent apparently became slower, and the 380 K level is reached only after 44 days. Finally, after 51 days air reached the 390 K level.

The apparent variation with altitude is again unlikely to be significant. The average ascent rate between 360 and 390 K was 0.6 K/day, equal to TROCCINOX.
The second approach as described in the previous section is to fit the CO_2 index to the

Table 5.1: Residence times and ascent rates for CO_2. See text for an explanation of the different columns.

Pot. temp.	alt	CO_2	t-slope	w-slope	t-fit(shifted)	w-fit(shifted)	t-fit(unshifted)	w-fit(unshifted)
K	km	ppm	days	K/day	day	K/day	days	K/day
APE-THESEO								
360	14.9	365.8	0	-	-	-	-	-
370	16.0	366.1	-11	-0.9	-	-	-	-
380	16.6	366.1	-15	-1.3	-	-	-	-
390	17.3	366.1	-13	-2.3	23 ± 7	1.3 ± 0.5	75	0.4
TROCCINOX								
360	13.7	378.4(index)	0	-	-	-	-	-
370	15.0	377.7	30	0.3	-	-	-	-
380	15.9	377.4	42	0.5	-	-	-	-
390	16.9	377.3	47	0.6	40 ± 10	0.75 ± 0.15	60	0.5
SCOUT-O3								
360	14.4	378.7	0	-	-	-	-	-
370	16.4	377.9	24	0.4	-	-	-	-
380	16.9	377.5	35	0.6	-	-	-	-
390	17.3	377.6	-	-	-	-	60 ± 25	0.5 ± 0.15
AMMA/SCOUT-O3								
360	14.3	380.1	0	-	-	-	-	-
370	15.0	380.5	15	0.7	-	-	-	-
380	16.1	381.3	44	0.5	-	-	-	-
390	16.6	381.5	51	0.6	-	-	43± 8	0.7 ± 0.1

aircraft data to be able to also assess ascent rates when the slope of the CO_2 index changes. The results of these fits can be seen in Figures 5.4, 5.5, 5.6, and 5.7. For this approach the assumption is made that the ascent rates are uniform, which may not be the case as observed in the first approach, but is used to give an approximation of the average ascent rate in the TTL between 360 and 390 K. In the figures only the flights of the campaign sampling the "background" TTL are shown. The data used are shown as red dots while data excluded by filtering with the CFC-12 and latitude filters are shown as grey dots. The black line gives the average profile during the campaign with error bars showing the standard deviation. The CO_2 index is fitted to the data for different vertical ascent rates. The different colored lines show the different fits. Fits were started at 360 K. If necessary, to achieve good fits, the fits allowed for a constant shift in mixing ratio of the CO_2 index, which would reflect discrepancies between the aircraft and surface data due to unknown systematic errors and calibration differences, or compensate for other inaccuracies in the approach. The TTL is the region between the horizontal black lines.
The average profile during APE-THESEO shows a negative slope, instead of the positive slope of the index. The data also show a large scatter and no coherent tape recorder signal below 380 K. Therefore the data do not well constrain a fit of the index. However, above 390 K the data are more coherent and a fit could be constrained with help of these data, which fits the data in the TTL as well. The fit, however, must be considered a coarse indication of

an average ascent rate between 360 K and 420 K. Ascent rates between 1.0 and 1.8 K/day match the data well, with the optically best fit for 1.3 K/day. A shift of -1.8 ppm of the CO_2 index was used to achieve a reasonable fit of the index to the data. A shift of -0.5 ppm is in any case justified due to the difference in CO_2 calibration scales (cf. Appendix A, APE-THESEO data are based on the WMO X93 scale). Assuming only this shift of -0.5 ppm, the fit profile would look like the brown curve in the figure, which roughly follows the highest observed mixing ratios up to 380 K and matches the mean profile at 390 K. The brown line has an ascent rate of 0.4 K/day, much lower than the fit with shift. This can be considered the minimum ascent rate still compatible with the observations.
During TROCCINOX the data below 370 K are still largely influenced by local processes, and therefore the fit was made between the 370 and 390 K levels. The CO_2 index had to be shifted by -0.5 ppm to fit the average measured profile. The best fit was found with an ascent rate of 0.75 K/day, with still good fits within a range of $\pm$ 0.15 K/day. This agrees still with the ascent rate as defined from the slope only (0.6 K/day). A fit without the shift of -0.5 ppm and an ascent rate of 0.5 K/day matches the observations at 390 K/day, but not below that level. It could be justified here only if it is assumed that below 390 K the air between the hemispheres has not completely mixed yet. In this case, the TROCCINOX data (mostly taken at 20-22° S) would lie closer to the CO_2 mixing ratios of Samoa (376.78 ppm for February 2005) and thus lower than the index.
The SCOUT-O3 profile reflects the curve of the CO_2 index clearly. A good fit to the index was found with ascent rates between 0.35 and 0.65 K/day, in agreement with the results of the calculation using the slope of the index up to 380 K. No shift was necessary to fit the index to the data. The ascent rate is found to be lower than during the APE-THESEO and TROCCINOX campaigns. This is consistent with the expected seasonality, since the air that arrives at 390 K crossed the 360 K level approximately 45-85 days before, i.e. in August/September when the Brewer-Dobson circulation was still weak, in contrast with the air which ascended since January during the APE THESEO and TROCCINOX campaigns, when the Brewer-Dobson circulation is at its strongest.
The AMMA/SCOUT-O3 observations can also be fitted well to the index without a shift for ascent rates between 0.6 and 0.8 K/day. The ascent rate of 0.6 K/day calculated before with help of the first method agrees rather well with these results.
All the results of these fits are summarized in the last four columns of Table 5.1. The first two columns give the residence time and ascent rates when shifts of the index were allowed, and the last two columns give the residence times and ascent rates when no shift of the index was applied. The "uncertainties" listed for the results represent the range within which good fits to the data are possible for the particular shift (or zero-shift) assumed and are thus only part of the overall uncertainties. A rigorous estimate of the true uncertainties would be difficult, but it is probably reasonable to assume that they would be at least twice as large as the ranges listed.

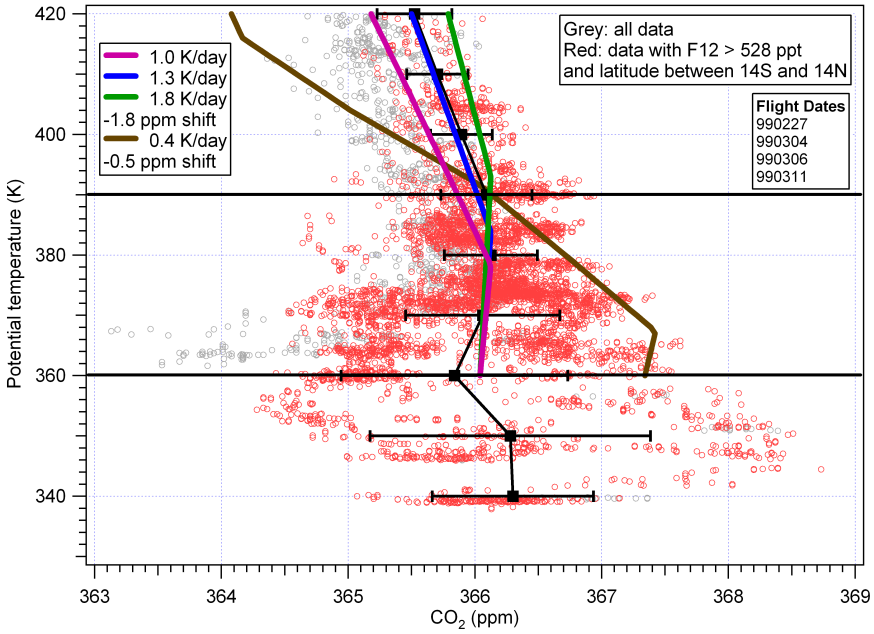

Figure 5.4: CO_2 profile measured during the APE-THESEO campaign. Red symbols show the data after filtering for latitude and extratropical influences. Grey symbols show data excluded from the analysis by this filtering. The black line is the mean profile. Error bars show one standard deviation. Coloured curves are the fits of the CO_2 index to the data for different constant vertical ascent rates. The brown line shows the fit without a shift (see text for explanation).

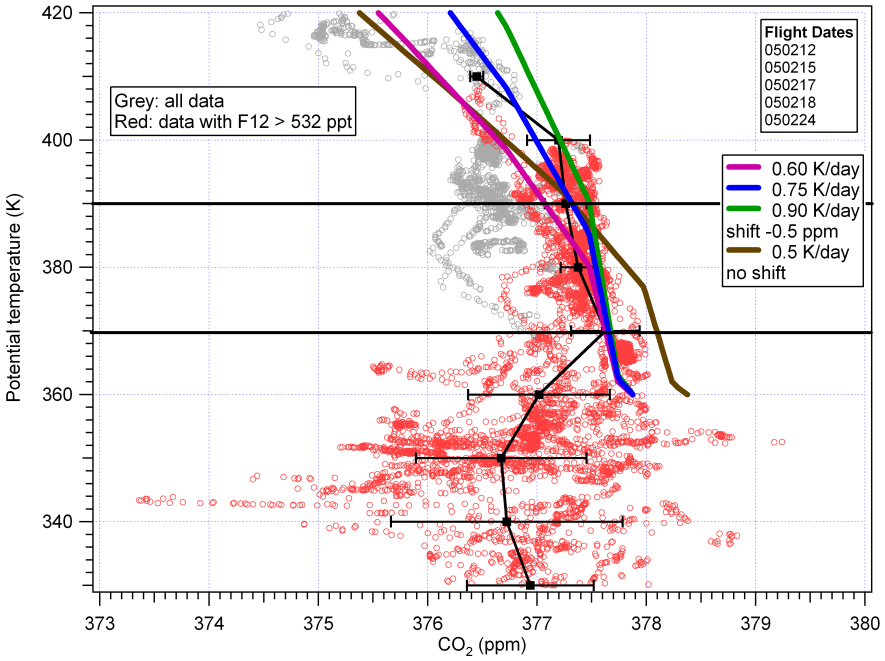

Figure 5.5: same as Figure 5.4 but for TROCCINOX

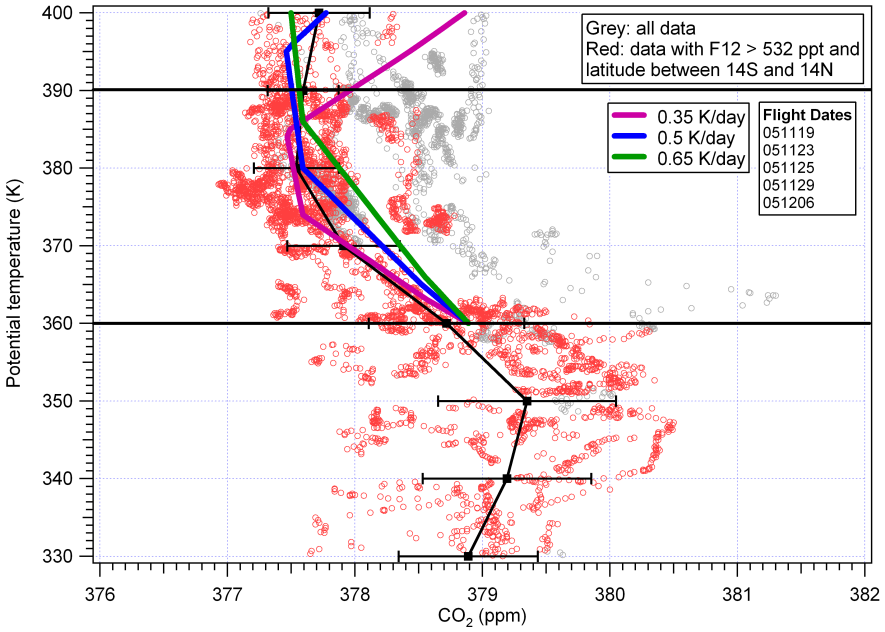

Figure 5.6: same as Figure 5.4 but for SCOUT-O3

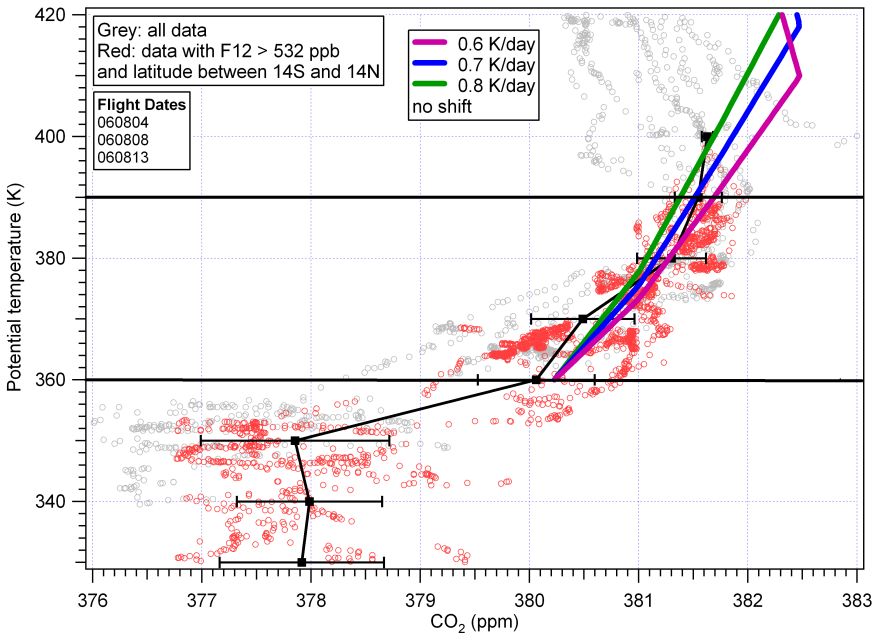

Figure 5.7: same as Figure 5.4 but for AMMA/SCOUT-O3

5.4 Discussion and Conclusions

The results show that the background TTL above 360 K indeed generally exhibits a coherent tape recorder signature in accordance with the tropospheric variation of CO_2, such that an ascent rate can be calculated, although with high uncertainties (in particular for the APE-THESEO campaign). The assumption that the air is well mixed between the hemispheres above 360 K seems to agree with the SCOUT-O3 and AMMA/SCOUT-O3 data, but not with the (southern subtropical) TROCCINOX data, where a smaller mixing ratio more in accordance with the mixing ratio at Samoa is found. This supports the idea that at the 360 K potential temperature the difference between both hemispheres is still observed. Darwin and Ouagadougou are located closer to the ITCZ and might therefore show a better mix of NH and SH air. More importantly, interhemispheric differences in CO_2 are minimal during August and November, when the AMMA/SCOUT-O3 and SCOUT-O3 campaigns took place. In February/March on the other hand, the interhemispheric difference is up to 2-3 ppm and appears to be reflected also in the APE-THESEO data, which were sampled right in the ITCZ region.

The first method of calculating the ascent is crude as it assumes that an average slope of the index over several months is a good approximation for the CO_2 trend during the transit period through the TTL. The method yields residence times for Australia, West Africa, and Brazil of the same order, 35-45 days to 380 K and 50 days to 390 K (where no value can be derived for Australia as the slope is changing approximately 1 month before the campaign). For APE-THESEO, the method does not yield reasonable results, apparently because the slope of the index during the preceding months is not representative for the CO_2-variation during February 1999. The principle advantage of this method is that it relies on relative changes in CO_2 rather than on absolute values and thus does not require an absolute match between the aircraft and surface data. For TROCCINOX, however, a background TTL value at 360 K could not be deduced from the aircraft data and was thus set equal to the CO_2 index value, thus de facto assuming an absolute match. Considering the observations rather suggest a significant offset between aircraft and CO_2 index data, the results for TROCCINOX have to be viewed with particular caution, although the resulting increase of the ascent rate with altitude (cf. Table 5.1) seems physically plausible.

The second method, fitting the CO_2 index directly to the vertical profiles assuming a constant ascent rate, is more sophisticated and can be used in all seasons. However, it relies on matching absolute values of CO_2 mixing ratio between the aircraft and surface data. Apart from perfect calibration of the observations on the same scale, this perfect match would also require stringent validity of the assumptions at 360 K, i.e. exactly zero age, no influence of local boundary layer conditions and perfect mixing between the hemispheres. Clearly these assumptions are not always strictly valid and in practice, observations at 360 K may not match the CO_2 index well. Significant offsets between the two data sets indeed occur for APE-THESEO and (less so) for TROCCINOX such that reasonably good fits of the index to the data can only be obtained by allowing for a constant shift in the data. Clearly the results for ascent rates are quite sensitive to the exact shift applied (although this was not demonstrated explicitly here). This is also true for the SCOUT-O3 and AMMA/SCOUT-O3 campaigns, where the data at 360 K match the index remarkably

well without a shift. For all campaigns, the data would in fact be consistent with a range of shifts and thus with a larger range of ascent rates than indicated in Figs. 5.4-5.7 and Table 5.1, and summarized in the next paragraph. Finally, there is no physical reason to assume that ascent rates will be approximately constant between 360 and 390 K, but the derived results can be considered as mean ascent rates over this interval.

The best estimates using the second method, as listed in Table 5.1, show moderate mean ascent rates of 0.5 ± 0.15 K/day for SCOUT-O3 (NH autumn) and 0.7 ± 0.1 K/day for AMMA/SCOUT-O3 (NH summer) corresponding to residence times between 360 and 390 K of 60 ± 25 days and 43 ± 8 days, respectively. For APE-THESEO and TROCCINOX the best fits (applying constant shifts of -1.8 ppm and -0.5 ppm, respectively) yield higher mean ascent rates of 1.3 ± 0.5 K/day and 0.75 ± 0.15 K/day, corresponding to residence times of 23 ± 7 and 40 ± 10 days, respectively, both during winter. These results agree roughly with those of Park et al. (2007a), who found an ascent rate of 1.2 ± 0.2 K/day, corresponding to a residence time of 26 ± 4 days during NH winter, essentially using the first method (employing the slope of the index). The results also correspond well to the expectations based on the seasonal variation of the Brewer-Dobson circulation that results in upwelling roughly a factor 2 stronger in NH winter than in NH summer (e.g. Holton et al., 1995). When not allowing for a shift in mixing ratio, i.e. requiring a strict match of absolute values for APE-THESEO and TROCCINOX, the ascent rates are 0.4 and 0.5 K/day, respectively, i.e. similar to those for summer and autumn (AMMA/SCOUT-O3 and SCOUT-O3). However, the poor agreement of the respective fits with the observations below 390 K (cf. Figs. 5.4 and 5.5) gives less credibility to these results.

Finally, it needs to be stressed that all these results are derived from a simple time lag between the surface (CO_2 index) and the "background TTL". This time lag represents the true transport time only in the case that slow diabatic ascent is the only transport process above 360 K that influences the background data selected for this study. Influences of other processes such as deep convection, vertical mixing, and isentropic inmixing of stratospheric air would bias the residence times derived here. Schoeberl et al. (2008) have pointed out this potential bias. In a re-analysis of the observations presented by Park et al.(2007a) together with a chemistry-climate model they claim that up to 50% of the apparent upwelling derived from the CO_2 time lag was due to vertical and horizontal eddy transport. Clearly, this critisism has to be taken seriously and needs further evaluation for the observations presented and analyzed here. While the data selected have been filtered to exclude observations influenced by local deep convection and stratospheric inmixing, this filtering is most effective at excluding recent influence of these faster transport processes with the primary goal of selecting background data with a coherent tape recorder signal. The coherent background profiles may still be influenced and shaped by the cumulative effects of these competing transport processes. In fact, as estimated in Section 3.2.2, the AMMA/SCOUT-O3 data between 380 and 390 K may contain about 20% of air entrained from the lowermost stratosphere (cf. Fig. 3.8). The CO_2 mixing ratio of this air depends on season, but is on the average less than that observed in the tropics. A significant influence on the tropical profiles is thus quite plausible. A quantitative assessment in how far the results may be biased by such effects is beyond the scope of this thesis, but should be adressed in future studies. Likely this will require involvement of more sophisticated

models. The results derived here have to be considered a first step towards a quantification of the ascent rates using a "CO_2 clock" and at the present stage serve to demonstrate that the results are consistent with other studies and with expectations, at least within the large associated uncertainties.

Chapter 6

Conclusions and Outlook

The previous three chapters have presented in situ measurements of long lived trace gases made during two aircraft campaigns in Darwin, Australia, and Ouagadougou, West-Africa. Different transport processes in the TTL were discussed: convection, vertical mixing following convective overshooting, vertical mixing along the subtropical jets, horizontal exchange along isentropes with the extratropical stratosphere, and slow diabatic ascent.
Measuring convective activity and the impact of high reaching convective systems was one of the main goals of both campaigns. As the SCOUT-O3 campaign took place during the pre-monsoon, and the AMMA/SCOUT-O3 campaign during the summer monsoon, the majority of the flights were potentially influenced by convection. The average level of main convective outflow was located at a potential temperature level of 360 K (14-15 km) during the SCOUT-O3 campaign, and between 350-360 K during the AMMA/SCOUT-O3 campaign. Only one flight during the last campaign shows a level of main convective outflow at 370 K. During the SCOUT-O3 campaign, low mixing ratios of ozone typical for the marine boundary layer are found at the level of main convective outflow, indicating an active convective regime. During the AMMA/SCOUT-O3 campaign, the low ozone mixing ratios of the boundary layer are not observed at the level of main convective outflow and ozone mixing ratios are up to twice as high in the TTL. The influence of local, very recent convection therefore seems to be minimal in the West African region. Also, hardly any signatures of overshooting convection are observed in the tracer data. It seems that long range transport, associated with the summer monsoon circulation, had a larger influence on this region. This long range transport is also important over nothern Australia. Although the SCOUT-O3 campaign focussed on the convective system Hector, appearing almost daily above the Tiwi islands, the measurements made with the HAGAR, FOZAN and COLD instruments in the direct vicinity of Hector do not give an indication of a large influence of this system on the TTL. Rather, the observations indicate possible influences of older systems and a more dominating influence of long-range transport. Probably convective transport of polluted air masses from Indonesia and subsequent ozone production in the TTL causes the high ozone and CO levels found in the TTL during the two flights on November 30. Vertical mixing in the vicinity of the subtropical jet, along which the air travelled on its way from Indonesia to Darwin, may also have contributed to the high anomalies in ozone and CO.

During both campaigns no large influence of horizontal inmixing from the extratropical stratosphere was observed. Below the tropical tropopause, correlation analysis of ozone and N_2O indicated no significant influence of stratospheric air, and based on N_2O observations the fraction of aged air was estimated for AMMA/SCOUT-O3 to be below 10% up to the tropopause (at 375 K), though increasing to 30% at 390 K.
The mean diabatic ascent was estimated for both campaigns and for two previous campaigns over Brasil (TROCCINOX, January/February 2005) and the Seychelles (APE-THESEO, February/March 1999) from the time lag of the seasonal variation of CO_2 between the TTL and the surface. The results confirm the notion that the Brewer-Dobson circulation is strongest in NH winter, when ascent rates are fastest. For APE-THESEO and TROCCINOX (both during winter) the estimated mean ascent rates of 1.3±0.5 K/day and 0.75±0.15 K/day agree roughly with those of Park et al. (2007a), who found an ascent rate of 1.2±0.2 K/day during NH winter over Australia and Costa Rica. For SCOUT-O3 and AMMA/SCOUT-O3 (in autumn and summer, respectively) smaller ascent rates of 0.5±0.15 and 0.7±0.1 K/day are derived.
The assumption that the air is well mixed between the hemispheres above 360 K seems to agree with the SCOUT-O3 and AMMA/SCOUT-O3 data, but not with the (southern subtropical) TROCCINOX data, where a smaller mixing ratio more in accordance with Southern Hemisphere mixing ratios is found. This supports the idea that at 360 K potential temperature the difference between both hemispheres is still observed. Darwin and Ouagadougou are located closer to the ITCZ and might therefore show a better mix of NH and SH air.
This thesis herewith gives more insight about the transport processes in the TTL and the importance of each of these processes. However, since the measurements only span a short time frame and a limited sampling region it would be extremely useful to support the analysis with global numerical and meso-scale simulations. Measurements can be compared to model results and be used to improve these models. On the other hand, models can give further insight into different explanations for the various observed features and derived results.
New aircraft campaigns in the tropics would be useful to extend the tropical dataset and to be able to compare data of different longitudes, latitudes and different seasons. Additionally, it would be interesting to study the influence of biomass burning on the TTL, since only few studies have been done on this subject. Therefore, measurements of typical biomass burning tracers, like for example CH_3Cl, should be performed on board the same measurement platform as CO and O_3. Another topic to study in more detail would be the vertical mixing along the subtropical jets. There are indications that mixing along these jets might be an important factor for vertical transport of trace gases through the TTL (Konopka et al., 2007), but more evidence is needed to prove this thesis.

Appendix A

Calibration standards

The Cal and Span values which are used to calculate the mixing ratios of the air samples from the SCOUT-O3 and AMMA-SCOUT campaign are dispayed in Table A.1. These working standards are accurately calibrated against a NOAA/CMDL standard (and are based on the WMO X93-scale). The values of this CMDL standard can be found in Werner et al. (2007).

The CO_2 mixing ratios of the Span and Cal standards are not directly defined by calibration against the NOAA/CMDL standard, but are calibrated in the laboratory against three standards intercalibrated by the Umweltbundesamt (UBA) based on the Scripps Institution for Oceanography (SIO) scale. These UBA standards were used until 2006 scale and measurements in the work of Werner (2007) are thus based on the SIO scale. After an intercalibration with the University of Heidelberg in 2006 and 2007 the UBA standards were rescaled to the new WMO'05 scale, and all measurements from 2005 onwards were recalculated based on this new scale in order to facilitate comparison with the NOAA/GMD surface data. The mixing ratios of the standards based on calibrations against the SIO and the WMO'05 scales and their difference are displayed in Table A.2.
Riediger (2000) actually based the CO_2 measurements in his thesis (including the APE-THESEO data) on a calibration of the HAGAR Cal and Span standards by the University of Heidelberg (I. Levin), whose scale was close to the WMO X93 scale at that time (1999). This scale yielded values about 0.2 ppm lower than the SIO scale (Riediger, 2000). Given that observed CO_2 values during APE-THESEO ($\sim$366 pm) are close to the UBA-1528 standard, these values as calculated by Riediger (2000) would thus have to be shifted by 0.2 ppm to be compatible with the SIO scale and by another 0.33 pm (cf. Table A.2), i.e. in total about 0.5 ppm, to be compatible with the WMO'05 scale.

Table A.1: Mixing ratios of the calibration gases used for the SCOUT-O3 and AMMA-SCOUT measurements.

Molecule	**Cal**	**Span**
N_2O (ppb)	318.95	191.54
CFC-12 (ppt)	542.08	322.66
H-1211 (ppt)	5.32	3.15
CFC-11 (ppt)	255.00	151.99
SF_6 (ppt)	5.91	3.55
CH_4 (ppb)	1832.63	1088.87
H_2 (ppb)	519.62	317.15
CO_2 (ppm)	392.29	371.7

Table A.2: CO_2 Mixing ratios of the UBA Standards scaled with the old SIO scale (Riediger, 2000) and the new WMO'05 scale (I.Levin). The new WMO´05 scale is used for calibrating measurements made from 2005 onwards.

Name	**CO_2 (ppm) SIO**	**CO_2 (ppm) WMO'05**	**shift (ppm)**
UBA-1546	389.51	390.45	0.94
UBA-1541	376.58	377.11	0.53
UBA-1528	362.20	362.53	0.33

List of abbreviations

ACTIVE	Aerosol and Chemical Transport in tropIcal conVEction
ALTO	Airborne Lidar for Tropospheric Ozone
AMMA	African Monsoon Multidisciplinary Analysis
APE-THESEO	Airborne Platform for Earth Observation – The Contribution to the Third European Stratospheric Experiment on Ozone
ASHOE	Airborne Southern Hemisphere Ozone Experiment
CALIPSO	Cloud-Aerosol Lidar and Infrared Pathfinder Satellite
CAO	Central Aerological Observatory
CCN	Cloud Condensation Nuclei
CFC	Chlorofluorcarbon
CH_4	Methane
CLaMS	Chemical Lagrangian Model of the Stratosphere
CMDL	Climate Monitoring and Diagnostics Laboratory
CNR	Italian National Research Council
CO	Carbon monoxide
CO_2	Carbon dioxide
COLD	Cryogenically Operated Laser Diode
COPAS	Condensation Particle System
CPT	Cold point tropopause
CR-AVE	Costa Rica Aura Validation Experiment
CRISTA-NF	Cryogenic Infrared Spectrometers and Telescopes for the Atmosphere New Frontier
DLR	Deutsches Zentrum für Luft- und Raumfahrt
ECD	Electron Capture Detector
ECMWF	European Center for Medium Range Weather Forecast
EOP	Enhanced Observing Period
EU	European Union
FISH	Fast In-situ Hygrometer
FLASH	Fluorescent Aircraft Stratospheric Hygrometer
FOZAN	Fast Ozone Analyzer

FSSP	Forward Scattering Spectrometer Probe
FZJ	Research Centre Jülich
GC	gaschromatography
GCM	Global Circulation Model
GMT	Greenwich Mean Time
H1211	Halon 1211 ($CBrClF_2$)
H_2	
HAGAR	High Altitude Gas Analyser
HALOX	HALogenOXide monitor
INOA	Istituto Nationale di Ottica Applica
IR	Infrared
ISAO	Institute for Atmospheric and Ocean Studies
ITCZ	InterTropical Convergence Zone
LZRH	Level of Zero net Radiative Heating
LOP	Long term Observing Period
MAESA	Measurements for Assessing the Effects of Stratospheric Aircraft
MAL	Microjoule Airborne Lidar
MARSCHALS	Millimetre-Wave Airborne Receivers for Spectroscopic CHaracterisation in Atmospheric Limb Sounding
MAS	Multi-Wavelength Aerosol Spectrometer
MCS	Mesoscale Convective System
MDB	Myasishchev Design Bureau
MIPAS-STR	Michelson Interferometer for Passive Atmospheric Sounding - Stratospheric Aircraft
MODIS	Moderate Resolution Imaging Spectroradiometer
MOPITT	Measurements of Pollution in the Troposphere
MPI	Max Planck Institute
NASA	National Aeronautics and Space Administration
NCAR	National Centre for Atmospheric Research
NOAA -ESRL	National Oceanic and Atmospheric Administration
NH	Northern Hemisphere
O_3	Ozone
ppb	parts per billion, SI: $\mathrm{nmol\,mol^{-1}}$
ppm	parts per million, SI: $\mathrm{\mu mol\,mol^{-1}}$
ppt	parts per trillion, SI: $\mathrm{pmol\,mol^{-1}}$
PV	Potential Vorticity
QBO	Quasi Biennial Oscillation
RAL	Rutherford Appleton Laboratories, UK
SCOUT-O3	Stratosphere-Climate Links with Emphasis on the Upper Troposphere and Lower Stratosphere
SF_6	Sulfurhexafluorid
SH	Southern Hemisphere
SIOUX	StratospherIc Observation Unit for nitrogen oXides

SOP	Special Observing Period
THESEO	Third European Stratospheric Experiment on Ozone
TROCCINOX	Tropical Convection and Nitrogen Oxides Experiment
TST	Troposphere-to-Stratosphere Transport
TTL	Tropical Tropopause Layer of Tropical Transition Layer
TWP-ICE	Tropical Warm Pool- International Cloud Experiment
UCSE	Unit for Connection with Scientific Equipment
UTC	Universal Time
UTLS	Upper-Troposphere Lower-Stratosphere
UV	Ultraviolet
VOC	Volatile Organic Compound
VSLS	Very Short Lived Species
WAS	WHO
World Health Organisation	
WMO	World Meteorological Organisation

Bibliography

Allen, G., Vaughan, G., Bower, K. N., Williams, P. I., Crosier, J., Flynn, M., Connolly, P., Hamilton, J. F., Lee, J. D., Saxton, J. E., Watson, N. M., Gallagher, M., Coe, H., Allan, J., Choularton, T. W., and Lewis,A. C.: Aerosol and trace-gas measurements in the Darwin area during the wet season, J. Geophys. Res., 113, D06306, doi:10.1029/2007JD008706, 2008.

AMMA Public: http://www.amma-international.org/rubrique.php3?id_rubrique=1, last access: 25 May 2009.

AMMA/SCOUT-O3 website: http://amma.igf.fuw.edu.pl/, last access: 30 December 2010.

Andreae, M.O., Anderson, B.E., Blake, D.R., Bradshaw, J.D., Collins, J.E., Gregory, G.L., Sachse, G.W., and Shipham, M.C.: Influence of plumes from biomass burning on atmospheric chemistry over the equatorial and tropical South Atlantic during CITE 3, J. Geophys. Res., 99, 12,793–12,808, 1994.

Andrews, A. E., Boering, K. A., Daube, B. C.,Wofsy, S. C., Hintsa, E. J., Weinstock, E. M., and Bui, T. P.: Empirical age spectra for the lower tropical stratosphere from in situ observations of CO2: Implications for stratospheric transport, J. Geophys. Res., 104(D21), 26 58126 596, 1999.

Baehr, J., Volk, C.M., Kuhn, A.C., Viciani, S., Ulanovski, A., Ravegnani, F., Schlager, H., and Stohl,A.: Influence of convection on the TTL over Brazil: Analysis of airborne in situ trace gas measurements, in preparation.

Barret, B., Ricaud, P., Mari, C., Atti ´ e, J.-L., Bousserez, N., Josse, B., Le Flochmoën, E., Livesey, 15 N. J., Massart, S., Peuch, V.-H., Piacentini, A., Sauvage, B., Thouret, V., and Cammas, J.-P.: Transport pathways of CO in the African upper troposphere during the monsoon season: a study based upon the assimilation of spaceborne observations, Atmos. Chem. Phys., 8, 3231-3246, 2008.

Barret, B., Williams, J. E. , Bouarar, I., Yang, X., Josse, B., Law, K., Pham, M., Le Flochmoën, E., Liousse, C., Peuch, V. H., Carver, G. D., Pyle, J. A., Sauvage, B., van Velthoven, P., Schlager, H., Mari, C., and Cammas, J.-P.: Impact of West African Monsoon convective transport and lightning NOx production upon the upper tropospheric composition: a multi-model study, Atmos. Chem. Phys. Discuss., 10, 2245-2302, 2010.

Berthet, G., Esler, J.G., Haynes, P.H.: A Lagrangian perspective of the tropopause and the ventilation of the lowermost stratosphere, J. Geophys. Res., 112, D18102, doi : 10.1029/2006JD008295, 2007.

Boering, K. A., Wofsy, S. C., Daube, B. C., Schneider, H. R., Loewenstein, M., and Podolske, J. R.: Stratospheric mean ages and transport rates from observations of carbon dioxide and nitrous oxide, Science, 274(5291), 13401343, 1996.

Bonazzola, M., and Haynes, P. H.: A trajectory- based study of the tropical tropopause region, J. Geophys. Res., 109, doi:10.1029/2003JD004356, 2004.

Brewer, A. W.: Evidence for a world circulation provided by the measurements of helium and water vapour distribution in the stratosphere, Quart. J. Roy. Meteor. Soc., 75, 351-363, 1949.

Bridgeman, C. H., Pyle, J. A., and Shallcross, D. E.: A three-dimensional model calculation of the ozone depletion potential of 1-bromopropane (1-C3H7Br), J. Geophys. Res., 105, 2649326502, 2000.

Brunner, D., Siegmund, P., May, P. T., Chappel, L., Schiller, C., Müller, R., Peter, T., Fueglistaler, S., MacKenzie, A. R., Fix, A., Schlager, H., Allen, G., Fjaeraa, A. M., Streibel, M., and Harris, N. R. P.: The SCOUT-O3 Darwin Aircraft Campaign: rationale and meteorology, Atmos. Chem. Phys., 9, 93117, 2009.

Cairo, F., Buontempo, C., MacKenzie, A. R., Schiller, C., Volk, M., Adriani, A., Mitev, V., Matthey, R., Di Donfrancesco, G., Oulanovsky, A., Ravegnani, F., Rudakov, S., Yushkov, V., Snels, M., Cagnazzo, C., and Stefanutti, L.: Morphology of the tropopause layer and lower stratosphere above a tropical cyclone: A case study on cyclone Davina (1999), Atmos. Chem. Phys., 8, 3411-3426, 2008.

Cairo F., Pommereau, J. P., Law, K. S., Schlager, H., Garnier, A., Fierli, F., Ern, M., Streibel, M., and the SCOUT-AMMA team: An overview of the SCOUT-AMMA stratospheric aircraft, balloons and sondes campaign inWest Africa, August 2006: rationale, roadmap and highlights, Atmos. Chem. Phys., 10, 2237-2256, 2010.

Chatfield, R. B., and Delany, A. C.: Convection links biomass burning to increased tropical ozone: however, models will tend to over predict O3. J. of Geophys. Res., 95, D12, 18473-18488, 1990.

Corti, T., Luo, B. P., Peter, T., Vomel, H., and Fu, Q.: Mean radiative energy balance and vertical mass fluxes in the equatorial upper troposphere and lower stratosphere, Geophys. Res. Lett., 32, L06 802, 2005.

Corti, T., Luo, B. P., Fu, Q., Vomel, H., and Peter, T.:The impact of cirrus clouds on tropical troposphere-to-stratosphere transport, Atmos. Chem. Phys., 6, 25392547, 2006.

Crutzen, P. J., Heidt, L. E., Krasnec, J.P., Pollock, W. H., and Seiler, W.: Biomass burning as a source of atmospheric gases CO, H2, N20, NO, CH3C1, and COS, Nature, 282, 253-256, 1979.

Crutzen, P. J., and Andreae, M. O.: Biomass burning in the tropics: impact on atmospheric chemistry and biogeochemical cycles, Science, 250, 1669-1678, 1990.

Danielsen, E. F.: A dehydration mechanism for the stratosphere, Geophys. Res. Lett., vol. 9, no. 6, 605–608, 1982.

Danielsen, E. F.: In situ evidence of rapid, vertical, irreversible transport of lower tropospheric air into the lower tropical stratosphere by convective cloud turrets and by larger-scale upwelling in tropical cyclones, J. Geophys. Res., 98, 86658681, 1993.

Douglass, A. R., Schoeberl, M. R., Rood, R. B., and Pawson, S.: Evaluation of transport in the lower tropical stratosphere in a global chemistry and transport model, J. Geophys. Res., 108, 4259, doi:10.1029/2002JD002696, 2003.

Duncan, B. N., Strahan, S. E., Yoshida, Y., Steenrod, S. D., and Livesey, N.: Model study of the cross-tropopause transport of biomass burning pollution, Atmos. Chem. Phys., 7, 3713-3736, 2007.

Fahey, D.W., Donelly, S.G., Keim, E.R., Gao, R.S. , Wamsley, R.C., Del Negro, L.A., Woodbridge, E.L., Proffitt, M.H., Rosenlof, K.H., Ko, M.K.W., Weisenstein, D.K., Scott, C.J., Nevison, C. , Solomon, S., and Chan, K.R.: In situ observations of NO_y, O_3 and the NO_y/O_3 ratio in the lower stratosphere, Geophys. Res. Lett., 23, 1653–1656, 1996.

Folkins, I., Chatfield, R.B., Baumgardner, D., and Profitt, M.: Biomass burning and deep convection in Southeast Asia: Results from ASHOE/MAESA, J. Geophys. Res., 102, 13.291–13.299, 1997.

Folkins, I., Braun, C., Thompson, M., and Witte, J.:Tropical ozone as an indicator of deep convection, J. Geophys. Res., 107, D13, 4184, 10.1029/2001JD001178, 2002.

Folkins, I., and Martin, R.V.:The vertical structure of tropical convection and its impact on the budgets of water vapor and ozone, J. Atmos. Sci., 62, 1560–1573, 2005.

Folkins, I., Bernath, P., Boone, C., Lesins, G., Livesey, N. Thompson,, A. M., Walker, K., and Witte, J. C.: Seasonal cycles of O3, CO, and convective outflow at the tropical tropopause, Geophys. Res. Lett., 33, L16802, doi:10.1029/2006GL026602, 2006.

Folkins I., Loewenstein M., Podolske J., Oltmans S. J. and Profitt M.: A barrier to vertical mixing at 14 km in the tropics: Evidences from ozonesondes and aircraft measurements, J. Geophys. Res., 104, 22095–22102, 1999.

Folkins, I., Oltmans, S. J., and Thompson, A. M.: Tropical convective outflow and near surface equivalent potential temperatures, Geophys. Res. Lett., 27, 2549–2552, 2000.

Fueglistaler, S., Dessler, A. E., Dunkerton, T. J., Folkins, I., Fu, Q., Mote, P. W.: Tropical tropopause layer, Rev. Geophys., 47, RG1004, doi:10.1029/2008RG000267, 2009.

Fueglistaler, S., and Fu, Q.: Impact of clouds on radiative heating rates in the tropical lower stratosphere, J. Geophys. Res., 111, D23202, doi:10.1029/2006JD007273, 2006.

Fueglistaler, S. and Haynes, P.H.: Control of interannual and longer-term variability of stratospheric water vapor, J. Geophys. Res., 110 (D24), doi:10.1029/2005JD006019, 2005.

Fueglistaler, S., Wernli, H., and Peter, T.: Tropical troposphere-to-stratosphere transport inferred from trajectory calculations, J. Geophys. Res., 109, D03108,doi:03110.01029/02003JD004069, 2004.

Gettelman A., Forster P. M. deF., A climatology of the tropical tropopause layer, J. Meteorol. Soc. Japan, 80, 911–924, 2002.

Gettelman, A., Birner, T., Eyring, V., Akiyoshi, H., Bekki, S., Brühl, C., Dameris, M., Kinnison, D. E., Lefevre, F., Lott, F., Mancini, E., Pitari, G., Plummer, D. A., Rozanov, E., Shibata, K., Stenke, A., Struthers, H., Tian, W.: The Tropical Tropopause Layer 19602100, Atmos. Chem. Phys., 9, 1621-1637, 2009.

Haynes, P. H., Shuckburg, E. F., Effective diffusivity as a diagnostic of atmospheric transport,1, Stratopshere, J. Geophys. Res., 105, 22.777–22794, 2000.

Haynes, P. H., Marks, C. J., McIntyre, M. E., Shepherd, T. G., Shine, K. P.: On the 'downward control' of extratropical diabatic circulations by eddy-induced mean zonal forces, J. Atmos. Sci., 48, 651–678, 1991.

Heyes, W. J., Vaughan, G., Allen, G., Volz-Thomas, A., Pätz, H.-W., and Busen, R.: Composition of the TTL over Darwin: local mixing or long-range transport?, Atmos. Chem. Phys. Discuss., 9, 72997332, 2009.

Highwood, E. J., Hoskins, B. J.: The tropical tropopause, Quart. J. Roy. Meteor. Soc., 124, 1579-1604, 1998.

Holton, J. R., Haynes, P. H., McIntyre, M. E., Douglass, A. R., Rood, R. B., and Pfister, L.: Stratosphere-Troposphere Exchange, Rev. Geophys., 33, 403439, 1995.

Hoskins, B. J., McIntyre, M. E., Robertson, A. W.: On the use and significance of isentropic potential vorticity maps, Quart. J. Roy. Meteor. Soc., 111:877946, 1985.

Hoor, P., Fischer, H., Lange, L., Lelieveld, J., Brunner, D.: Seasonal variations of a mixing layer in the lowermost stratosphere as identified by the CO-O3 correlation from in situ measurements, J. Geophys. Res., 107, NO. D5, 4044, doi: 10.1029/2000JD000289, 2002.

Ivanova, E. I.: Evaluation of transport and ozone loss in the Antarctic polar vortex by using tracer-based coordinates, Ph.D. thesis, Johann Wolfgang Goethe-Universität Frankfurt, Germany, 2007.

Janicot, S., Thorncroft, C. D., Ali, A., Asencio, N., Berry, G., Bock, O., Bourles, B., Caniaux, G., Chauvin, F., Deme, A., Kergoat, L., Lafore, J.-P., Lavaysse, C., Lebel, T., Marticorena, B., Mounier, F., Nedelec, P., Redelsperger, J.-L., Ravegnani, F., Reeves, C. E., Roca, R., de Rosnay, P., Schlager, H., Sultan, B., Tomasini, M., Ulanovsky, A., and ACMAD forecasters team: Large-scale overview of the summer monsoon over West Africa during the AMMA field experiment in 2006, Ann. Geophys., 26, 2569-2595, 2008.

Keenan, T. D., and Carbone, R. E.: A preliminary morphology of precipitation systems in tropical northern Australia, Quart. J. Roy. Meteor. Soc., 118, 283–326, 1992

Kita, K., Kawakami,S. , Miyazaki, Y., Higashi, Y., Kondo, Y., Nishi, N., Koike, M., Blake, D. R., Machida, T., Sano, T., Hu, W., Ko, M., and Ogawa, T.:Photochemical production of ozone in the upper troposphere in association with cumulus convection over Indonesia, J. Geophys. Res., 108, D3, 8400, doi:10.1029/2001JD000844, 2003.

Konopka, P., Günther,G., Müller, R., dos Santos, F. H. S., Schiller, C., Ravegnani, F., Ulanovsky, A., Schlager, H., Volk, C.M., Viciani, S., Pan, L., McKenna, D.-S., and Riese, M.: Contribution of mixing to the upward transport across the TTL, Atmos. Chem. Phys., 7, 3285-3308, 2007.

Kremser, S., Wohltmann, I., Rex, M., Langematz, U., Dameris, M., and Kunze, M.:Water vapour transport in the tropical tropopause region in coupled Chemistry-Climate Models and ERA-40 reanalysis data, Atmos. Chem. Phys., 9, 26792694, 2009.

Krüger, K., Tegtmeier, S., and Rex, M.: Long-term climatology of air mass transport through the Tropical Tropopause Layer (TTL) during NH winter, Atmos. Chem. Phys., 8, 813823, 2008.

Krüger, K., Tegtmeier, S., and Rex, M.: Variability of residence time in the Tropical Tropopause Layer (TTL) during Northern Hemisphere winter, Atmos. Chem. Phys., 9, 67176725, 2009.

Laursen, K. K., Hobbs, P. V., Radke, L.F., and Rasmussen, R. A.: Some trace gas emissions from North American biomass with an assessment of regional and global fluxes from biomass burning, J. Geophys. Res., 97, 20,687-20,701, 1992.

Law, K.S., Fierli, F., Cairo, F., Schlager, H., Borrman, S., Ravegnani, F., Real, E., Kunkel, D., Schiller, C., Streibel, M., Ulanovsky, A., Viciani, S., Volk, C.M.: Air mass origins influencing TTL chemical composition over West Africa during the 2006 summer monsoon, Atmos. Chem. Phys. Discuss., 10, 1548515536, 2010.

Levine, J. G., Braesicke, P., Harris, N. R. P., Savage, N. H., and Pyle, J. A.: Pathways and timescales for troposphere to stratosphere transport via the tropical tropopause layer and their relevance for very short lived substances, J. Geophys. Res., 112, D04308, doi:10.1029/2005JD006940, 2007.

Liu, C., and Zipser, E. J.: Global distribution of convection penetrating the tropical tropopause, J. Geophys. Res., 110, D23104, doi:10.1029/2005JD006063, 2005.

Marcy T. P., Popp, P. J., Gao, R. S., Fahey, D. W., Ray, E. A., Richard, E. C., Thompson, T. L., Atlas, E. L., Loewenstein, M., Wofsy, S. C., Park, S., Weinstock, E. M., Swartz, W. H., and Mahoney, M. J.: Measurements of trace gases in the tropical tropopause layer, Atmospheric Environment, 41, 7253–7261, doi:10.1016/j.atmosenv.2007.05.032, 2007.

Mauzerall, D. L., Logan, J. A., Jacob, D. J., Anderson, B. E., Blake, D. R., Bradshaw, J. D., Heikes, B., Sachse, G. W., Singh, H., Talbot, B.: Photochemistry in biomass burning plumes and implications for tropospheric ozone over the tropical South Atlantic, J. Geophys. Res., 103, 8401-8423, 1998.

McKeen, S. A., and Liu, S. C.: Hydrocarbon ratios and photochemical history of air masses, Geophys. Res. Lett., 20, 2362-2366, 1993.

Minschwaner, K., Dessler, A.E., Elkins, J.W., Volk, C.M., Fahey, D.W., Loewenstein, M., Podolske, J.R., Roche, A.E., and Chan, K.R.: Bulk properties of isentropic mixing into the tropics in the lower stratosphere, J. Geophys. Res., 101, 9433–9439, 1996.

MODIS Rapid Response System - Global Firemaps: http://rapidfire.sci.gsfc.nasa.gov/firemaps, last access: 05 September 2010.

Park, S., Jiménez, R., Pfister, L., Conway, T. J., Gottlieb, E. W., Chow, V. Y., Curran, D. J., Matross, D. M., Bright, A., Atlas, E. L., Bui, T. P., Gao, R. -S, Twohy, C. H., Wofsy, S. C.: The CO_2 tracer clock for the Tropical Tropopause Layer, Atmos. Chem. Phys., 7, 3989–4000, 2007.

Park, M., Randel, W. J., Gettelman, A., Massie, S. T., and Jiang, J.H.: Transport above the Asian summer monsoon anticyclone inferred from Aura Microwave Limb Sounder tracers, J. Geophys. Res., 112, D16309, doi:10.1029/2006JD008294, 2007b.

Parrish, D.D., Holloway, J.S., Trainer, M., Murphy, P.C., Forbes, G.L., and Fehsenfeld, F.C.: Export of North American ozone pollution to the North Atlantic Ocean, Science, 259, 1436–1439, 1993.

Pickering, K. E., et al., Convective transport of biomass burning emissions over Brazil during TRACE A, J. Geophys. Res., 101, 23,993–24,012, 1996.

Plumb, R. A., and Ko, M. K. W.: Interrelationships between mixing ratios of long-lived stratospheric constituents, J. Geophys. Res., 97, 10145-10156,1992.

Randel, W.J., Park, M., Wu, F., and Liveseya, N.: A large annual cycle in ozone above the tropical tropopause linked to the BrewerDobson Circulation, J. Atmos. Sci., 64, 4479–4488, DOI: 10.1175/2007JAS2409.1, 2007.

Redelsperger, J.-L., Thorncroft, C., Diedhiou, A., Lebel, T., Parker, D., and Polcher, J.: African Monsoon Multidisciplinary Analysis (AMMA): An International Research Project and Field Campaign, B. Am. Meteorol. Soc., 87, 17391746, 2006.

Reid, G.C., and Gage, K.S.: On the annual variation in the height of the tropical tropopause, J. Atmos. Sci., 38, 1928–1938, 1981.

Reus de, M., Borrmann, S., Bansemer, A., Curtius, J., Frey, W.,Heymsfield, A. J., Kürten, A., Ravegnani, F., Schiller, C., Sitnikov, N. M., Ulanovsky, A., and Weigel, R.: Evidence for ice particles in the tropical stratosphere from in-situ measurements, Atmos. Chem. Phys. Discuss., 8, 1931319355, 2008.

Ricaud P., Barret, B., Attié, J. -L., Motte, E., Le Flochmoën, E., Teyssèdre, H., Peuch, V. -H., Livesey, N., Lambert, A., and Pommereau, J. -P.: Impact of land convection on troposphere-stratosphere exchange in the tropics, Atmos. Chem. Phys., 7, 5639–5657, 2007.

Riediger, O.: Entwicklung und Einsatz eines flugzeuggetragenen Instrumentes zur in-situ-Messung langlebiger Spurengase in der Stratosphäre, Ph.D. thesis, Johann Wolfgang Goethe Universität Frankfurt, Germany, 195 pp., 2000.

Rossow, W. B., and Pearl, C.: 22-Year survey of tropical convection penetrating into the lower stratosphere, Geophys. Res. Lett., 34, L04803, doi:10.1029/2006GL028635, 2007.

Sauvage, B., Gheusi, F., Thouret, V., Cammas, J.-P., Duron, J., Escobar, J., Mari, C., Mascart, P., Pont,V.: Medium-range mid-tropospheric transport of ozone and precursors over Africa: two numerical case studies in dry and wet seasons, Atmos. Chem. Phys., 7, 5357-5370, 2007.

Schiller, C., Grooß, J.-U., Konopka, P., Plöger, F., Silva dos Santos, F. H., Spelten, N.: Hydration and dehydration at the tropical tropopause,Atmos. Chem. Phys., 9, 9647-9660, 2009.

Schoeberl, M. R., Douglass, A. R., Stolarski, R. S., Pawson, S., Strahan, S. E., Read, W.: Comparison of lower stratospheric tropical mean vertical velocities, J. Geophys. Res., 113, D24109, doi:10.1029/2008JD010221, 2008.

SCOUT-O3 Home: http://www.ozone-sec.ch.cam.ac.uk/scout$_o$3, *lastaccess* : 25 *May* 2009.

Seidel, D.J., Ross, R.J., Angell, J.K., Reid, G.C.: Climatological characteristics of the tropical tropopause as revealed by radiosondes, J. Geophys. Res., 106, D8, 7857-7878, 2001.

Sherwood, S. C.: A ßtratospheric drainöver the maritime continent, Geophys. Res. Lett., 27, 677-680, 2000.

Sherwood, S. C. and Dessler, A. E.: Convective mixing near the tropical tropopause: Insights from seasonal variations, J. Atmos. Sci., 60, 26742685, 2003.

Shindell, D.T., Rind, D., and Lonergan, P.: Climate change and the middle atmosphere. Part IV: Ozone response to doubled CO_2. J. Climate, 11, 895-918, doi:10.1175/1520-0442, 1998.

Sinnhuber, B.-M. and Folkins, I.: Estimating the contribution of bromoform to stratospheric bromine and its relation to dehydration in the tropical tropopause layer, Atmos. Chem. Phys., 6, 4755 - 4761, 2006.

Stefanutti, L., MacKenzie, A. R., Santacesaria, V., Adriani, A., Balestri, S., Borrmann, S., Khattatov, V., Mazzinghi, P., Mitev, V., Rudakov, V., Schiller, C., Toci, G., Volk, C. M., Yushkov, V., Flentje, H., Kiemle, C., Redaelli, G., Carslaw, K. S., Noone, K. and Peter, T.: The APE-THESEO tropical campaign: an overview. J. Atmos. Chem., 48, 1-33, doi: 10.1023/B:JOCH.0000034509.11746.b8 (online publication), 2004.

Strunk, M. An Experimental Study on the Mean Age of Stratospheric Air, Ph.D. thesis, Johann Wolfgang Goethe-Universität Frankfurt, Germany, 1999.

Sultan, B., Janicot, S., and Drobinski, P.: Characterization of the Diurnal Cycle of the West African Monsoon around the Monsoon Onset. J. Climate, 20, 4014-4032, 2007.

Thompson, A.M., Doddridge, B.G., Witte, J.C., Hudson, R.D., Luke, W.T., Johnson, J.E., Johnson, B.J., Oltmans, S.J., Weller, R.:A tropical atlantic paradox: shipboard

and satellite views of a tropospheric ozone maximum and wave-one in January-February 1999, Geophys. Res. Lett., 27, 3317-3320, 2000.

Thuburn, J., Craig, G. C.: On the temperature structure of the tropical substratosphere. J. Geophys. Res., 107, doi:10.1029/2000JD000285, 2002.

Tuck, A. F., Brune, W.H., Hipskind, R. S.: TThe Airborne Southern Hemisphere Ozone Experiment/Measurements for Assessing the Effects of Stratospheric Aircraft (ASHOE/MAESA): A road map."J. Geophys. Res. 102.D3: 3901-3904, 1997.

Tuck, A.F., Hovde, S. J., Kelly, K. K., Mahoney, M. J., Proffitt, M. H., Richard, E. C. and Thompson, T. L.: Exchange between the upper tropical troposphere and the lower stratosphere studied with aircraft observations, J. Geophys. Res., 108, no. D23, 4734, doi:10.1029/2003JD003399, 2003.

Ulanosvky, A.E., Yushkov, V.A., Sitnikov, N.M., and Ravegnani, F.: The FOZAN-II Fast-Response Chemiluminescent Airborne Ozone Analyzer, Instruments and Experimental Techniques, Vol. 44, No. 2, 249-256, 2001.

Vaughan, G., Schiller, C., MacKenzie, A. R., Bower, K., Peter, T., Schlager, H., Harris, N. R. P., and May, P. T.: SCOUTO3/ACTIVE: High-altitude aircraft measurements around deep tropical convection, B. Am. Meteorol. Soc., 89, 647662, doi:10.1175/BAMS-89-5-647, 2008.

Viciani, S., D'Amato, F., Mazzinghi, P., Castagnoli, F., Toci, G., and Werle, P.: A cryogenically operated laser diode spectrometer for airborne measurement of stratospheric trace gases, Applied Physics B, 90, 581-592, DOI 10.1007/s00340-007-2885-2, 2008.

Voigt, C., Schlager, H., Roiger, A., Stenke, A., de Reus, M., Borrmann, S., Jensen, E., Schiller, C., Konopka, P. and Sitnikov, N.: Detection of reactive nitrogen containing particles in the tropopause region evidence for a tropical nitric acid trihydrate (NAT) belt, Atmos. Chem. Phys., 8, 74217430, 2008.

Volk, C. M., Elkins, J. W., Fahey, D. W., Salawitch, R. J., Dutton, G. S., Gilligan, J. M., Proffitt, M. H., Loewenstein, M., Podolske, J. R., Minschwaner, K., Margitan, J. J., and Chan, K. R.: Quantifying transport between the tropical and mid-latitude lower stratosphere, Science, 272, 1763–1768, 1996.

Werner, A.: Quantifying transport into the lowermost stratosphere, Ph.D. thesis, Johann Wolfgang Goethe-Universität Frankfurt, Germany, 2007.

Wernli, H. and Davies, H. C.: A Lagrangian-based analysis of extratropical cyclones. Part I: The method and some applications, Q. J. Roy. Meteor. Soc., 123, 467489, 1997.

WMO (World Meteorological Organization), Scientific Assessment of Ozone Depletion: 2006, Global Ozone Research and Monitoring Project - Report No. 50, 572 pp., Geneva, Switzerland, 2007.

Wohltmann, I. and Rex, M.: Improvement of vertical and residual velocities in pressure or hybrid sigma-pressure coordinates in analysis data in the stratosphere, Atmos. Chem. Phys., 8, 265272, 2008.

World Bank Indonesia Office, Indonesia Environment Monitor 2003, 50pp., Jakarta, Indonesia, 2003.

Zipser, E.J., Cecil, D.J., Liu, C.T., Nesbitt, S.W., and Yorti, D.P.: Where are the most intense thunderstorms on earth? B. Am. Meteorol. Soc., 87(8), 1057–1071, 2006.

Summary

The goal of this thesis is to study different transport processes in the Tropical Tropopause Layer (TTL). The TTL is the transition layer between the tropical troposphere and stratosphere, and is the main region where tropospheric air enters the stratosphere. Different transport processes are important for the physical and chemical properties of this layer, and define the rate of exchange between troposphere and stratosphere. This is important for understanding to know the influence of, for example, very short-lived species (VSLS), which can destroy ozone if they reach the stratosphere within a few days.
In this thesis different transport processes are studied by using in situ measurements of tracers. Tracers are gases whose lifetimes are longer than the processes transporting them, such that their distribution is mainly determined by dynamics. Long-lived tracers were measured with the High Altitude Gas Analyzer (HAGAR) on board the M55 Geophysica aircraft. The instrument was developed by the University of Frankfurt and measures the long-lived tracers CO_2, N_2O, CFC-12, CFC-11, H-1211, SF_6, CH_4 and H_2 with two gas chromatographic channels and a CO_2 sensor (LICOR). The measurements are supported by CO measurements of the Cryogenically Operated Laser Diode (COLD) instrument, O_3 measurements of the Fast Ozone ANalyzer (FOZAN), as well as by backward trajectories provided by D. Brunner.
Two campaigns were conducted to obtain measurements in the TTL. The first campaign, the SCOUT-O3 campaign, took place in November and December 2005 in Darwin, Australia. During eight (mostly northbound) flights in situ trace gas measurements were made within the tropical tropopause layer (TTL) and the lower stratosphere (up to 20 km). The campaign included both survey flights designed to sample the background TTL and flights sampling the plume, turret, and outflow of the deep convective cell "Hector" frequently appearing north of Darwin and reaching up close to the tropopause. The second campaign, the AMMA-SCOUT-O3 campaign took place in July and August 2006 in Ouagadougou, Burkina Faso. Five local flights were performed, as well as four transfer flights between Verona, Italy, Marrakech, Maroc, and Ouagadougou. The flights were focused on long-range transport, satellite validation and on the mesoscale convective systems travelling to the west during the monsoon period.
After a general introduction of this thesis in chapters one and two, the third chapter of this thesis describes the findings during this last campaign. The five local flights are analyzed to study the different transport processes that occur in the tropical tropopause layer above West-Africa: deep convection up to the level of main convective outflow, vertical mixing after overshooting of air in deep convection, horizontal inmixing from the

extratropical lower stratosphere, and horizontal transport across the subtropical barrier. Except for one flight (on 13 August), a distinct convective outflow level is present, indicating high convective activity. CO_2 profiles show that the average level of main convective outflow is located between 350 and 360 K. Only on 11 August, the level of main convective outflow is higher, up to 370 K. The O_3 profiles on the other hand indicate that no fresh convection is observed, but air of older origin. When the average O_3 profile is compared with the O_3 profiles measured over northern Australia (SCOUT-O3 campaign), there is a less distinct level of main convective outflow observed, as well as higher O_3 concentrations throughout the TTL.

Signatures of irreversible mixing after overshooting of convective air are scarce. On 4 and 8 August there are only some small signatures found between 390 and 410 K. On 7 August, there is a signature seen in the CO data at 410 K, but this seems to be highly unusual because it would imply mixing between potential temperature levels of 380 K and 460 K. Also, no similar evidence was found in these cases in other tracer data.

The amount of air mixing in from the extratropical stratosphere is found to be not significant. The fraction of extratropical stratospheric air in the TTL due to isentropic mixing, as calculated from N_2O data, is 0.0 ± 0.1 up to 370 K during the local flights. This fraction is increasing above this level up to a maximum of 0.3 ($\pm$ 0.1) at 390 K.

The subtropical barrier, as indicated by the slope of the correlation between N_2O and O_3, appears not as an abrupt border between the tropics and extratropics, but more as a region of transition between 10°N and 20°N where the values change from tropical to extratropical. This is in agreement with observations during the ASHOE/MAESA campaigns in 1994.

Chapter 4 presents the results obtained during the SCOUT-O3 campaign. From the eight local flights the last four flights (051129, 051130a, 051130b, 051206) show enhanced values of ozone, CO and CO_2 between 355 and 380 K potential temperature in comparison with the first four flights (051116, 051119, 051123, 051125). This suggests vertical mixing through the TTL, influence of boundary layer pollution (local or remote) or stratospheric influence.

The absence of a negative correlation between O_3 and N_2O in the TTL and the presence of enhanced CO excludes horizontal inmixing from the extra-tropical stratosphere as an explanation for the enhancements. Also, the convective system Hector cannot explain the enhanced values of the two flights on 30 November, when flights were made just before, during and after the development of the system. Satellite pictures, in combination with the flight paths show that the signatures were already observed before the development of the Hector system, and at all sides of the system. Therefore, other possible explanations for these enhanced CO, CO_2 and ozone levels are proposed.

The first explanation is vertical mixing in the vicinity of the jet stream. At the time of the campaign the subtropical jet was located just south of Darwin. Backward trajectories show that the air measured on the 30th of November crossed the subtropical jet 3-4 days before. Particular strong mixing can occur in this region, due to the strong wind shear and resulting deformation of the flow field. However, the jet cannot explain the differences between the flights on 30 November and the flights on 29 November and 5 December.

Another possible explanation is influence of polluted boundary layer air masses from the

Indonesian region. The flights took place at the end of the biomass burning season in Indonesia. Especially air sampled during the flights on November 30 crossed large parts of northern Indonesia between 8 and 10 days before the measurements. Convective uplift of biomass burning and other pollution plumes can transport CO and ozone precursors into the upper troposphere, where they can significantly enhance the ozone production. Enhancement ratios calculated for the flights in question are indeed consistent with expectations for old plumes (older than 6 days).

The last chapter deals with the vertical ascent rate in the TTL and uses measurements of both the SCOUT-O3 and AMMA-SCOUT-O3 campaign as well as data from previous aircraft campaigns, namely the TROCCINOX and APE-THESEO campaigns. The TROCCINOX campaign took place in January/February 2005 in Brazil, and the APE-THESEO campaign in February/March 1999 in the Seychelles.

Time scales and residence times for mean vertical transport in the background TTL are estimated for different seasons and over different geographic regions using in situ observations of CO_2 and long-lived tracers. The vertical transport time scales are constrained using the seasonal variation of CO_2 in the tropical troposphere ("CO_2 index") as a "tracer clock" for vertical ascent.

Two methods are applied to calculate the residence time in the layer between 360 and 390 K potential temperature. The first method uses the slope of the CO_2 index, the second method fits the CO_2 index directly to the measurements assuming a constant ascent rate. The results show that the background TTL above 360 K indeed shows a coherent "tape recorder" signature in accordance with the tropospheric variation of CO_2, such that an ascent rate can be calculated, although with high uncertainties (in particular for the APE-THESEO campaign). The assumption that the air is well mixed above 360 K seems to agree with the SCOUT-O3 and AMMA/SCOUT-O3 data, but not with the (southern subtropical) TROCCINOX data, where a smaller mixing ratio more in accordance with Southern hemispheric mixing ratios is found. This supports the idea that at 360 K potential temperature the difference between both hemispheres is still observed.

The first method of calculating the ascent yields residence times for Australia, West Africa, and Brazil of the same order, 35-45 days to 380 K and 50 days to 390 K (where no value can be derived for Australia as the slope is changing approximately one month before the campaign). For APE-THESEO, the method does not yield reasonable results, apparently because the slope of the index during the preceding months is not representative for the CO_2-variation during February 1999.

The second method, fitting the CO_2 index directly to the vertical profiles assuming a constant ascent rate, is more sophisticated and can be used in all seasons. However, it relies on matching absolute values of CO_2 mixing ratio between the aircraft and surface data. Significant offsets between the two data sets occur for APE-THESEO and (less so) for TROCCINOX such that reasonably good fits of the index to the data can only be obtained by allowing for a constant shift in the data. In this case the results for ascent rates are quite sensitive to the exact shift applied.

The best estimates using the second method show moderate mean ascent rates of 0.5 ± 0.15 K/day for SCOUT-O3 (NH autumn) and 0.7 ± 0.1 K/day for AMMA/SCOUT-O3 (NH summer) corresponding to residence times between 360 and 390 K of 60 ± 25 days and

43±8 days, respectively. These results agree well with the results calculated using the first method. For APE-THESEO and TROCCINOX the best fits (applying constant shifts of -1.8 ppm and -0.5 ppm, respectively) yield higher mean ascent rates of 1.3±0.5 K/day and 0.75±0.15 K/day, corresponding to residence times of 23±7 and 40±10 days, respectively, both during winter. These results agree roughly with those of Park et al. (2007a), who found an ascent rate of 1.2±0.2 K/day, corresponding to a residence time of 26±4 days during NH winter, essentially using the first method (employing the slope of the index). The results also correspond well to the expectations based on the seasonal variation of the Brewer-Dobson circulation that results in upwelling roughly a factor 2 stronger in NH winter than in NH summer (e.g. Holton et al., 1995). When not allowing for a shift in mixing ratio, i.e. requiring a strict match of absolute values for APE-THESEO and TROCCINOX, the ascent rates are 0.4 and 0.5 K/day, respectively, i.e. similar to those for summer and autumn (AMMA/SCOUT-O3 and SCOUT-O3). However, the poor agreement of the respective fits with the observations below 390 K gives less credibility to these results.

Zusammenfassung

Einleitung

Der Übergang zwischen der Troposphäre und der Stratosphäre in den Tropen ist nicht als eine scharfe Grenze zu verstehen, sondern vielmehr als eine vertikal ausgedehnte Region, die sowohl Eigenschaften der konvektiv geprägten Troposphäre als auch solche der von Strahlung dominierten Stratosphäre aufweist. Diese Region wird die Tropische Tropopausenregion genannt (auf Englisch TTL: Tropical Tropopause Layer). Hier findet der größte Teil des Transports zwischen Troposphäre und Stratosphäre statt. Aufsteigende Luftmassen erfahren ihre letzte Austrocknung, und Transportzeiten (zusammen mit washout Prozessen) bestimmen den Fluss von Wasserdampf und kurzlebigen Ozon abbauenden Substanzen in die Stratosphäre. Der TTL kommt als "Pforte zur Stratosphäre" deshalb eine besondere Bedeutung für das globale Klimasystem zu.
Verschiedene Transportprozesse bestimmen die Zusammensetzung der TTL und den Transport von Ozon(vorläufern), Aerosolen und kurzlebigen Spurengasen in die Stratosphäre. Auf der globalen Skala wird der Transport in die TTL durch die Brewer-Dobson-Zirkulation bestimmt. Innerhalb dieser Zirkulation werden Luftmassen langsam innerhalb der tropischen Stratosphäre aufwärts bewegt und anschließend horizontal in höhere Breiten transportiert, wo die Luft schließlich allmählich absinkt. Die Brewer-Dobson-Zirkulation verstärkt sich auf der jeweiligen Winterhemisphäre. Neben diesem großräumigen Troposphären-Stratosphären-Transport bestimmen andere Prozesse, wie Strahlungsheizung, Konvektion oder horizontaler Austausch mit der extratropischen unteren Stratosphäre die Zusammensetzung der TTL sowie die Transportzeiten zwischen Troposphäre und Stratosphäre.
Diese Doktorarbeit soll dazu beitragen, das Verständnis dieser verschiedenen Prozesse zu verbessern.

Messungen

Im Rahmen dieser Arbeit wurden zwei Messkampagnen durchgeführt, wobei mit Hilfe von Spurengasmessungen die verschiedenen Transportprozesse untersucht wurden. Die Messungen wurden mit dem High Altitude Gas AnalyzeR (HAGAR) durchgeführt, der an der Universität Frankfurt entwickelt wurde. HAGAR beinhaltet zwei gaschromatographische Kanäle, die zur Messung der langlebigen Spurengase N_2O, CFC-12, CFC-11, H-1211 ($CBrClF_2$), SF_6, CH_4, H_2 verwendet werden, und einen LI-COR Detektor, der mit Hilfe von Infrarotabsorption CO_2 messen kann. Zusätzlich wurden (von anderen Forscher-

gruppen) die Konzentrationen von Ozon (mit Hilfe des Fast Ozone Analyzer (FOZAN)) und CO (mit dem Cryogenically Operated Laser Diode (COLD) Messgerät) gemessen. Als Plattform für die Messgeräte diente das Höhenforschungsflugzeug M55 Geophysica, ein durch MDB (Myasishchev Design Bureau) in Russland entwickeltes Flugzeug, das eine Höhe von 21 Kilometer erreichen kann.
Die erste Messkampagne fand im Rahmen der SCOUT-O3 Tropical Aircraft Campaign in November und Dezember 2005 in Darwin, Australien (12°S, 130°E) statt. Neben insgesamt 12 Transferflügen wurden acht lokale Flüge in der TTL und der untere Stratosphäre durchgeführt, sowohl Flüge zur Vermessung der "Hintergrund TTL", als auch Flüge mit dem Ziel, die tiefe Konvektion in der Region zu untersuchen.
Die zweite Messkampagne, AMMA/SCOUT-O3, führte im August 2006 nach Ouagadougou, Burkina Faso. Dabei fanden fünf lokale und vier Transferflüge zwischen Verona, Italien und Ougadougou statt, mit dem Ziel, den Einfluss von großräumigen Transport und mesoskaliger konvektiver Systeme zu bestimmen, sowie eine Validation des Calypso Satelliten durchzuführen.

Spurengasmessungen in der TTL während der AMMA/SCOUT-O3 Messkampagne.

Das dritte Kapitel dieser Dissertation beschreibt die Ergebnisse der AMMA/SCOUT-O3 Kampagne. Dabei werden fünf lokale Flüge analysiert, um die dominierenden Transportprozesse in der TTL zu studieren: tiefe Konvektion bis zum Level of main convective Outflow, Vertikalmischung nach überschießender Konvektion, isentrope Mischung entlang der subtropischen Tropopause, und horizontaler Transport in der Region der subtropischem Barriere.
Die CO_2 Profile (mit Ausnahme des Flugs am 13. August) weisen deutliche Minima in der TTL auf, was auf Ausströmung von CO_2-armer Grenzschichtluft hindeutet. Diese Minima zeigen, dass i) der konvektive Einfluss in der untersuchten TTL-Region sehr signifikant ist und ii), dass das Niveau des main convective Outflow im potenziellen Temperaturbereich zwischen 350 und 360 K (13-14 km) lag, für den Flug am 11. August mit 370 K sogar darüber ($\sim$15 km). Die Ozonprofile andererseits zeigen, dass der größte Teil der gesammelten konvektiv beeinflussten Luftmassen älteren Ursprungs sein muss (mehrere Tage), weil Mischungsverhältnisse von 30 ppb, die in der regionalen Grenzschicht gemessen wurden, nur bei einem der Flüge in der TTL beobachtet wurden. Die mittleren gemessenen Mischungsverhältnisse in der TTL lagen bei etwa 50 ppb oder darüber.
Der Einfluss von überschießender Konvektion auf die Vertikalprofile der Spurengase scheint gering zu sein, da diese ein ziemlich kohärentes Profil oberhalb des Levels of main convective Outflow zeigen. Einige schwache Signaturen, die potentiell auf überschießende Konvektion hindeuten, wurden in den CO_2-Daten vom 4. und 8. August gefunden, ein anderes potentielles Signal wurde in den CO-Daten vom 7. August beobachtet. Gleichzeitige Messungen anderer Spurengase bestätigen diese Beobachtungen jedoch nicht.
Stratosphärische Einmischung von photochemisch gealterter Luft aus der extratropischen Stratosphäre ist sehr gering bis zum Tropopausenniveau von durchschnittlich 376 K potentieller Temperatur. Der Anteil gealterter extratropischer Luft in der TTL, abgeschätzt

mit Hilfe der N_2O Profile, beträgt 0.0 ± 0.1 bis zur 370 K-Isentrope und nimmt oberhalb dieses Levels zu bis auf 0.3 (± 0.1) bei 390 K.
Die subtropische Barriere zeigt sich nicht als eine scharfe Grenze in der Spurengasverteilung, sondern eher wie eine Übergangsregion zwischen ungefähr 10°und 25°N, innerhalb derer sich die Mischungsverhältnisse der Spurengase langsam von tropischen zu extratropischen Werten verändern. Die subtropische Barriere auf der Sommerseite der Tropen scheint daher ziemlich durchlässig für horizontale Einmischung in den Sommersubtropen unterhalb 20 km Höhe zu sein.

Einfluss von verschmutzten Grenzschicht-Luftmassen, Konvektion und des subtropischen Jetstreams auf die TTL über Darwin während der SCOUT-O3 Messkampagne.

Kapitel 4 zeigt die Resultate der SCOUT-O3 Messkampagne. Von den acht lokalen Flügen weisen die vier letzten Flüge (051129, 051130a, 051130b, 051206) im Niveau zwischen 355 und 380 K potenzieller Temperatur im Vergleich mit den ersten vier Flügen (051116, 051119, 051123, 051125) erhöhte Ozon-, CO- und CO_2-Werte auf. Dies suggeriert vertikale Mischung in die TTL durch überschießende Konvektion oder stratosphärischen Einfluss.
Das Fehlen einer negativen Korrelation zwischen O_3 und N_2O in der TTL und die Beobachtung erhöhter CO-Werte schließt horizontale Einmischung aus der extratropischen Stratosphäre aus. Auch Hector, das konvektive System, das sich fast jeden Tag über den Tiwi-Inseln nördlich von Darwin entwickelt, kann die erhöhten Werte für die beiden Flüge am 30. November nicht erklären. Am 30. November wurden zwei Flüge durchgeführt - vor, während und nach der Entwicklung von Hector. Mit Hilfe von Satellitenbildern und anhand der Flugstrecken wird deutlich, dass die erhöhten Mischungsverhältnisse schon vor der Entwicklung des Systems, und auch an allen Seiten des Systems auftraten. Deswegen werden andere Erklärungen für die erhöhten Mischungsverhältnisse vorgeschlagen.
Eine mögliche Erklärung ist durch vertikale Mischung in der Nähe des Jetstreams gegeben. Während der Kampagne lag der Jet nicht weit südlich von Darwin. Rückwartstrajektorien zeigen, dass die Luft, die am 30. November gemessen wurde, während der letzten drei bis vier Tage entlang des subtropischen Jets transportiert wurde. In dieser Region kann aufgrund starker Windscherung und der daraus resultierenden Deformation des Stromfeldes sehr starke Mischung auftreten. Der Jet kann aber nicht die einzige Erklärung der erhöhten Werte sein, weil die am 29. November beobachteten Luftmassen auch entlang des Jets transportiert wurden, die Messungen aber deutlich niedrigere Erhöhungen zeigen.
Eine andere mögliche Ursache liegt im Einfluss von verschmutzten Grenzschicht-Luftmassen über Indonesien. Die Flüge fanden am Ende der Biomassen-Verbrennungs-Saison statt. Dabei durchqueren insbesondere die Rückwartstrajektorien der Flüge vom 30. November große Teile von Nord-Indonesien zwischen 8 und 10 Tagen vor den Messungen. Konvektion von Biomass Burning Plumes und anderen Luftverschmutzungen kann CO und Ozonvorläufer in die TTL transportieren und dort für erhebliche Ozonproduktion sorgen. Die beobachteten Anreicherungen zeigen Signaturen die für alte Biomass Burning Plumes typisch sind.

Bestimmung von Verweilzeiten und vertikalen Transportgeschwindigkeiten in der Hintergrund-TTL mit Hilfe von in situ Spurengasmessungen.

Das letzte Kapitel behandelt die vertikale Aufstiegsgeschwindigkeit in der TTL und benutzt Messungen von sowohl der SCOUT-O3 und AMMA/SCOUT-O3 Kampagne, als auch von früheren Messkampagnen, namentlich die TROCCINOX und APE-THESEO Kampagnen. Die TROCCINOX Kampagne fand im Januar/Februar 2005 in Brasilien statt, die APE-THESEO Kampagne im Februar/März 1999 auf den Seychellen.
Zeitskalen und Verweilzeiten für vertikalen Transport in der Hintergrund-TTL wurden für verschiedene Jahreszeiten und verschiedene geographische Regionen mit Hilfe von CO_2 Messungen und langlebigen Spurengase abgeschätzt. Die vertikalen Transportzeiten wurden anhand der zeitlichen Verzögerung der saisonalen Variation von CO_2 bestimmt, die als CO_2 "tracer clock" benutzt wird.
Zwei Methoden werden angewandt um die Verweilzeit zu bestimmen. Die erste Methode benutzt den mittleren zeitlichen Gradienten von CO_2 in der tropischen Troposphäre ("CO_2-Index") über mehrere Monate, die zweite Methode arbeitet mit direktem Anpassen des CO_2-Index an die Messdaten unter Annahme einer konstanten Aufstiegsgeschwindigkeit als Fit-Parameter.
Die Resultate zeigen, dass die Hintergrund-TTL ein kohärentes "Tape Recorder"-Signal in Übereinstimmung mit der troposphärische Variation von CO_2 zeigt. Eine Aufstiegsrate kann berechnet werden, wenn auch mit großen Unsicherheiten, insbesondere für APE-THESEO. Die Annahme, dass Luft oberhalb von 360 K gut gemischt ist stimmt für die SCOUT-O3 und AMMA/SCOUT-O3 Daten, aber nicht für die (südlichen subtropischen) TROCCINOX Daten, die niedrigere Mischungsverhältnisse eher charakteristisch für die Südhemisphäre zeigen. Das bestätigt die Annahme, dass bei 360 K potentieller Temperatur die Unterschiede zwischen beiden Hemisphären noch wahrgenommen werden.
Die erste Methode liefert Verweilzeiten in Australien, Brasilien und Westafrika liegen in der gleichen Größenordnung, 35-45 Tage bis zu 380 K und 50 Tage bis zu 390 K (wobei auf 390 K kein Wert für Australien ermittelt werden kann weil der Gradient sich ungefähr einen Monat vor der Kampagne ändert). Für APE-THESEO konnte kein Resultat berechnet werden, weil der zeitliche Gradient über die vorherigen Monat offensichtlich nicht representativ für die CO_2-Variationen während Februar 1999 ist.
Die zweite Methode, bei der CO_2-Index an die gemessenen Daten angepasst wird, kann in allen Jahreszeiten benutzt werden. Im Gegensatz zu der ersten Methode verlangt diese Methode im Prinzip perfekte Übereinstimmung der Flugzeugdaten mit den troposphärischen Daten des CO_2-Index, die in der Praxis schon aufgrund von Messfehlern und unterschiedlichen Kalibrationen nicht immer gegeben ist. In der Tat ergeben sich signifikante Differenzen zwischen den Flugzeugdaten und dem CO_2-Index für APE-THESEO und in geringerem Maße für TROCCINOX, so dass gut Fits des CO_2-Index mit den TTL-Beobachtungen nur erreicht werden, wennn eine konstante Verschiebung zugelassen wird. Für AMMA/SCOUT-O3 und SCOUT-O3 ergibt sich jedoch auch ohne Verschiebung gute Übereinstimmung.
Die besten Schätzungen zeigen moderate Aufstiegsraten von 0.5 ± 0.15 K/Tag für SCOUT-O3 (NH-Herbst) und 0.7 ± 0.1 K/Tag für AMMA/SCOUT-O3 (NH-Sommer)

entsprechend Verweilzeiten zwischen 360 und 390 K von 60 ± 25 Tagen bzw. 43 ± 8 Tagen. Diese Resultate stimmen gut mit den Resultaten der ersten Methode überein. Für APE-THESEO und TROCCINOX haben die besten Fits (mit einer Verschiebung von -1.8 ppm bzw. -0.5 ppm) höhere Aufstiegsraten von 1.3 ± 0.5 K/Tag und 0.75 ± 0.15 K/Tag, entsprechend Verweilzeiten von 23 ± 7 und 40 ± 10 Tagen, beide während dem Nordhemisphären-Winter. Diese Resultate stimmen relativ gut mit den Resultaten von Park et al. (2007a) überein, die eine Aufstiegsrate von 1.2 ± 0.2 K/Tag entsprechend einer Verweilzeit von 26 ± 4 Tagen während des Nordhemisphären-Winter abgeleitet haben.
Die Resultate sind auch in Einklang mit der jahreszeitlichen Variation der Brewer-Dobson Zirkulation, die einen um etwa einen Faktor zwei stärkeren Aufstieg im Winter als im Sommer erwarten lässt (z.B. Holton et al., 1995). Wenn der CO_2-Index für APE-THESEO und TROCCINOX ohne Verschiebung angepasst wird so dass der Fit die Werte bei 390K trifft, dann erhält man eine Aufstiegsrate von 0.4 bzw. 0.5 K/Tag, d.h. ähnlich den Werten für Sommer und Herbst. Allerdings passen die entsprechende Fits in diesem Fall unterhalb von 390 K schlecht mit den TTL-Daten zusammen, so dass diese Resultate wenig glaubhaft sind.

Acknowledgements

Another chapter comes to its end. Four years in Frankfurt had already come to an end last September. It seems like ages ago when I arrived in Frankfurt with just some school-German and not knowing that you are not allowed to enter a bus when the bus driver is not in yet.
After two months I already left Frankfurt for the first campaign in Australia. Both the campaigns in Darwin and in Ouagadougou are experiences I will never forget. Not only the stress and the long nights we made to get our HAGAR working in time for the next flight. How I sometimes was swearing, when, again, we were the only ones left in the hangar, and again had to remove the 40 screws (or so) to open up the instrument and replace some broken piece. Also the sight of the Geophysica safely landing and giving us loads of interesting data. Also the fun I had with all the colleagues from all over Europe and who felt like a kind of big family. I will not forget the campaign parties and the early morning runs with Fred and Marc through the Botanical Gardens in Darwin and during many other conferences that followed.
Thanks Michael for giving me the opportunity to visit so many conferences and so many places in the world: Darwin, Ouagadougou, La Reunion, Cambridge, Manchester, Crete, Vienna, Aachen, Oberpfaffenhofen, Schliersee and not to forget Jülich. Thanks for giving me the opportunity to do a PhD in your group, thanks for always correcting my work very thoroughly, although maybe not always that fast... Thanks for taking the time to explain me everything in detail and helping to solve any problems I was encountering.
Thanks to the other Hagaristi: Anna Christina, Janine, Katja and Anja. You were really nice colleagues to work with. And thanks for having the patience to learn me how to deal with HAGAR. Thanks to Olli for helping during the AMMA campaign, and for the Latex files of your thesis, which made it a lot easier for me to write down this one.
A very grateful thank you to Ulrich Schmidt, for giving me the possibility to do a thesis within your group and for the support you gave me at the end of my thesis, although already in retirement. Thanks also to Joachim Curtius, who became the professor after the retirement of Prof. Schmidt and let me keep my office in Frankfurt after being actually employed by the University of Wuppertal.
A lot of thanks also for Sven, who took the effort of taking out all the German grammar errors in the Zusammenfassung. A special thanks to Christine, much more than the secretary of the group! Thanks for all the nice conversations we had and all the tips you gave me.
This research would not have been possible without support of the European Community

under the Integrated Project SCOUT-O3 (505390-GOCE-CT-2004) as well as by the AMMA-EU project. Many thanks as well to the pilot and the crew of the M55 Geophysica and all the other colleagues who made the SCOUT-O3 and AMMA/SCOUT-O3 campaign a success. The third year of my research was granted with an Excellence Stipendium of the Otto Stern School.

Luckily there were also a lot of people who made it possible to forget work now and then. Thanks to the Merton Lauftreff for the many rounds along the Nidda we ran together! Ludz, I am still training for the 2:52. Thanks to the Uni Wandergruppe, especially to Stefan and Bernd, for organising wonderful walks around Frankfurt. Thanks to Meiko, Stas, Daniel, Bilal, Katja, Philipp, Hoyoung, Stefan, Dirk, Zuzana, Sebastian, Sven, Jeroen and all the other people who made my stay in Frankfurt a wonderful time. Keep ice-skating! Thanks to the Niederländische Stammtisch to make me not forget my Dutch and share tips where to buy 'stroopwafels' in Frankfurt.
Thanks as well to my Dutch friends and family, who always kept interested in the progress of my thesis and always kept in touch, although I saw them a lot less: Jorick, Miranda, Kim, Danneke, Corien, Rob, Maarten´s family.
There are a lot more people to thank but who I cannot all name here, from the friendly ladies at the mensa to the Sport-Uni: thanks to all the people who made my stay in Frankfurt an unforgettable time!
Thanks mum. Thanks for all the support you gave me, also when things did not go very smoothly.
Almost last, but not least: thanks Maarten. It was not easy to live so far away from each other for such a long time. Thanks for spending all the hours on the ICE to visit me. Thanks for letting me forget all my worries when I was on Texel. Thanks for the patience. Thanks for always letting me believe I could do it. Thanks for being there!

And last, sorry to the busdriver that I still did not read the "Busgesetz".

The end!
Einde!
Ende!

Curriculum Vitae

Carine Homan was born on 2 August 1981 in Amsterdam, Netherlands. After finishing "Gymnasium" (high school) at the Alkwin Kollege in Uithoorn she started her studies "Soil, Water and Atmosphere" at Wageningen University in 1999. After obtaining her propaedeuse in 2000 (cum laude), she continued with her doctoraal (MSc) and choose the specialisation Meteorology and Air Quality. She conducted two practical times, one at the Ministry of Housing, Spatial Planning and Environment to study the point of views of climate sceptics and one at the Netherlands Assessment Agency to relate satellite measurement of Aerosol Optical Thickness with ground based measurements of particulate matter. Her first master thesis was performed at research institute Alterra in Wageningen with Dr. B. Kruijt, and comprised a study on fluxes of CO_2 from different soil types. The second and largest master thesis was written at Monash University in Melbourne, Australia with Dr. S. Siems, and comprised a study with an air pollution model on the influence of the sea breeze on the passage of fronts at the coast of Tasmania. After finishing her studies in November 2004, Carine continued her work on satellite measurements at the Netherlands Assessment Agency as a junior researcher. In September 2005 she started her PhD research at the Johann Wolfgang Goethe University of Frankfurt under the supervision of Prof. Dr. U. Schmidt and Dr. C.M. Volk. She also pursued post-graduate education at the International Max Planck Scool on Atmospheric Chemistry and Physics (IMPRS). Currently, Carine Homan is working at the Royal Dutch Meteorological Institute in De Bilt, Netherlands, as a researcher in the division Climate Services.

Publications:

Homan, C. D., Volk, C.M., Kuhn, A.C., Werner, A., Baehr, J., Viciani, S., Ulanovski, A. and Ravegnani, F.: Tracer measurements in the tropical tropopause layer during the AMMA/SCOUT-O3 aircraft campaign, Atmos. Chem. Phys., 10, 3615-3627, 2010.

Homan, C. D., Volk, C.M., Baehr, J., Kuhn, A.C., Werner, A., Viciani, S., Ulanovski, A., Ravegnani, F., Günther, G., Konopka, P., and Brunner, D.: Vertical mixing of air in the TTL during the SCOUT-O3 and AMMA/SCOUT aircraft campaigns, proceedings of the Reunion Island International Symposium on tropical stratosphere and upper troposphere (Riis), Reunion Island, 2007.

Koelemeijer, R.B.A., **Homan, C. D.**, Matthijsen, J.: Comparison of spatial and temporal variations of aerosol optical thickness and particulate matter over Europe, Atmospheric Environment 40, 5304-5315, 2006.

Koelemeijer, R.B.A., Schaap, M., Timmermans, R.M.A., **Homan, C. D.**, Matthijsen, J., Van de Kassteele, J., and Builtjes P.J.H.: Monitoring aerosol concentrations and optical thickness over Europe- PARMA final report, MNP report 555034001, 2006.

Van de Kassteele, J., Koelemeijer, R.B.A., Dekkers, A.L.M., Schaap, M., **Homan, C. D.**, Stein, A.: Statistical mapping of PM10 concentrations over Western Europe using secondary information from dispersing modelling and MODIS satellite observations, Stoch. Environ. Res. Risk Assess., DOI 10.1007/s00477-006-0055-4, 2006.

Homan, C. D., R.B.A. Koelemeijer, and J. Matthijsen: Modis aerosol optical thickness over Europe compared to surface PM data, proceedings of the 5th Urban Air Quality Conference, Valencia, Spain, on CDROM, 2005.

Presentations at international conferences:

Homan, C. D., C. M. Volk, J. Baehr, A.C. Kuhn, A. Werner, S. Viciani, A. Ulanovski, F. Ravegnani: Tracer measurements in the tropical tropopause layer during the AMMA/SCOUT-O3 aircraft campaign, Talk at the SCOUT-O3 Final meeting, Schliersee, Germany, 15-17 June 2009.

Homan, C. D., C. M. Volk, J. Baehr, A.C. Kuhn, A. Werner, S. Viciani, A. Ulanovski, F. Ravegnani, D. Brunner: Influence of biomass burning, convection and the subtropical jet on the TTL over Darwin, Poster presented at the SCOUT-O3 Final meeting, Schliersee, Germany, 15-17 June 2009.

Homan, C. D., C. M. Volk, J. Baehr, A.C. Kuhn, A. Werner: Residence times and vertical transport rates in the background TTL derived from in situ tracer measurements, Poster presented at the SCOUT-O3 Final meeting, Schliersee, Germany, 15-17 June 2009.

Homan, C. D., C. M. Volk, J. Baehr, A.C. Kuhn, A. Werner, S. Viciani, A. Ulanovski, F. Ravegnani, P. Konopka, D. Brunner: Vertical Mixing and Ascent in the TTL during the SCOUT-O3 and AMMA/SCOUT Aircraft Campaigns, Talk at the at the

EGU Assembly, Vienna, Austria, 13-18 April 2008, Geophys. Res. Abstr., Vol. 10, EGU2008-A-09782, 2008.

Homan, C. D., C. M. Volk, J. Baehr, A.C. Kuhn, A. Werner, S. Viciani, A. Ulanovski, F. Ravegnani, P. Konopka, D. Brunner: Vertical Mixing in the TTL during the SCOUT-O3 and AMMA/SCOUT Aircraft Campaigns, Talk at the SCOUT-O3/ACTIVE/TWP-ICE workshop on tropical UTLS, Manchester, England, 11 January 2008.

Homan, C. D., C. M. Volk, J. Baehr, A.C. Kuhn, A. Werner, S. Viciani, A. Ulanovski, F. Ravegnani, G. Günther, D. Brunner: Vertical Mixing of Air in the TTL during the SCOUT-O3 and AMMA/SCOUT Aircraft Campaigns, Talk at the Reunion Island International Symposium on Upper Troposphere, Lower Stratosphere, Reunion Island, 07 November 2007.

Homan, C. D., C. M. Volk, J. Baehr, A.C. Kuhn, A. Werner, S. Viciani, A. Ulanovski, F. Ravegnani, G. Günther, D. Brunner: Vertical mixing in the TTL during the SCOUT-O3 Aircraft Campaign, Poster presented at the SCOUT-O3 Annual Meeting, Iraklion, Greece, 7-10 May 2007.

Homan, C. D., C. M. Volk, J. Baehr, A.C. Kuhn, A. Werner, S. Viciani, A. Ulanovski, F. Ravegnani, G. Günther, D. Brunner: Mixing of overshooting air in the TTL during the SCOUT-O3 Aircraft Campaign, Poster presented at the EGU Assembly, Vienna, Austria, 16-20 April 2007, Geophys. Res. Abstr., Vol. 9, 08238, 2007.

Homan, C. D., C. M. Volk, J. Baehr, A.C. Kuhn, A. Werner, S. Viciani, P. Mazzinghi, A. Ulanovski, F. Ravegnani, G. Günther: Mixing of overshooting air in the TTL during the SCOUT-O3 Aircraft Campaign, Talk at the ACTIVE/SCOUT-O3 Workshop, Cambridge, England, 6-8 November 2006.